# Enhancing anti-tumor immunity to MHC class I-deficient tumors: role of regulatory T cells and type I IFN

**Dissertation**
**submitted to the**
**Combined Faculties for the Natural Sciences and for Mathematics**
**of the Ruperto-Carola University Of Heidelberg, Germany**
**for the degree of**
**Doctor of Natural Sciences**

**presented by**
**Ioanna Evdokia Galani**
born in Acharnes, Greece

**Dissertation**
**submitted to the**
**Combined Faculties for the Natural Sciences and for Mathematics**
**of the Ruperto-Carola University Of Heidelberg, Germany**
**for the degree of**
**Doctor of Natural Sciences**

**presented by**
**Ioanna Evdokia Galani**
born in Acharnes, Greece

Oral examination: 20.06.2008

# Enhancing anti-tumor immunity to MHC class I-deficient tumors: role of regulatory T cells and type I IFN

| | |
|---|---|
| 1. Referee: | Prof. Dr. G. Hämmerling |
| 2. Referee: | PD Dr. A. Cerwenka |

The work described in this thesis was performed from September 2004 to April 2008 at the German Cancer Research Center, Germany, in the laboratory of PD Dr. Adelheid Cerwenka.

**Parts of this thesis have been published in:**

Galani I.E., M. Wendel, C. Schellack, E. Suri-Payer and A. Cerwenka. Treg suppress leukocyte accumulation and macrophage activation in lymphoma. Manuscript in preparation.

Nausch N., I.E. Galani and A. Cerwenka. Myeloid-derived ‚suppressor' cells express RAE-1 and activate NK cells. Manuscript in revision.

Wendel M., I.E. Galani, E. Suri-Payer and A. Cerwenka. NK cell accumulation in tumors is dependent on IFN-γ and CXCR3 ligands. Manuscript submitted.

Kiessling M., C.D. Klemke, M. Kamiński, I.E. Galani, P.H. Krammer and K. Gülow. Survival of primary T cell lymphomas is dependent on regulation of Ferritin Heavy Chain by constitutively activated NF-κB. Manuscript submitted.

**Conference presentations:**

Galani I.E., M. Wendel, C. Schellack, E. Suri-Payer and A. Cerwenka. IFN-γ dependent rejection of the NK cell dependent RMA-S tumor in the absence of regulatory T cells. 16$^{th}$ European Congress of Immunology, September 2006, Paris, France.

Galani I.E., M. Wendel, C. Schellack, E. Suri-Payer and A. Cerwenka. Regulatory T cells suppress IFN-γ dependent rejection of the NK cell sensitive RMA-S tumor. Natural Killer Cell Symposium 2006 Heidelberg, December 2006, Heidelberg, Germany.

Galani I.E., M. Wendel, C. Schellack, E. Suri-Payer and A. Cerwenka. Rejection of the NK cell sensitive tumor RMA-S via IFN-γ in the absence of regulatory T cells. Keystone Symposia meeting 'Mechanisms Linking Inflammation and Cancer', February 2007, Santa Fe, New Mexico, USA.

Galani I.E., M. Wendel, C. Schellack, E. Suri-Payer and A. Cerwenka. Treg suppress leukocyte accumulation and macrophage activation in RMA-S lymphoma. 10th Meeting of the Society for Natural Immunity, April 2007, Cambridge, UK.

Galani I.E., M. Wendel, C. Schellack, E. Suri-Payer and A. Cerwenka. Regulatory T cells suppress IFN-γ dependent leukocyte accumulation and macrophage activation in lymphoma. 37th Annual Meeting of the German Society for Immunology (DGfI), September 2007, Heidelberg, Germany.

# CONTENTS

# 1 Zusammenfassung

Natürlich vorkommende $CD4^+CD25^+Foxp3^+$ regulatorische T Zellen (Treg) besitzen die Fähigkeit, Immunantworten, wie z.B. die Tumorabwehr, zu unterdrücken. In klinischen Studien in Krebspatienten wird gegenwärtig untersucht, ob durch Manipulation der Treg Population die Wirksamkeit von Vakzinen, deren Ziel die Stärkung des adaptiven Immunsystems ist, gesteigert werden kann. Viele Tumore verlieren jedoch die Expression von MHC Klasse I Molekülen, die zur direkten Erkennung und Eliminierung durch $CD8^+$ T Zellen führen. Eine effiziente Beseitigung dieser Art von Tumoren kann allerdings durch Zellen des angeborenen Immunsystems erfolgen, die nicht auf die Erkennung von Antigen-MHC Klasse I Komplexen angewiesen sind. Die Funktion regulatorischer T Zellen in der Abwehr von Tumoren, deren Wachstum überwiegend durch das angeborene Immunsystem kontrolliert wird, ist bislang nur sehr wenig erforscht.

In dieser Arbeit wurde der Einfluss von Treg auf die Immunantwort gegen subkutan injizierte RMA-S Zellen untersucht. RMA-S Zellen sind Maus-Lymphom-Zellen, die nur eine geringe MHC Klasse I Expression aufweisen. Unsere Experimente zeigten, dass sich Treg im Tumorgewebe sowie in den lymphoiden Organen Tumor-tragender Mäuse anreichern. Die Depletion von Treg mittels eines monoklonalen anti-CD25 Antikörpers ermöglichte die Abstoßung großer Mengen injizierter RMA-S Zellen, die in unbehandelten Mäusen zu progressivem Tumorwachstum führten. In Abwesenheit von Treg wurde eine sehr hoher Anzahl an $NK1.1^+$, $CD8^+$ und $CD4^+CD25^+$ T Zellen in das Tumorgewebe rekrutiert. Alle diese Zellpopulationen waren an der Abstoßung von RMA-S Tumoren beteiligt. Die in Abwesenheit der Treg ausgelöste primäre Immunantwort führte zur Entstehung von immunologischem Gedächtnis; In Mäusen, die den ursprünglichen Tumor abgestoßen hatten und anschließend erneut mit entweder RMA-S oder MHC Klasse I exprimierenden RMA Zellen injiziert wurden, wurde Tumorabstoßung beobachtet. Darüber hinaus konnten wir zeigen, dass Tumor-infiltrierende Leukozyten nach Depletion von Treg IFN-γ in größeren Mengen produzierten. Eine Neutralisation von IFN-γ hemmte die Anreicherung von Leukozyten im Tumor und verhinderte die normalerweise nach Treg Depletion beobachtete Tumorabstoßung. In Abwesenheit von Treg stellten Makrophagen die größte Zell-Population unter den Tumor-infiltrierenden Leukozyten

dar. Makrophagen, die in Tumore Treg-depletierter Mäuse eingewandert waren, zeigten eine verstärkte Expression von MHC Klasse II und eine gesteigerte Produktion von Chemokinen und Entzündungs-fördernden Zytokinen. Diese Makrophagen waren in der Lage die Proliferation von Tumorzellen durch einen Mechanismus zu unterbinden, der unabhängig von iNOS, PGE2 und IDO war.

Diese Arbeit untermauert somit die Bedeutung von Treg für die Hemmung der Immunantwort gegen Tumorzellen mit geringer MHC Klasse I Expression. In Abwesenheit von Treg bestand zudem eine Korrelation zwischen einer hohen Anzahl Tumor-infiltrierender Makrophagen und der Abstoßung des Tumors. Diese Daten beschreiben zum ersten Mal dass in Tumor-tragenden Mäusen Makrophagen durch Treg gehemmt werden können.

Der zweite Teil dieser Arbeit diente der Untersuchung weiterer Kontrollmechanismen der Immunantwort gegen RMA-S Tumore. Hierbei konzentrierten wir uns auf die Bedeutung von endogen produzierten Typ I Interferonen. Obwohl die exogene Applikation von Typ I Interferonen bereits zur Behandlung verschiedener Krebsarten angewandt wird, ist ihre endogene Produktion und Funktion nur sehr wenig erforscht. In diesen Experimenten untersuchten wir das Tumorwachstum von RMA-S Tumoren in IFNAR1$^{-/-}$ Mäusen, die nicht auf Typ I Interferone reagieren können, da sie keinen Rezeptor für Typ I Interferone exprimieren. In IFNAR1$^{-/-}$ Mäusen stellten wir ein beschleunigtes Tumorwachstum fest. Wir generierten Knochenmark-Chimären, in denen entweder die hämatopoetischen oder die nicht-hämatopoetischen Zellen unfähig waren auf Typ I Interferon zu reagieren und beobachteten, dass die Fähigkeit zur Reaktion auf Typ I Interferone in beiden Zellpopulationen gegeben sein muss. Der IFNA-Rezeptor zeigte sich insbesondere für die zytotoxische Aktivität von NK Zellen und für eine fehlerfreie Entwicklung von Blutgefäß-Netzwerken verantwortlich. Im Gegensatz hierzu beeinträchtigte seine Abwesenheit weder die Effektorfunktionen von Makrophagen noch die Anreicherung von Leukozyten im Tumorgewebe.
Zusammenfassend zeigten unsere Studien, dass endogen produzierte Typ I Intereferone einen Beitrag zur Kontrolle des Wachstums von RMA-S Tumoren ohne MHC Klasse I Expression leisten. Dies könnte durch Beeinflussung sowohl der hämatopoetischen wie auch der nicht-hämatopoetischen Zellen und durch Regulation der Aktivität von NK Zellen und der Bildung Tumor-versorgender Blutgefäße geschehen.

# 2 SUMMARY

Naturally occurring $CD4^+CD25^+Foxp3^+$ regulatory T cells (Treg) have been shown to suppress immune responses, including anti-tumor immunity. Strategies of manipulating Treg in cancer patients are currently evaluated in clinical trials with the aim of enhancing the efficiency of vaccinations, targeting the adaptive arm of immunity. Many tumors, however, lose expression of MHC class I and thus become protected from $CD8^+$ T cell-mediated recognition and elimination. Such types of tumors can still be efficiently eliminated by cells of the innate immune system, in particular NK cells, through antigen- and MHC class I-independent mechanisms. The role of Treg in the rejection of tumors, which are predominantly under the control of innate immune cells has been poorly addressed so far.

In this study, we investigated the influence of Treg on the immune response against the MHC class I-deficient mouse lymphoma RMA-S after subcutaneous injection. We showed that Treg accumulate in the tumor tissue and lymphoid organs of tumor-bearing animals. Treg depletion upon application of an anti-CD25 monoclonal antibody led to the rejection of high tumor cell numbers, which in contrast grew progressively in untreated mice. Our experiments demonstrated that $NK1.1^+$ cells, $CD8^+$ and $CD4^+CD25^-$ T cells are recruited in high cell numbers to the tumor site in the absence of Treg and that all of these three cell populations contribute to RMA-S tumor rejection. Primary immune responses elicited during Treg depletion led to the generation of protective immunological memory; rechallenge of mice that had rejected the initial tumor with either RMA-S or MHC class I-sufficient RMA tumor cells resulted in immediate tumor rejection. Furthermore, we showed that IFN-γ is produced in higher amounts by the tumor-infiltrating lymphocytes in the absence of Treg. Neutralization of IFN-γ completely abrogated the tumor rejection observed after Treg depletion, which correlated with the inhibition of accumulation of leukocytes at the tumor site. Among the tumor-infiltrating leukocytes, macrophages constituted the major cell population infiltrating the RMA-S tumor tissue in the absence of Treg. Tumor-infiltrating macrophages from Treg depleted mice expressed increased amounts of MHC class II and produced highly enhanced levels of chemokines and pro-inflammatory cytokines as compared to control mice. Macrophages isolated from the tumors also inhibited tumor cell proliferation through a mechanism independent of iNOS, PGE2 and IDO.

In conclusion, this study supports a role for Treg in blunting the immune response to a MHC class I-deficient tumor target, by interfering with leukocyte accumulation at the tumor site. In addition, high numbers of activated tumor-infiltrating macrophages correlated with tumor rejection in the absence of Treg. These data identify macrophages as novel potential targets for Treg mediated immune suppression in cancer.

In the second part of this study, we aimed at defining further mechanisms controlling the immune response against the MHC class I-deficient RMA-S tumor. For this purpose, we focused on the role of endogenously produced type I IFN. Although exogenously administered type I IFN have been used to treat various types of cancer, their endogenous production and function during an anti-tumor response has not been extensively studied. We studied the growth of RMA-S tumor in mice that cannot respond to type I IFN (IFNAR1$^{-/-}$ mice) and observed an acceleration in the tumor growth. In addition, we prepared bone marrow chimeras in which either the hematopoietic or the non-hematopoietic cells cannot respond to type I IFN and we found that type I IFN responsiveness is required in both compartments. Namely, IFNAR1 was important for NK cell cytotoxicity and proper development of the vessel network in the tumor tissue. In contrast, its absence did neither affect macrophage effector functions nor accumulation of leukocytes within the tumor tissue.
In summary, endogenously produced type I IFN contribute to the control of the MHC class I-deficient RMA-S tumor growth, via targeting both the hematopoietic and non-hematopoietic compartments, and regulate NK cell activity and tumor vessel formation.

# 3 INTRODUCTION

## 3.1 The immune system

The immune system is a complex and highly developed system, which has evolved to protect the host against the attack of foreign pathogens as well as tumors. In vertebrates, it consists of the innate and the adaptive immunity. The non-specific component of the immune system – innate immunity – is a set of mechanisms that are not specialized for a particular pathogen. Adaptive immunity, on the contrary, displays a higher degree of specificity in recognizing foreign antigens than innate immunity as well as the property of memory. Typically, an adaptive immune response against an antigen is raised five or six days after the initial exposure to that antigen. Subsequent exposure to the same antigen results in a memory response, which is faster, stronger, and often more effective in neutralizing or clearing the pathogen than the first one. Due to this attribute, the immune system can confer life-long immunity to many infectious agents after an initial encounter. Adaptive and innate immunity, however, do not operate independently of each other but rather function as a highly interactive and cooperative system.

The cells of the immune system originate in the bone marrow (BM), where many of them also mature, from the same progenitor, the hematopoietic stem cells. Initially, they give rise to stem cells of more limited potential, i.e. the common myeloid progenitor and the common lymphoid progenitor. The first one is the precursor of granulocytes, macrophages, dendritic cells (DC) and mast cells, while the second one gives rise to the lymphocytes.

### 3.1.1 The immune response to tumors

In order to fulfill its role, the immune system has developed mechanisms for the discrimination of self and non-self antigens, preventing the host from suffering autoimmune diseases via tolerance to self-antigens, while recognizing and eliminating the foreign pathogens. Cancer cells can be viewed as altered self-cells that have escaped normal growth-regulating mechanisms.

The theory of immune surveillance suggests that cancer cells arise frequently in the body, are recognized as foreign and are eliminated by the immune system; when tumor cells escape immune surveillance, tumors form that grow too large for the immune system to control. A more elaborate theory on how the immune system responds to a tumor is cancer immunoediting [1-5], which is comprised of three phases: elimination, equilibrium and escape. The elimination phase

basically refers to the immune surveillance. In the equilibrium phase, the tumor cell variants that have survived the elimination phase and the immune system enter into a dynamic equilibrium leading to a population of tumor clones with reduced immunogenicity. Evidence for the equilibrium phase was provided by a clinical case where metastatic melanoma occurred 1-2 years post-transplant in the two recipients who each received a kidney from the same donor [6]. In the escape phase, finally, the tumor cell variants surviving the equilibrium phase grow and become clinically detectable (Figure 3.1).

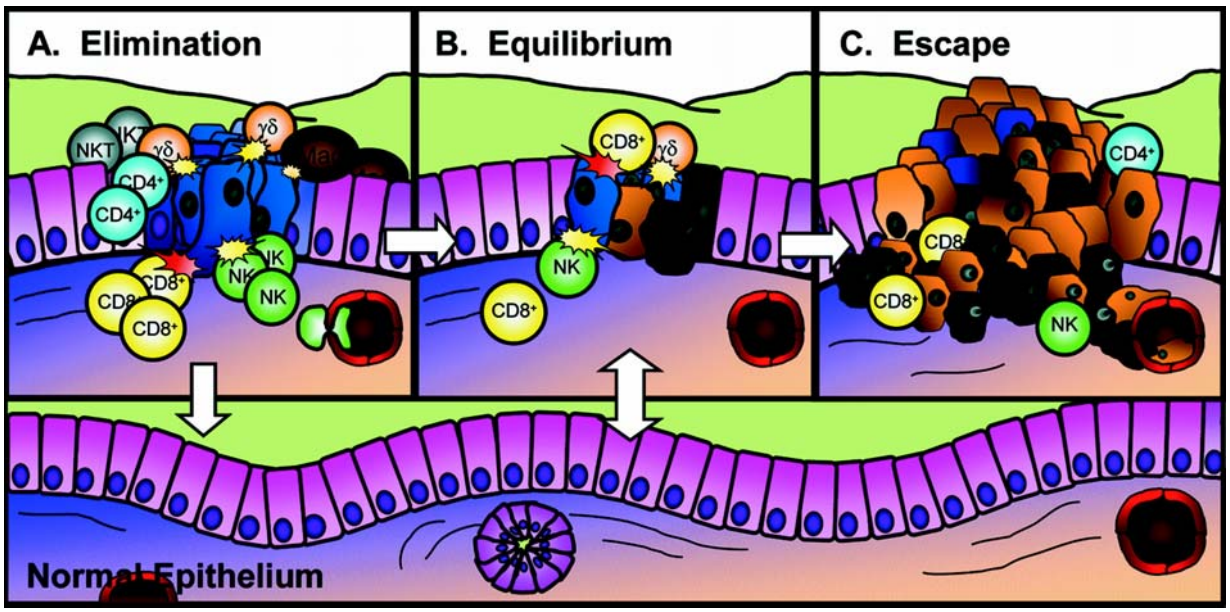


**Figure 3.1.** The three Es of cancer immunoediting: elimination, equilibrium, and escape. (Dunn *et al*. *Annu Rev Immunol*. 2004;22:329-60)

The immune system can detect the tumor cells by the recognition of the so called tumor-specific antigens (TSA) or tumor-associated antigens (TAA). TSA are unique to tumor cells and not present on normal cells, while TAA are not unique to tumor cells but quite often proteins either expressed at low levels by normal cells or expressed on normal cells during fetal development when the immune system is immature to respond. However, the tumor can impede the immune response directly e.g. by the shedding of recognition structures or indirectly e.g. by the production of immunosuppressive cytokines (TGF-β, IL-10) or the induction of immunosuppressive cell populations.

The immune system itself can form tumors that are classified as lymphomas or leukemias. Lymphomas are solid tumors which form within a lymphoid tissue, such as the bone marrow,

lymph nodes or thymus, while leukemias – either of lymphoid or myeloid lineage – proliferate as single cells.

### 3.1.2 The innate immune system

The innate immune system is a collection of distinct subsystems that appeared at different stages of evolution including anatomic, physiologic, phagocytic and inflammatory barriers that prevent the entrance and establishment of infectious agents. A summary of the main subsystems found in mammals and their function in innate host defence can be found in Table 3.1.

Innate immune recognition is also known as pattern recognition and is based on the detection of molecular structures unique to microorganisms. The innate immune system senses pathogens through pattern-recognition receptors (PRR), which trigger the activation of antimicrobial defenses. The targets of PRR are named pathogen-associated molecular patters (PAMP), although they are present on both pathogenic and non-pathogenic microorganisms. Bacterial PAMP are often components of the cell wall, such as lipopolysaccharide (LPS), peptidoglycan, lipoteichoic acids and cell-wall lipoproteins. β-glycan is an important fungal PAMP, which is present on the fungal cell wall. The detection of these structures by the innate immune system can signal the presence of microorganisms. Moreover, the recognition of viruses also follows this principle; however, since viral components are synthesized within the host cells, the main targets of innate immune recognition in this case are the viral nucleic acids. In addition, the innate immune system is able to discriminate between self and viral nucleic acids based on specific chemical modifications unique to viral RNA and DNA, as well as on the cellular compartments where viral, but not host-derived, nucleic acids are found [7]. There are several classes of PRR, the best characterized being Toll-like receptors (TLR), which can elicit inflammatory and antimicrobial responses after activation by their microbial ligands [8].

The innate immune response depends on the coordinate activity of several effector cells, like natural killer cells, monocytes/macrophages, DC and granulocytes.

#### 3.1.2.1 Natural Killer cells

Natural Killer (NK) cells constitute one of the major lymphocyte populations, representing 5-10% of cells among peripheral blood lymphocytes (PBL). They differ from the

other lymphocytes by the absence of clonally distributed receptors derived via somatic gene rearrangement. NK cells were first described in the early 1970's by R. Kiessling and R.B. Herberman [9-12] and defined based on their functional entity, i.e. cells that are capable of recognizing and killing tumor cells without a prior exposure. Afterwards, they were described to

| **Innate subsystem** | **Primary sensors** | **Prototypical responses** |
|---|---|---|
| Mucosal epithelia | TLR and NOD proteins | Production of antimicrobial peptides<br>Production of mucins |
| Phagocytes | TLR, dectins and NOD proteins | Production of antimicrobial proteins<br>Production of cytokines: IL-1β, IL-6 and TNF |
| Acute-phase proteins and complement system | Collectins, pentraxins and ficolins | Lysis or opsonization of pathogens<br>Chemotactic attraction of leukocytes |
| Inflammasomes | NALP and NAIP | Production of IL-1-family members<br>Apoptosis of infected host cells |
| NK cells | ND | Apoptosis of infected host cells |
| Type-I-IFN-induced antiviral proteins | RIG-I, MDA5, DAI and TLR | Induction of an antiviral state<br>Apoptosis of infected host cells |
| Eosinophils and basophils | ND | Contraction of smooth muscle<br>Production of mucins<br>Peristalsis<br>Production of biogenic amines<br>Production of cytokines: IL-4, IL-5, IL-9, IL-13 and TNF |
| Mast cells | ND | Contraction of smooth muscle<br>Production of mucins<br>Peristalsis<br>Production of biogenic amines<br>Production of cytokines: IL-4, IL-5, IL-9, IL-13 and TNF |
| **ND, not determined** | | |

**Table 3.1.** Subsystems of the innate immune system. (Adapted from R. Medzhitov, Nature, 2007 )

have a large granular lymphocyte morphology [13]. Phenotypically, they are defined as $CD3^-CD56^+$ cells in humans [14], and can be further divided into two subpopulations, the $CD56^{bright}CD16^-$ subset, which can be found mainly in the LN and produces high amounts of cytokines, and the $CD56^{dim}CD16^+$ subset which is found predominantly in the blood and is cytolytic. There are indications that $CD56^{bright}$ NK cells could be precursors of the $CD56^{dim}$ subset [15]. In mice, depending on the strain, the combination of $CD3^-NK1.1^+$ or $CD3^-DX5^+$ is commonly used to identify NK cells. Recently, NKp46 (CD335) has been described to be uniquely expressed on NK cells of various species, including human and mice [16]. Importantly, NKp46 is not expressed on NKT cells, a population that shares many common markers with NK cells, such as NK1.1. NKp46 appears early during NK cell development, so it can be used to characterize NK cells of different maturation stages.

Stages of NK cell development have been described based on phenotypical and functional analysis [17]. Committed NK cell progenitors express CD122 and no other lineage-specific markers (stage I). Subsequently, immature NK cells express NK1.1 – only on the C57BL/6 strain – (stage II) followed by the acquisition of the whole repertoire of activating and inhibitory receptors of the CD94-NKG2 and Ly49 families (stage III). DX5 appears on stage IV and NK cell maturation is completed with the expression of the markers CD11b and CD43, which accompanies acquisition of cytotoxicity and the ability to produce cytokines (stage V). In mice, it has been reported that the mature $CD11b^{high}$ NK cell population can be further distinguished into two phenotypically and functionally distinct subsets based on the expression of the marker CD27 [18]. The $CD11b^{high}CD27^{high}$ NK cell population exhibited enhanced effector functions, i.e. higher cytotoxic ability and enhanced IFN-γ production upon stimulation with IL-12 and IL-18 *in vitro*, when compared to the $CD11b^{high}CD27^{low}$ NK cell subset. In addition, $CD11b^{high}CD27^{high}$ NK cells specifically expressed the chemokine receptor CXCR3 and possessed higher proliferating activity [18]. Similar subdivision was also proposed for human NK cells [19]. Stimulation of NK cells with CD27 ligand (CD70) artificially expressed on tumor cells could enhance proliferation and IFN-γ production of freshly isolated NK cells and potentated the rejection of MHC class I-deficient tumor cells via perforin- and IFN-γ- dependent mechanisms [20].

NK cells require interaction with bone marrow stromal cells for functional maturation [21,22]. Their development is mainly independent of the thymus, since they appear in normal numbers and function in athymic (nude), SCID and, $RAG1^{-/-}$ and $RAG2^{-/-}$ mice. Nevertheless,

there is accumulative evidence that not all of the NK cells derive from a unique peripheral pool. 'Bipotent' NK cell – T cell progenitors have been described in the thymus in both humans and mice [23-25]. Mouse thymic NK cells were shown to be different from BM NK cells, with regards to higher expression of GATA-3 and CD127 (IL-7Rα) and to their preferential homing to the lymph nodes. They exhibited low cytotoxic ability and high IFN-γ production, resembling the $CD56^{high}CD16^{-}$ human NK cell subset [26]. Mouse liver contains a NK cell subset, which does not express the DX5 marker and constitutively expresses TRAIL. This effector molecule may be involved in the immunosurveillance of liver tumors [27]. In addition, a $CD34^{+}$ subset which can differentiate into the $CD56^{bright}$ NK cell subset was identified in human LN [28].

There are various mutations described causing impairment of NK cell numbers and/or function. Lists of genes coding for different transcription factors, surface receptors or cytokines leading to such impairments are shown in Tables 3.2-3.4.

| Gene deleted | Effect | Reference |
|---|---|---|
| **Ikaros** | **NK cells absent** | **29, 30** |
| **PU.1** | **NK cell number decreased, normal lytic function** | **31** |
| **Ets-1** | **NK cell number decreased, decreased lytic function** | **32** |
| **Id2** | **NK cell number decreased or absent, reduced lytic function** | **33, 34** |
| **TCF-1** | **Altered acquisition of Ly49s** | **34, 35** |
| **IRF-1** | **NK cell number decreased, lytic function impaired** | **36, 37** |
| **IRF-2** | **NK cell number decreased, lytic function impaired** | **38** |

**Table 3.2.** Transcription factor deficiencies leading to NK cell impairments.

| Gene deleted | Effect | Reference |
|---|---|---|
| **LTβr** | **NK cells severely decreased** | **39** |
| **$LT\alpha_1\beta_2$** | **NK cells severely decreased, reduced lytic function** | **40, 41, 42** |
| **IL-15Rα** | **NK cells severely decreased** | **43** |

| | | |
|---|---|---|
| **IL-2/15Rβ** | **NK cells absent** | **[44, 45]** |
| **c-kit** | **NK cells decreased, impaired lytic function** | **[46]** |

**Table 3.3.** Surface receptor deficiencies leading to NK cell impairments.

| Gene deleted | Effect | Reference |
|---|---|---|
| **IL-15** | **NK cells absent, no lytic function** | **[47, 48]** |
| **Flt3-ligand** | **NK cells severely decreased, impaired lytic function** | **[49]** |

**Table 3.4.** Cytokine deficiencies leading to NK cell impairments.

#### *3.1.2.1.1 NK cells and tumor*

NK cells were the first cells shown to effectively eliminate tumor cells from the circulation of mice [50,51]. Mice with an autosomal mutation called *beige* lack NK cells, and are more susceptible than normal mice to tumor growth following injection with live tumor cells [52]. Likewise, humans suffering from the Chediak-Higashi syndrome, an autosomal recessive disorder associated with impairment in neutrophils, macrophages and NK cells, have an increased incidence of lymphomas [53].

NK cells, unlike $CD8^+$ T cells, do not require expression of MHC class I determinants for recognition of target cells. In fact, there is an inverse relationship between expression of MHC class I and susceptibility to lysis by NK cells. This observation is the milestone for the 'missing self hypothesis' [54], describing that cells which have normal expression of MHC class I molecules are not lysed by NK cells, while if self is absent, NK cells are activated to lyse the abnormal cells. Reduced MHC class I expression is often observed in virus-infected cells and tumor cells, which downregulate MHC class I expression as a mechanism to escape $CD8^+$ T cell-mediated lysis. Thus, NK cells can kill virus-infected or transformed cells [55] and are especially effective at killing cells with low MHC class I expression [54,56]. More recent studies confirmed the importance of NK cell cytotoxicity – mediated via perforin – against MHC class I-deficient tumors *in vivo* [57-59]. Besides perforin, NK cells can express death ligands, i.e. CD95L, TNF-α and TNF-related apoptosis-inducing ligand (TRAIL), via which they can induce apoptosis to their targets [60-62].

The more recent concept about NK cell recognition of targets involves a set of activating receptors which stimulate NK cell functions, in addition to the inhibitory receptors, which sense

the absence of MHC class I [63,64]. The dynamic balance between these activating and inhibitory signals controls NK cell activation (Figure 3.2).

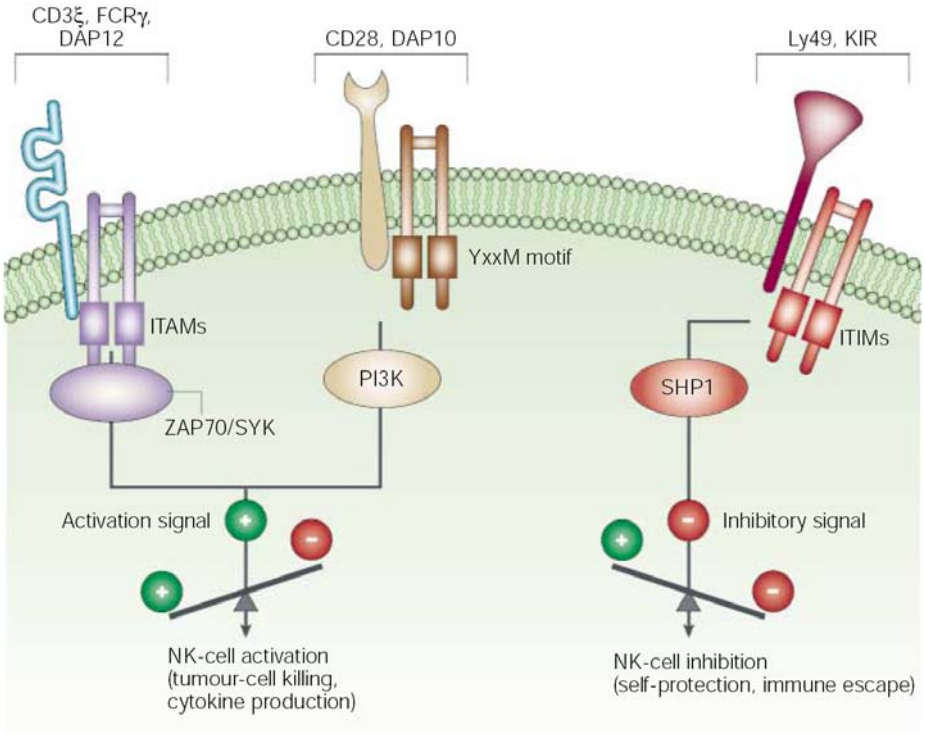


**Figure 3.2.** Control of NK cell functions by the balance of activating and inhibitory signals (Smyth MJ *et al*. *Nature Reviews Cancer* **2**, 850-861).

NKG2D is an example of an activating receptor expressed on human and mouse NK cells that recognize a diversity of ligands, including the RAE-1 family (α, β, γ, δ and ε), H60 and MULT-1 in the mouse and the MICA and ULBP families in humans [65,66]. NKG2D ligands are not expressed on the surface of normal cells, but their expression is induced in virally infected, stressed and DNA damaged cells [65-68]. In tumor cell lines that fail to express NKG2D ligands, ectopic expression of RAE-1 leads to their elimination *in vivo* [69,70]. Moreover, NKG2D neutralization led to increased incidence of methylcholanthrene (MCA)-induced fibrosarcomas [71]. Finally, increased incidence of tumors was observed in NKG2D-deficient mice [72].

Although tumors quite often bear recognition structures for NK cells, they might escape NK cell killing by desensitizing the receptor via soluble ligands released by the tumor cells, as in the case of the NKG2D pathway; in individuals with epithelial derived tumors, soluble, surface-shed MICA was detected in the sera and resulted in down-regulation of NKG2D and subsequent impairment of NK cell cytotoxicity [73]. In cancer patients, NK cell function was shown to be

impaired, as determined by reduced proliferation, response to IFN and cytotoxicity after *ex vivo* isolation of the cells [74,75]. Nevertheless, in a 11-year follow-up study of a Japanese population, medium and high cytolytic function of peripheral blood NK cells was associated with reduced cancer risk, while low cytolytic function was associated with increased cancer risk [76].

Several studies aim at improving the anti-tumor effect of NK cells for cancer immunotherapy. These approaches include endogenous activation of NK cells via the administration of cytokines [77-79] or adoptive transfer of *ex vivo* expanded and activated NK cells [80,81]. Unfortunately, the application of IL-2 for the activation of NK cells has been controversial because of its accompanying toxicity *in vivo*. In addition, adoptive immunotherapy of cancer with systemic administration of autologous NK cells has also proven to be not so successful, as the cells are difficult to expand and localize poorly to the tumors. Based on this observation, it is necessary to develop alternative approaches to enhance anti-tumor immunity.

#### *3.1.2.1.2 NK cells as regulatory cells*

Besides their ability to lyse target cells, an important function of NK cells is the production of cytokines, such as IFN-γ, TNF-α and GM-CSF. In the past few years, evidence for a role for NK cells in promoting adaptive immune responses via their interaction with DC has been reported [82-87]. These data have provided a new appreciation for the interrelated nature of innate and adaptive immunity. NK cells were shown to kill immature DC, despite high expression of MHC class I [83]. It has also been described that NK cells with an immature phenotype were found in increased numbers in a leukemia mouse model and these immature NK cells could suppress DC functions, rather than killing them, by down-regulating the expression of I-$A^d$ or inhibiting allo-T cell stimulatory activity [88]. During early pregnancy in humans and rodents, c-kit$^+$CD25$^+$CD122$^+$CD16$^-$CD56$^{bright}$ NK cells and Thy-1$^+$NK1.1$^+$asialo-GM1$^+$ cells, respectively, were reported to accumulate in the uterine deciduas [89,90]. These uterine NK cells produce TGF-β1 and are thought to have immunoregulatory functions [91-93]. Finally, NK cells are thought to play an immunoregulatory role in the prevention of autoimmune diseases, as autoimmune condition is typically deteriorated when there are NK cell defects [94].

### 3.1.2.2 Macrophages

Macrophages originate from the common myeloid progenitor in the bone marrow. They are then released in the blood where they differentiate into mature monocytes, comprising ~5% of peripheral blood leukocytes. When monocytes migrate into the tissues, they eventually differentiate into tissue-specific macrophages. This process is accompanied by several changes: increase in size, increase in number and complexity of organelles, acquisition of phagocytic ability and secretion of various soluble factors. Macrophages serve different functions in various tissues, such as alveolar macrophages in the lung, histiocytes in connective tissues, Kupffer cells in the liver, mesangial cells in the kidney, microglial cells in the brain and osteoclasts in the bones.

Monocytes/macrophages are identified by the expression of CD14 marker in humans and F4/80 marker in mice [95]. In addition, macrosialin or CD68, a lysosomal marker, can be used to identify all tissue macrophages of both mouse and human origin [96]. Nevertheless, peripheral blood monocytes are not a homogeneous population and they can be divided into two functional subsets in mice; a $CX_3CR1^{low}CCR2^{+}Gr\text{-}1^{+}$ 'inflammatory subset' which has a short half-life and is actively recruited to inflamed tissues, and a $CX_3CR1^{high}CCR2^{-}Gr\text{-}1^{-}$ 'resident subset' which has a longer half-life and is recruited to non-inflammed tissues in a $CX_3CR1$-dependent manner [97]. Both subsets have the potential to differentiate *in vivo* into DC. In addition, the level of expression of CX3CR1 correlates with the two described monocyte subpopulations in humans, the $CD14^{+}CD16^{-}$ and $CD14^{low}CD16^{+}$ subsets, resembling the murine inflammatory and resident subsets, respectively.

Macrophages can be activated via various stimuli during an immune response, which determine their subsequent phenotype. Macrophage activation can be triggered via TLR pathways (see Table 1.1) and/or cytokines secreted by lymphocytes, the most potent of which is IFN-γ [98]. Activation of macrophages via LPS, a ligand for TLR4, and IFN-γ leads to the 'classically' activated macrophages, also known as M1, which are linked to the response to intracellular pathogens and promote Th1 responses. They are characterized by their ability to secrete significant amount of proinflammatory cytokines, such as IL-1β, IL-15, IL-18, TNFα and IL-12, and the enhanced expression of MHC class II and co-stimulatory molecules CD80 and CD86 [95]. By contrast, an 'alternative' activation pathway has also been described. Such macrophages are associated with parasitic infections, allergic and humoral responses [99]. More recently, the alternatively activated macrophages or M2 have been further subdivided into 3

categories depending on the activation trigger: M2a macrophages arise after exposure to IL-4 or IL-13, M2b macrophages after engagement of Fcγ receptors in combination with IL-1β or LPS, and M2c macrophages are induced by IL-10, TGF-β or glucocorticoids [95]. The activation pattern of macrophage populations in tumors is not so well defined, but in some cases it bears similarities with the alternative activation phenotype.

Activated macrophages can produce cytotoxic substances which can be divided into oxygen-dependent and oxygen-independent. Oxygen-dependent substances include the reactive oxygen intermediates, such as hydrogen peroxide ($H_2O_2$) and the reactive nitrogen intermediates, such as nitric oxide (NO). NO is produced by the enzyme inducible nitric oxide synthase (iNOS) via the following reaction:

L-arginine + $O_2$ + NADPH $\rightarrow$ **NO** + L-citrulline + NADP

The oxygen-independent substances include various hydrolytic enzymes, such as lysozyme, various antimicrobial and cytotoxic peptides, known as defensins, and cytokines, such as TNF-α.

Only a limited number of mutations which lead to macrophage deficiency have been described. In the osteopetrotic op/op mouse, a naturally occurring mutation of the gene coding for colony stimulating factor (CSF)-1 leads to differential deficiency of various macrophage subpopulations, dividing the macrophage lineage into CSF-1-dependent and CSF-1-independent [100]. The PU-1 knockout mouse, in contrast, was artificially generated [101]. PU.1 is a transcription factor specifically expressed in hematopoietic cells. Homozygosity for the mutant gene leads to lethality in mice in the prenatal stage; nevertheless, analysis of embryos up to day 18 of gestation revealed that no macrophages could be detected in these mice. The development of liposome-encapsulated clodronate (dichloromethylene diphosphonate) is the most commonly used method to eliminate macrophages *in vivo* [102].

#### *3.1.2.2.1 Tumor associated macrophages*

The tumor microenvironment has many factors that can recruit and differentiate the infiltrating macrophages, which are defined as tumor-associated macrophages (TAM) [103]. TAM quite often represent the major infiltrating cell population of various tumors, and can exert tumor promoting or tumor suppressing functions.

TAM isolated from mice bearing mammary tumors were shown to be poor producers of NO and exhibited low cytotoxic ability [104]. In addition, macrophages positive for iNOS were

rarely found in human ovarian cancer and were only localized in the periphery [105]. Induction of angiogenesis by the production of angiogenic factors such as vascular epithelial growth factor (VEGF) and platelet-derived endothelial cell growth factor (PD-ECGF) has often been linked with the TAM. In breast cancer patients, TAM density positively correlated with VEGF expression and microvessel density, while all of them negatively correlated with disease-free survival [106]. TAM have been shown to express high levels of both the scavenger receptor A [107] and the mannose receptor [95], which is compatible with the M2 macrophage phenotype.

On the other hand, TAM have the potential to directly control tumor cell proliferation when appropriately stimulated, and thus exert tumor suppressing functions. In two murine models of melanoma, engineered to produce granulocyte/macrophage-CSF (GM-CSF), macrophage density inversely correlated with tumorigenicity; these macrophages produced macrophage metalloelastase (MME or MMP-12) and angiostatin, which suppressed the growth of metastases [108]. MHC class II-negative myeloma cells injected into mice were readily infiltrated by macrophages and were crucial in inhibiting tumor growth after activation by $CD4^+$ T cell-derived IFN-γ [109]. Finally, CpG-oligodeoxynucleotide treatment allowed the control of weakly immunogenic tumors, such as the B16 melanoma and the NXS2 neuroblastoma by macrophages [110].

#### *3.1.2.2.2 Myeloid-Derived Suppressor Cells*

In cancer patients and tumor-bearing mice, a subpopulation of myeloid cells, characterized as myeloid-derived suppressor cells (MDSC), myeloid suppressor cells (MSC) or immature myeloid cells (iMC), has been described to accumulate and exert immunosuppressive function [111,112]. MDSC represent a heterogeneous population of myeloid cells comprising of immature macrophages, granulocytes and DC; the addition of cytokines is able to differentiate these cells into mature macrophages, granulocytes or DC *in vitro* [113]. In mice, MDSC are identified by the expression of the markers CD11b and Gr-1, while other markers have also been described for this population, such as CD31 [113], CD115 [114] and CD124 [114]. Interestingly, this population can be detected in low numbers also in the BM, blood and spleen of healthy mice, lacking however immunosuppressive function. Human equivalent MDSC were originally described in patients with head and neck cancer as $CD34^+$ cells [115]. Afterwards, they were also characterized in the peripheral blood of patients with squamous cell carcinoma, non-small cell lung cancer and breast

cancer [116]. Human MDSC also exhibit an immature phenotype, as shown by the expression of the markers CD34, CD33, CD13 and the absence of CD15.

Accumulating findings suggest that tumor-derived factors are responsible for the generation of MDSC. Conditioned media from tumor cell lines could inhibit the differentiation of DC from their precursors *in vitro* [117]. In addition, immunosuppressive cells arose from bone marrow cells after culture with Lewis lung carcinoma S/N [118]. MDSC expansion in tumor-bearing hosts has been correlated with T cell dysfunction. Indeed, it was shown that MDSC induce decrease or loss of the expression of the TCR ζ chain [119], inhibit the CD3/CD28-induced T cell proliferation by the production of nitrogen and oxygen intermediates [120] as well as the $CD8^+$ T cell IFN-γ production [121]. Recently, it was shown that MDSC suppress IL-2-mediated NK cell cytotoxicity via interfering with Stat5 activation [122]. For this purpose, depletion of MDSC in therapeutic settings is under investigation. In mice, an anti-Gr-1 mAb has been used to deplete MDSC and enhance anti-tumor responses [123]. However, a similar treatment is difficult to be applied in humans, since total granulocyte depletion removes also neutrophils which could render the individual susceptible to infections.

### 3.1.3 The adaptive immune system

The two main components of the adaptive immune system are B and T lymphocytes. B cells constitute part of the humoral-mediated response which specializes in the recognition and elimination of the extracellular pathogens, while T cells generate cell-mediated immune responses which target the intracellular pathogens. B lymphocyte maturation takes place within the bone marrow and is accompanied by the acquisition of a unique antigen-binding receptor on their surface, called the B cell receptor (BCR); the BCR constitutes a membrane-bound antibody. Upon antigen encounter, B cells differentiate into memory and effector cells, called plasma cells; the latter produce antibodies in a secreted form.

T lymphocytes also arise in the BM but, subsequently, migrate to the thymus for their maturation. During their maturation, T cells express a unique antigen binding molecule, the T cell receptor (TCR). Both the BCR and TCR are products of somatic gene rearrangement during maturation. The genes encoding these receptors are assembled from variable and constant fragments through recombination activation gene (RAG) protein-mediated somatic recombination. However, the TCR in contrast to the BCR can only recognize antigen bound to

MHC molecules. T cells are distinguished by the presence of either CD4 or CD8 membrane glycoproteins on their surface. The $CD4^+$ T cells recognize antigens in the context of MHC class II molecules on the surface of antigen-presenting cells, while the $CD8^+$ T cells recognize antigens presented by MHC class I molecules found on all cells of a healthy individual. After a $CD4^+$ T cell recognizes and interacts with a MHC class II-peptide complex, it is activated and secretes various cytokines, which play an important role in activating other immune cells, as B cells, $CD8^+$ T cells, macrophages, etc. Thus, $CD4^+$ T cells play a central role in both humoral and cell-mediated immunity. $CD8^+$ T cells exhibit high cytotoxic activity upon activation and act on eliminating potentially dangerous cells, like virus-infected cells, tumor cells or cells of a foreign tissue graft.

Besides the conventional B and T cells, adaptive immunity encompasses the so-called innate-like lymphocytes, i.e. the B1 cells, the marginal-zone B cells, natural killer T (NKT) cells and subsets of γδ T cells; the diversity of antigen receptors expressed by these cells is restricted and not entirely random and their specificities are skewed towards a predefined set of ligands [124].

In certain individuals, the discrimination of self from non-self malfunctions, leading to an immune attack upon the host, a condition termed as autoimmunity. During an autoimmune response, self-reactive clones of B or T cells are activated, generating humoral or cell-mediated responses against self-antigens. Normal healthy individuals are believed to possess self-reactive lymphocytes [125,126]. However, since the presence of these cells does not necessarily lead to autoimmunity, mechanisms which regulate their activity exist.

#### 3.1.3.1 Mechanisms of T cell tolerance

Random rearrangement of the TCR genes generates an enormous TCR repertoire, leading to specificities which in theory could also recognize soluble antigens, self antigens or antigens presented in non-self MHC molecules. Positive selection of T cells in the thymus ensures that TCR expressed on mature T cells will bind only to self MHC molecules; the T cells that fail to do so are eliminated by apoptosis. In a second step termed negative selection, T cells bearing a high-affinity receptor for self antigens presented in self MHC are also eliminated. This selection procedure leads to the apoptosis of ~98% of all T cells in the thymus and ensures the generation of T cells, which are self-MHC restricted and self-tolerant. B cell progenitors undergo a similar process in the BM. This control of self-responsiveness that occurs during lymphocyte

development in the central lymphoid organs is known as central tolerance [127]. One constraint of central tolerance is the requirement for the autoantigens to be present in the thymus. Although many tissue-specific antigens are represented in the thymus, at least at the mRNA level [128], whether or not they are expressed as proteins at levels sufficient to induce T cell deletion is not clear. In fact, healthy individuals have been shown to harbor self-reactive T cells in the periphery [125,126] and these T cells are more likely to bear a low-affinity TCR for self-antigens [129]. Mechanisms of peripheral tolerance protect us from these escaping self-reactive clones.

In the periphery, recognition of a peptide–MHC complex on an APC can result either in the activation and clonal expansion of the T cell or in some cases in a state of non-responsiveness called anergy. In contrast to central tolerance, anergy does not lead to the apoptosis of the T cell but allows its survival in the periphery for an extensive period of time in a hyporesponsive state. Whether a T cell will be activated or subjected to anergy in the presence of peptide-MHC complex is determined by the presence or absence of sufficient co-stimulatory signals, delivered through the CD28-B7-1/2 interaction [130], or the ligation of ligands like the cytotoxic T lymphocyte associated antigen 4 (CTLA-4), a homologue of CD28 with inhibitory function [131]. Dendritic cells (DC) have emerged as key APC in this process, regulating immunity versus tolerance. In fact, immature DC have been described to inhibit T cell responses, and are thus characterized as tolerogenic DC [132]. This second level of control which regulates the responsiveness of mature lymphocytes against unwanted responses to self in the periphery is known as peripheral tolerance [133,134].

In addition to the mechanisms of clonal deletion and anergy that physically eliminate or functionally inactivate potentially hazardous self-reactive lymphocytes, other mechanisms of tolerance include T cell ignorance of self antigens and the phenotype skewing. T cell ignorance occurs either because the antigen is expressed in sites not easily accessible to T cells or because the amount of antigen does not reach the threshold required to trigger a T cell response [135]. In the phenotype skewing, effective tolerance might be maintained, even in the presence of an active immune response, depending on the nature of the response. Th2 cytokines, in particular, have been linked with downregulation of autoimmunity in experimental autoimmune encephalomyelitis [136] and diabetes [137].

Finally, there is accumulating evidence that a subset of $CD4^+$ T cells, named regulatory T cells, actively suppresses the activation and expansion of self-reactive T cells, thereby preventing autoimmune diseases [138-140].

### 3.1.3.2 Regulatory T cells

Naturally occurring regulatory T cells (Treg) constitute 5-10% of all $CD4^+$ T cells and possess potent ability to suppress immune cell effector functions in *in vitro* functional assays. They are present in the normal thymus, as a functionally mature and distinct T cell subpopulation [141,142]. Thus, Treg are already specialized for suppressive function before antigen encounter. This differentiates them from other types of regulatory T cells, such as Tr1 and Th3 cells, which under certain conditions arise in the periphery from naïve T cells following antigen exposure; these are termed induced Treg (iTreg), in contrast to the naturally occurring Treg (nTreg), which arise from the thymus [143,144]. The TCR repertoire of Treg is broad and more diverse than the one of the naïve T cells, however, more self-reactive than other T cells [145,146]. They appear to either escape thymic deletion or may indeed be positively selected as part of an 'anti-self' repertoire. This may explain why some Treg are in a more proliferative state than other T cells in the periphery of normal animals, presumably due to the recognition of self-antigens [147]. Treg do not produce pro-inflammatory cytokines upon antigenic stimulation and therefore do not harm the host, despite their high self-reactivity [148,149]. Naturally occurring Treg are widely believed to exert their suppressive effect in a contact-dependent manner, in contrast to induced Treg which exert their suppressive function via cytokines, despite the fact that controversy has emerged from *in vivo* data, where in various models nTreg were shown to act through cytokine-dependent manner [150-152].

#### *3.1.3.2.1 Phenotypic characterization of Treg*

Treg are characterized by the expression of cell surface markers, which are usually also found on activated T cells, like the α chain of the IL-2R (CD25), the glucocorticoid-induced TNF-receptor family-related gene/protein (GITR) and the cytotoxic T-lymphocyte-associated antigen-4 (CTLA-4, CD152). Currently, the most specific and reliable molecular marker for the identification of Treg in rodents and humans is the transcription factor Foxp3, which is expressed in a highly Treg-specific manner and controls the development and function of Treg [153-155]. Although Foxp3 expression is more restricted to $CD4^+$ Treg identified in mice, human Foxp3 expression is not as restricted as the mouse counterpart; several reports document its expression in effector T cells upon activation, although at a relatively lower level when compared to Treg [156-162]. Retroviral transduction of mouse Foxp3 to mouse $CD4^+CD25^-$ T cells can convert them to

Treg-like cells, both phenotypically and functionally [153,154]. Surprisingly, when human Foxp3 and/or Foxp3δ2, an isoform of Foxp3 present on human Treg, are ectopically overexpressed in human $CD4^+$ T cells, it does not lead to the acquisition of significant suppressor activity *in vitro* [163], suggesting that the mouse and human Foxp3 may have some differences.

The gene *foxp3* was identified as the defective gene in the *Scurfy* mouse strain, which has a X-linked recessive mutation leading to lethality in hemizygous males or homozygous females within a month after birth [164]. Mutations of the human gene FOXP3, the ortholog of the murine f*oxp3* gene, were subsequently found to be the cause of the Immune dysregulation, Polyendocrinopathy, Enteropathy, X-linked immunodeficiency (IPEX) syndrome, which leads to the development of organ-specific autoimmune diseases, inflammatory bowel disease (IBD), allergic dermatitis, food allergy, hematological disorders, hyperimmunoglobulinemia E, and serious infections [165,166]. Although IPEX is a rare disease, its clinical picture and its causative factor as a deficiency or malfunction of Treg underlies the role of Treg in maintaining immunologic self-tolerance.

Recent analysis of Foxp3-reporter mice and intracellular staining of the Foxp3 protein revealed a correlation between the ontogeny of CD25-expressing Treg and Foxp3-expressing T cells [167]. This analysis confirmed the finding that natural Treg become detectable in the periphery of normal mice a few days after birth and thymectomy around day 3 after birth abrogates the thymic production of natural Treg from the beginning of their ontogeny [168]. There is substantial evidence that CD25 is not a mere indicator of the chronically activated state of Treg, but is a functionally essential molecule for their survival and function. For example, IL-2, IL-2Rα (CD25) and IL-2Rβ (CD122) deficiencies produce similar fatal lymphoproliferative inflammatory disease, as the Foxp3 deficiency, with autoimmune components, generally characterized as 'IL-2 deficiency syndrome' [169-173]; while deficiency of the common γ chain completely abrogates the development of the other T cells as well. In addition, neutralization of circulating IL-2 resulted in selective reduction of $CD4^+CD25^+Foxp3^+$ T cells in the thymus and periphery. These findings collectively indicate that the IL-2 and transcription factor Foxp3 are key control molecules for the development and function of natural $CD4^+CD25^+$ Treg. Since Foxp3 is a nuclear factor, the combination of CD4 and CD25 markers have been more commonly used for the isolation or depletion of Treg.

#### *3.1.3.2.2 Treg and autoimmunity*

Treg play an indispensable role in the mechanism of self-tolerance, since depletion of these cells from normal animals by the use of a mAb directed against CD25 leads to the spontaneous development of various autoimmune diseases, such as autoimmune gastritis, thyroiditis, type I diabetes (TID) and IBD; reconstitution of the animals with normal $CD4^+CD25^+$ T cells prevents these disorders [174,175]. In addition, the incidence of autoimmune disease in IPEX patients, which have a mutated Foxp3 gene, is approximately 90%, with approximately 80% incidence of TID within a year after birth [176]. Some patients, in fact, already manifest the disease at the time of birth [176]. The high incidence of autoimmune disease in IPEX patients suggests that most of normal individuals may harbor potentially pathogenic self-reactive T cell clones, capable of mediating common autoimmune diseases. This is an indication that dominant self-tolerance is physiologically operating in humans as well as rodents with the purpose of preventing autoimmune disease.

Treg not only inhibit autoimmune responses but also suppress a variety of immune responses to non-self antigens. Depletion of $CD4^+CD25^+$ T cells from animals enhances immune responses to microbes, triggers allergic responses and breaks feto-maternal tolerance during pregnancy. In addition, depletion of Treg provokes effective tumor immunity to autologous tumor cells in otherwise nonresponding animals [138]. Conversely, natural Treg can be exploited to treat autoimmune diseases and to establish immunologic tolerance to non-self antigens as in organ transplantation.

#### *3.1.3.2.3 Treg and tumor immunity*

Although Treg play a crucial role in preventing autoimmunity by inducing immune tolerance, they might inhibit anti-tumor immunity and promote tumor growth by suppressing host immune responses against non-self antigens. Sakaguchi and colleagues first demonstrated that the removal of $CD4^+CD25^+$ T cells can induce antitumor responses, establishing a 'common basis' between tumor immunity and autoimmunity [177]. In later studies, many groups reported elevated percentages of $CD4^+CD25^+$ Treg in the total T cell population isolated from tumor tissues or peripheral blood in a variety of cancers, including lung cancer [178], breast cancer [179], ovarian cancer [180], melanoma [181], liver cancer [182], gastric cancer [183] and lymphoma [184]. From these studies, two are of a particular interest. Curiel *et al*. reported that Treg preferentially accumulate

in ovarian tumors and in malignant ascites attracted by CCL22 and that the high percentage of Treg is associated with the poor prognosis of cancer patients [180]. This study suggests that Treg may mostly interfere with the function of effector T cells and not so much with their priming phase. Viguier at al., on the other hand, found higher accumulation of Treg in the draining lymph nodes infiltrated by melanoma cells, suggesting that Treg contribute to the local immunosuppressive milieu [181]. Increasing number of evidence indicates that Treg in the tumor microenvironment inhibit anti-tumor immunity, which represents a major obstacle for developing effective therapeutic cancer vaccines.

#### *3.1.3.2.4 Treg and innate immunity*

The suppressive effect of Treg on the adaptive responses mediated by T cells is well documented. However, the effect of Treg on cells of the innate immune system is less well studied. A potential role for Treg in dampening NK cell functions was first suggested by Sakaguchi in a murine leukemia model [177]. More recently, it was reported that Treg depletion *in vivo* led to the rejection of NK cell sensitive cell lines expressing RAE-1, the ligand for the activating receptor NKG2D [69,70] *in vivo* [185,186]. *In vitro*, NK cell cytotoxicity was largely inhibited by Treg through a TGF-β-dependent and IL-10-independent mechanism [185,186]. These studies suggest that Treg directly inhibit NK cell activation towards NKG2D ligand-expressing targets *in vitro* and *in vivo*. In another recent study, Treg could induce NK cell death in a granzyme B- and perforin-dependent manner [187]. In a model of hybrid resistance during allogeneic BM transplantation, Treg removal significantly enhanced NK cell-mediated BM graft rejection [188].

It has been proposed that Treg can directly suppress monocyte/macrophage activation and their effector functions *in vitro*. Pre-incubation of human blood monocytes with Treg or the presence of Treg in the monocyte culture impaired cytokine production [189,190] and the upregulation of HLA II, CD40 and CD80 activation markers by monocytes upon LPS stimulation [190]. Kryczek *et al.* reported upregulation of the inhibitory molecule B7-H4 on isolated human monocytes mediated by Treg [191]. In addition, B7-H4 expression on macrophages infiltrating ovarian tumors inversely correlated with the patients' survival [192]. The ability of Treg to steer monocyte differentiation towards an alternative activated phenotype, marked by an upregulation of CD206 and CD163 markers, was also demonstrated *in vitro* [193]. In addition to macrophages, one study provided data that Treg could inhibit reactive oxygen intermediates and cytokine

production by neutrophils, although this phenomenon was only observed after *in vitro* treatment of both Treg and neutrophils with LPS [194]. Finally, in a model of acute *in vivo* ablation of Treg, it was observed that various types of innate immune cells, including $NK1.1^+$ cells and macrophages ($F4/80^+CD11c^-$ cells) increased in numbers in the secondary lymphoid organs after Treg ablation [195]. Nevertheless, it is possible that Treg do not exert their suppressive effect on innate immune cells via direct interaction but in an indirect manner as visualized for T cells. Treg inhibited the activation of autoreactive T cells in the LN by impeding the formation of stable contacts between T cells and DC [196,197].

#### *3.1.3.2.5 Manipulation of the suppressive function of Treg*

Given the observations that Treg exercise a negative role in tumor immunity, a key question in cancer immunotherapy is how to eliminate or to reverse the suppressive function of Treg. Cyclophosphamide is a chemotheurapeutic agent with anti-mitotic action, used to treat various types of cancer. High doses of this drug lead to immunosuppression, the basis of other clinical uses, as preventing organ rejection in organ transplantation [198,199]. Low doses of this drug, however, lead to enhanced immune responses against a variety of antigens [200,201]. The chemotherapeutic activity of cyclophosphamide was readily linked with the elimination of tumor-induced suppressor T cells [202,203] and later, namely, with its effect on Treg. Controversy still exists, however, on whether cyclophosphamide solely decreases Treg cell numbers [204], interferes with their suppressive function [205] or influences both numbers and suppressive ability [206], and on the mechanism of action. Another approach used in clinical studies is the administration of an anti-CTLA-4 mAb; however, the antitumor effects of CTLA-4 blockade were shown to be due to increased T cell activation rather than inhibition or depletion of the CTLA-4-expressing Treg [207,208]. Presently, several investigators are targeting the specific elimination of Treg with a fusion protein of diphtheria toxin and the IL-2 cytokine (ONTAK, Denileukin diftitox, $DAB_{389}$IL-2). Administration of ONTAK could efficiently eliminate CD25-expressing Treg and yielded effector functions in patients with melanoma or renal cancer [209,210]. Another recombinant immunotoxin, LMB-2, has been used for the same purpose. LMB-2 is a fusion of a single-chain Fv fragment of the CD25-specific, anti-Tac mAb to a truncated form of the bacterial Pseudomonas exotoxin A, which has been shown to selectively eliminate human Treg *in vitro* without impairing the function of the remaining lymphocytes [211]. *In vivo*, the administration of

this toxin in metastatic melanoma patients before vaccination led to a transient reduction in circulating Treg numbers without augmenting, however, the efficiency of the vaccination [212].

An alternative approach to Treg depletion *in vivo* is to reverse the suppressive function of Treg. It has been demonstrated that TLR signaling activation on DC can render naïve T cells refractory to suppression mediated by Treg in mice [213]. In humans, Poly-G oligonucleotides, which are recognized by TLR8, can directly reverse the suppressive effect of Treg in the absence of DC [214]. Poly-G oligonucleotides could not reverse the suppressive activity of murine Treg [215], because TLR8 is not functional in mice. In addition, activation of TLR2 with its ligand Pam3Cys directly increased the proliferation of murine Treg and temporally reversed their suppressive function [216,217]. Other TLR ligands, however, fail to do so. Human TLR5, for example, enhanced rather than reversed the suppressive function of Treg [218]. Further studies are needed to define the role of other TLR on the function of mouse and human Treg and effector cells.

## 3.2 Type I IFN

Type I IFN are a family of glycoproteins which includes several members, namely IFN-α, IFN-β, IFN-δ, IFN-ε, IFN-κ, IFN-τ, IFN-ω and IFN-ζ, also known as limitin [219]. All the members bind to the same receptor complex known as the IFN-α receptor (IFNAR), which constitutes of two subunits, the IFNAR1 and the IFNAR2 [220]. 13 isoforms have been described for IFN-α, and one for IFN-β, -ε, -κ, -τ and -ζ; although IFN-ω has only one functional form, several pseudogenes have been identified. Type I IFN and IFN-induced proteins have a crucial role in the defense against viruses and are unique in vertebrates. They are produced in response to viral infections by many cell types, including lymphocytes, macrophages, fibroblasts, endothelial cells, osteoblasts etc. These proteins trigger the expression of more than 100 genes, the products of which have diverse antiviral activities [221]. Type I IFN can be induced early during infection, and can thus activate promptly the cells of the innate immune system such as NK cells and macrophages [222].

In principle, all virally infected cells can produce type I IFN, resulting in autocrine and paracrine IFN-mediated signaling, which confers an antiviral state on the infected and neighboring cells. Type I IFN production has been originally studied in virus-infected fibroblasts, where the role of IRF-3 and IRF-7 has been demonstrated [223,224]. Both of these factors reside in

the cytoplasm and require phosphorylation in their C-terminal region for their activation and translocation to the nucleus, where they activate their target genes. *In vivo* observations further supported the importance of these factors. *Irf3*$^{-/-}$ mice are vulnerable to encephalomyocarditis virus (EMCV) infection [225]. Subsequent generation of the *Irf7*$^{-/-}$ mice showed that these mice are more susceptible to infections of both DNA and RNA viruses, such as Herpes simplex virus (HSV)-1 and EMCV, than wt or *Irf3*$^{-/-}$ mice, establishing IRF-7 as a master regulator of type I IFN-mediated immune responses [225]. The IRF-7-dependent pathway is often referred to as the classical pathway of IFN gene induction.

Alternatively, type I IFN production can be elicited in response to viral or bacterial nucleic acids by the engagement of TLR, namely TLR3, TLR7/TLR8 and TLR9. These receptors detect viral double-stranded RNA, single stranded RNA or unmethylated CpG motifs present in microbial DNA, respectively [226,227]. An exception to this rule seems to be the IFN-β production in response to TLR4 ligands, which are not nucleic acids [7]. TLR4 is activated by LPS or the lipid A component of Gram-negative bacteria, as well as some viral components [228]. Plasmacytoid DC (pDC) can produce systemic levels of IFN-α after engagement of TLR and thus are often referred to as specialized type I IFN producing cells [229].

### 3.2.1 Regulatory effects of type I IFN

Although first characterized based on their potent antiviral functions, type I IFN can also mediate a variety of immunoregulatory effects, suggesting that they can be important links between innate and adaptive immune responses. First of all, it has been shown that type I IFN can regulate their own expression. Particular IFN genes, namely IFN-β and/or IFN-α4, are first induced in virally infected cells; the products of their target genes can then act on the neighboring cells to induce the expression of other IFN-α subtypes [224,230]. The most well known effect of type I IFN is the enhancement of antigen processing and antigen presentation via the MHC class I pathway, leading thus to an enhancement of $CD8^+$ T cell-mediated responses [231]. Type I IFN contribute to the maturation of DC and the induction of co-stimulatory molecules [232,233]. Type I IFN have been proposed to induce the expression of IL-15 [234], which has been linked with the enhanced NK cell and memory $CD8^+$ T cell proliferation early during viral infections [222,235]. In contrast, type I IFN have been shown to negatively regulate the expression of IL-12 in mice both *in vitro* and *in vivo* during infection with MCMV [236] and in human *in vitro* generated DC co-

cultured with $CD4^+$ T cells [237]. Since IL-12 is a potent stimulator of IFN-γ production, type I IFN can control the subsequent immune response. Interestingly, IFN-γ production was enhanced by type I IFN in a IL-12-independent manner during a LCMV infection [238].

Type I IFN or chemical type I IFN inducers, i.e. tilerone, or analogues of viral nucleic acids such as polyinosinic-polycytidylic acid [poly(I:C)] were shown to enhance NK cell cytotoxicity and their *in vivo* trafficking [239-241]. Only recently, however, it was clearly demonstrated – with the use of an *in vivo* mouse model of inducible depletion of DC – that type I IFN do not directly activate NK cells but rather indirectly via DC, which in turn produced and trans-presented IL-15 to NK cells *in vivo* [87]. Finally, in addition to their regulatory effects, type I IFN affect the development and homeostasis of B and T cells, DC and osteoclasts [242-244].

### 3.2.2 Type I IFN and tumor

In addition to their antiviral activity, exogenously administered type I IFN have been shown to suppress the growth of transplantable tumors of different origins as well as pulmonary metastases in mice [245-247]. Type I IFN could have a direct inhibition on tumor cell proliferation *in vitro* by promoting cell growth arrest in the G1 and S phases [248,249]. In addition, type I IFN treatment resulted in vascular endothelial cell damage that preceded tumor necrosis [250] and restored the levels of other tumor-promoting factors, such as down-regulating matrix metalloproteinase (MMP)-9 and up-regulating E-cadherin [251]. For these reasons, exogenously administered type I IFN have also been used in clinical applications for the treatment of a range of malignancies such as hairy cell leukemia, melanoma, renal cell carcinoma and Kaposi sarcoma [252]. Nevertheless, clinical success has been limited due to the short half-life of type I IFN, which is less than 5h, and the side effects from the high dose administration required for effective therapy [253,254].

Besides the well documented role of type I IFN administration for tumor treatment, there are few reports documenting a role for endogenous type I IFN in the control of tumor growth of transplantable tumors [255-257]. Although much progress has been made in understanding the mechanisms of type I IFN responses to infection and inflammation, it is less clear how type I IFN production is stimulated during an anti-tumor response, which cells produce them, which cells respond to them and what is the importance of type I IFN for anti-tumor immunity.

Recently, a role for type I IFN in tumor immunoediting has been described [258]; MCA-induced sarcomas arising in $IFNAR1^{-/-}$ mice exhibited an unedited phenotype, i.e. they were

immunogenic and were rejected in a T cell-dependent manner when transplanted into wt recipients. In addition, type I IFN have been shown to control NK cell-mediated anti-tumor responses against MCA-induced sarcomas, MHC class I deficient RMA-S tumors and cytokine immunotherapy of lung metastases [259]. Interestingly, a role for IFN-α in downregulating the recognition of tumor cells by NK cells has also been proposed by the inhibition of the expression of H60 and, to a lesser extent, of MULT1 on MCA-induced sarcoma lines from 129/Sv mice after *in vitro* culture with IFN-α [260].

# 4 AIM OF THE STUDY

In cancer patients, many tumors downregulate expression of MHC class I molecules in order to escape direct recognition by $CD8^+$ T cells, which is MHC class I restricted [261]. At the same time, these tumors become more susceptible to NK cell attack due to the lack of self MHC class I [63]. However, upon inoculation of higher tumor cell numbers, tumors escape the control of the immune system. Therefore, it is essential to define mechanisms to strengthen the immune response against a high tumor cell load and tumors with poor immunogenicity. Strategies to enhance anti-tumor immune responses include activation of anti-tumor effector functions via the administration, for example, of cytokines [262,263] or, on the other hand, the removal of suppressive signals counteracting activation.

In this regard, the aim of our study is to strengthen the immune response against a MHC class I-deficient tumor, the RMA-S lymphoma. For this purpose, the role of immunosuppressive Treg in inhibiting innate immune cell functions during the anti-tumor response *in vivo* is addressed. In order to achieve this, we experimentally remove Treg before *s.c.* inoculation of mice with RMA-S tumor cells and analyze the emerging anti-tumor effector functions.

The second part of this study deals with the role of type I IFN in the anti-tumor immunity against the RMA-S lymphoma. Type I IFN have been well characterized for their contribution in anti-viral responses [264]. In parallel, they have been extensively used in clinical practice to treat various types of cancers [265]. Few reports exist, however, documenting the production of type I IFN during an anti-tumor response as well as their contribution to the control of tumor growth. In order to pinpoint the role of type I IFN in the anti-tumor response, we are monitoring the growth of RMA-S lymphoma in mice unresponsive to type I IFN ($IFNAR1^{-/-}$ mice), and characterizing the anti-tumor mechanisms which are under their control.

# 5 MATERIALS AND METHODS

## 5.1 MATERIALS

### 5.1.1 Laboratory equipment

(listed in alphabetical order)

| **Equipment** | **Company** |
|---|---|
| Anesthesia machine, Vapor 19.1 | Drägerwerk AG |
| Beta-counter, MicroBeta TriLux 1450 LSC | PerkinElmer |
| Bio-plex array system | Bio-rad |
| Cell culture incubator, Heraeus BBD 6220 ($CO_2$ ) | Kendro |
| Centrifuge, Heraeus Multifuge 4 K-R/3 S-R | Kendro |
| Centrifuge 5415 R (table) | Eppendorf |
| Centrifuge, Sorvall Evolution RC | Kendro |
| ELISA microplate reader, GENios | TECAN |
| FACS sorter, FACSDiva | BD |
| FACS sorter, FACSVantage SE | BD |
| Flow cytometer, FACSCalibur | BD |
| Flow hood, Heraeus Hera Safe | Kendro |
| Fridge, premium | Liebherr |
| Freezer -20°C, comfort/profi line | Liebherr |
| Freezer -86°C, VIP series | Sanyo |
| Gamma-counter, Cobra auto-gamma | Packard, PerkinElmer |
| Gamma cell 1000 | Atomic Energy of Canada Ltd |
| Harvester 96-well automated, TOMTEC | PerkinElmer |
| Heat sealer | PerkinElmer |
| Ice machine | Hoshizaki |
| Incubator Shaker, Innova 4200 | New Brunswick Scientific |
| Magnetic stirrer, MR3001 K | Heidolph |
| Microscope, WILOWERT30 | Neolab |
| Microscope (Stereo Microscope) | Hund |

| | |
|---|---|
| Microscope C1Si (confocal) | Nikon |
| Minifuge, GalaxyMini | VWR |
| $N_2$ tank, CryoSystem 6000 | MVE |
| pH meter | WTW |
| Photometer, Ultraspec 3100 | Amersham Biosciences |
| Pump, Econo Pump | Bio-Rad |
| Rotating wheel | Labor-Brand |
| Scales, PB602-S | Heidolph |
| Scales (micro), AG285 | Heidolph |
| Vortex, VortexGenie2 | VWR/Scientific Industries |
| Water bath, Heraeus Julabo TW20 | Kendro |

### 5.1.2 Cell culture products

| **Product** | **Source** | **Cat. No.** |
|---|---|---|
| Standard tissue culture flasks/filter screw caps – 25 $cm^2$ | TPP | 90026 |
| Standard tissue culture flasks/filter screw caps – 75 $cm^2$ | TPP | 90076 |
| Standard tissue culture flasks/filter screw caps – 150 $cm^2$ | TPP | 90151 |
| Tissue culture flasks/filter screw caps – 182 $cm^2$ | Greiner | 660175 |
| 96-well U-bottom with lid – Standard TC | BD | 353077 |
| 96-well flat-bottom with lid – Standard TC | BD | 353072 |
| 96-well flat-bottom with transwell insert | Corning | 3381 |
| 48-well flat-bottom with lid – Standard TC | BD | 353078 |
| 24-well flat-bottom with lid – Standard TC | BD | 353047 |
| 12-well flat-bottom with lid – Standard TC | BD | 353043 |
| 6-well flat-bottom with lid – Standard TC | BD | 353046 |
| 50ml conical tubes Falcon™ | BD | 352070 |
| 15ml conical tubes | Greiner | 188271 |

| | | |
|---|---|---|
| 5 ml round-bottom polypropylene test tube | BD | 352008 |
| 5 ml round-bottom polystyrene test tube with cell strainer | BD | 352235 |
| 0,6 ml round-bottom test tube | Greiner | 101101 |
| Eppendorf tubes | | |
| 70 μm cell strainer Falcon™ | BD | 352350 |
| 40 μm cell strainer Falcon™ | BD | 352340 |
| Cryovial®, 2ml sterile | Roth | E309.1 |
| Nalgene™ Cryo 1°C Freezing Container, "Mr. Frosty" | Nunc | 5100-0001 |
| 35mm FluoroDish™ | WPI | FD35-100 |
| HiTrap Protein G HP, 5ml | GE Healthcare | 17-0405-01 |

### 5.1.3 Cell culture media

| **Product** | **Source** | **Cat. No.** |
|---|---|---|
| RPMI 1640 (1x) w/o L-Glutamine | GIBCO-Invitrogen | 31870 |
| D-MEM (1x) (High Glucose) with L-Glutamine, 4500 mg/L D-Glucose, w/o sodium pyruvate | GIBCO-Invitrogen | 41965 |
| D-PBS (1x) w/o Ca, Mg, sodium bicarbonate | GIBCO-Invitrogen | 14190 |
| IMDM Iscoves Modified Dulbecco Medium (1x) | GIBCO-Invitrogen | 21980032 |
| Fetal Bovine Serum, Origin: EU Approved | GIBCO-Invitrogen | 10270 |
| Penicillin/Streptomycin-Solution<br>10000 U/ml penicillin, 10000 μg/ml streptomycin | GIBCO-Invitrogen | 15140 |
| L-Glutamine 200 mM (100x), 29.2 mg/ml | GIBCO-Invitrogen | 25030 |
| Non-essential amino acids (100X) | GIBCO-Invitrogen | 11140035 |
| Sodium pyruvate MEM 100mM | GIBCO-Invitrogen | 11360088 |
| β-mercaproethanol 50mM | GIBCO-Invitrogen | 31350010 |
| Trypsin –EDTA (1x) HBSS w/o $Ca^{2+}$/$Mg^{2+}$ w/ EDTA | GIBCO-Invitrogen | 25300 |
| Dimethylsulphoxide Hybri Max® (DMSO) | Sigma-Aldrich | D2650 |
| Cell Dissociation Solution Non-enzymatic 1x | Sigma-Aldrich | C5914 |

### 5.1.4 Solutions

(listed in alphabetical order)

| | | |
|---|---|---|
| ACK lysis buffer | 0.829 g | $NH_4Cl$ |
| | 0.1 g | $KHCO_3$ |
| | 0.38 mg | EDTA |
| | 100 ml | $ddH_2O$ |
| | | pH 7.3 |
| FACS buffer | 1x | PBS |
| | 0.02 % (v/v) | $NaN_3$ in PBS |
| | 1% | FCS |
| | 0.5 mM | EDTA |
| Freezing medium | 1x | FCS |
| | 10% | DMSO |
| MACS buffer | 1x | PBS |
| | 1% | FCS |
| | 0.5 mM | EDTA |
| Primary cell culture medium | 1x | RPMI |
| | 10% | FCS |
| | 2 mM | L-glutamine |
| | 100 U/ml | Penicillin |
| | 100 µg/ml | Streptomycin |
| | 1 mM | Sodium Pyruvate |
| | 1x | Non-essential amino acids |
| | 0.25 mM | β-mercaptoethanol |
| PBS (10x) | 1.37 M | NaCl |
| | 27 mM | KCl |

| | | |
|---|---|---|
| | 100 mM | $Na_2HPO_4$ (anhydrous) |
| | 20 mM | $KH_2PO_4$ |
| *Antibody purification:* | | |
| Binding buffer | 20 mM | Sodium phosphate |
| | | $ddH_2O$ |
| | | pH 7.0 |
| Elution buffer | 0.1 M | Glycin HCl |
| | | $ddH_2O$ |
| | | pH 2.7 |
| Neutralization buffer | 1 M | Tris-HCl |
| | | $ddH_2O$ |
| | | pH 9 |
| Precipitation buffer | 29.1 g | $(NH_4)_2SO_4$ |
| | 100 ml | $ddH_2O$ |

### 5.1.5 Chemicals

(listed in alphabetical order)

| **Product** | **Source** | **Cat. No.** |
|---|---|---|
| 1-methyl- L -tryptophan (1MT) | Sigma-Aldrich | 860646 |
| Brefeldin A | Sigma-Fluka | B7651 |
| Carboxyfluorescein succinimidyl ester (CFSE) | Sigma-Fluka | 21888 |
| Chromium-51 | PerkinElmer | NEZ030005MC |
| Collagenase, type IV from *Clostridium histolyticum* | Cell systems | LS004188 |
| DNAse I | Sigma | DN25-1G |
| FACS lysing solution (10x) | BD | 349202 |
| Heparin-Sodium, 25 000 Units | B Braun | 1708.00.00 |
| IFN-γ, recombinant mouse | BD | 51-9000889 |

| | | |
|---|---|---|
| Indomethacin | Sigma-Fluka | 57413 |
| Isofluoran | B Braun | 6724123.00.00 |
| Lipopolysaccharide (LPS) | Sigma-Fluka | L4391 |
| *Lycopersicum esculentum* lectin | Vector Labs | FL-1171 |
| [methyl-$^3$H] Thymidine | Amersham | TRK637-5MCI |
| $N^G$-Monomethyl-D-arginine monoacetate | Alexis | ALX-106-002 |
| $N^G$-Monomethyl-L-arginine monoacetate | Alexis | ALX-106-001 |
| PMSF | Applichem | A0999 |
| Paraformaldenhyde (PFA) | Applichem | A3813 |
| Propidium Iodide (PI) | Sigma-Fluka | 70335-5ML-F |
| TNFa, recombinant human | Kindly provided by Dr. Rüdiger Arnold, DKFZ | |
| TRAIL, recombinant mouse | Biomol | SE-722 |
| Triton X-100 | Sigma-Fluka | T9284 |
| Saponin from quillaja bark | Sigma | S4521 |

### 5.1.6 Antibodies

#### 5.1.6.1 Antibodies for FACS analysis

The following antibodies against mouse antigens were used (listed in alphabetical order):

| **Ab specificity** | **Conjugate** | **Clone** | **Isotype** | **Dilution** | **Source** | **Cat. No.** |
|---|---|---|---|---|---|---|
| B7-H4 | PE | 188 | rat IgG2a, κ | 1:100 | eBioscience | 12-5972 |
| CD3 | FITC | 145-2C11 | armenian hamster | 1:100 | BD | 553062 |
| CD3 | APC | 145-2C11 | armenian hamster IgG, κ | 1:100 | BD | 553066 |
| CD4 | FITC | GK1.5 | rat IgG2a | 1:100 | BD | 553046 |
| CD4 | PECy5 | H129.19 | rat IgG2a | 1:100 | BD | 553654 |
| CD8 | PE | 53-6.7 | rat IgG2a, κ | 1:100 | BD | 553033 |

| | | | | | | |
|---|---|---|---|---|---|---|
| CD11b | FITC | M1/70 | rat IgG2b | 1:100 | BD | 557396 |
| CD11b | APC | M1/70 | rat IgG2b | 1:100 | BD | 553312 |
| CD11c | FITC | HL3 | hamster IgG1 | 1:100 | BD | 557400 |
| CD25 | FITC | 7D4 | rat IgM | 1:100 | BD | 553071 |
| CD25 | PE | PC61 | rat IgG1 | 1:100 | BD | 553866 |
| CD45.1 | FITC | A20 | mouse IgG2a | 1:1000 | BD | 553775 |
| CD45.1 | PE | A20 | mouse IgG2a | 1:100 | BD | 553776 |
| CD80 (B7-1) | PE | 16-10A1 | rat IgG2a, κ | 1:100 | BD | 553692 |
| CD86 (B7-2) | PE | GL1 | rat IgG2a, κ | 1:100 | BD | 553692 |
| CD95 | FITC | Jo2 | armenian hamster IgG2, λ | 1:20 | BD | 554257 |
| CD119 (IFN-γR, a chain) | biotin | GR20 | rat IgG1 | 1:100 | BD | 558771 |
| CD273 (B7-DC) | PE | TY25 | rat IgG2a, κ | 1:100 | BD | 557796 |
| CD274 (B7-H1) | PE | MIH5 | rat IgG2, λ | 1:100 | BD | 558091 |
| CD275 (B7-H2) | PE | HK5.3 | rat IgG2a, κ | 1:100 | eBioscience | 12-5985 |
| CD276 (B7-H3) | PE | M3.2D7 | rat IgG2a | 1:100 | eBioscience | 12-5973 |
| F4/80 | Alexa488 | BM8 | rat IgG2a | 1:100 | Caltag | MF48020 |
| Foxp3 | PE | FJK-16s | rat IgG2a | 1:100 | eBioscience | 12-5773 |
| Gr-1 | APC | RB6-8C5 | rat IgG2a | 1:100 | BD | 553129 |
| H-2Kb | PE | AF6-88.5 | mouse IgG2a, κ | 1:100 | BD | 553570 |
| I-$A^b$ | PE | AF6-120.1 | mouse IgG2a | 1:200 | BD | 553552 |
| IFN-γ | FITC | XMG1.2 | rat IgG1 | 1:50 | BD | 554411 |
| Ly-6C/G (Gr-1) | APC | RB6-8C5 | rat IgG2b | 1:1500 | BD | 553129 |

| | | | | | | |
|---|---|---|---|---|---|---|
| NK1.1 | PE | PK136 | mouse IgG2a | 1:1500 | BD | 557391 |
| ***Isotypes*** | | | | | | |
| Isotype | FITC | R3-34 | rat IgG1 | | BD | 554684 |
| Isotype | PE | MOPC-21 | mouse IgG1 | | BD | 559320 |
| Isotype | PE | R35-95 | rat IgG2a | | BD | 553930 |
| Isotype | APC | A95-1 | rat IgG2b | | BD | 553991 |
| Streptavidin | APC | | | 1:1000 | BD | 554067 |

#### 5.1.6.2 Antibodies for *in vitro* activation

The following antibody against mouse CD3 was used *in vitro* for the activation of T cells:

| **Ab specificity** | **Clone** | **Isotype** | **Source** | **Cat. No.** |
|---|---|---|---|---|
| CD3 | 145-2C11 | armenian hamster IgG1, κ | BD | 553057 |

#### 5.1.6.3 *In vivo* administered antibodies

The following antibodies against mouse antigens were injected *i.p.* in mice for the depletion of cell populations or the neutralization of cytokines (listed in alphabetical order):

| **Ab specificity** | **Clone** | **Isotype** | **Source** |
|---|---|---|---|
| CD4 | GK1.5 | rat IgG2a | Purification from hybridoma |
| CD8 | 2.43 | rat IgG2b | Bioexpress |
| CD25 | PC61 | rat IgG1 | Purification from hybridoma |
| CD95L | MFL 4 | armenian hamster IgG | Kindly provided by Prof. Yagita, Juntendo University School of Medicine, Kyoto, Japan |
| IFN-β | 7FD3 | rat IgG1 | Purification from hybridoma |
| IFN-γ | XMG1.2 | rat IgG1 | Bioexpress |
| IL-10R | YL03.1B1.3a | rat IgG1 | DNAX |
| NK1.1 | PK136 | mouse IgG2a | Bioexpress |
| TGF-β | 1D11 | mouse IgG1 | Bioexpress |

### 5.1.7 Cell lines

The cell lines that were used in this study are listed below (in alphabetical order):

| Cell line | Cell type | Medium* | Reference |
|---|---|---|---|
| 2.4G2 | anti-CD16/CD32 hybridoma | RPMI 1640 | [266] |
| 7FD3 | anti-IFN-β hybridoma | RPMI 1640 | Kindly provided by Dr. Rainer Zawatzky, DKFZ |
| EC7.1 | MHC class I-deficient variant of RMA-S | IMDM | [267] |
| Jurkat | human T cell leukemia | RPMI 1640 | [268] |
| L929 | mouse fibroblast | DMEM | [269] |
| PC61 | anti-CD25 hybridoma | RPMI 1640 | [270] |
| RMA | mouse T cell lymphoma | RPMI 1640 | [271] |
| RMA-S | TAP2-deficient variant of RMA | RPMI 1640 | [271] |
| RMA-RAE-1γ | RAE-1γ transfectant of RMA | RPMI 1640 | [69] |
| YAC-1 | mouse lymphoma | RPMI 1640 | [9] |

*All media were supplemented with 10% heat-inactivated fetal bovine serum, 2 mM L-glutamine, 100 U/ml penicillin and 100 µg/ml streptomycin with the exception of PC61 which was supplemented with 5% FCS, 2 mM L-glutamine, 100 U/ml penicillin and 100 µg/ml streptomycin, 1 mM sodium pyruvate and 0.25 mM ß-mercaptoethanol.

Cell lines were regulary checked for mycoplasma contamination using PCR based assay.

### 5.1.8 Magnetic Cell Sorting (MACS) beads and columns

| Product | Source | Cat. No. |
|---|---|---|
| anti-CD4 beads | Miltenyi Biotec | 130-049-201 |
| anti-CD8 beads | Miltenyi Biotec | 130-049-401 |
| anti-CD11b beads | Miltenyi Biotec | 130-049-601 |
| anti-CD90 beads | Miltenyi Biotec | 130-049-101 |

| | | |
|---|---|---|
| anti-DX5 beads | Miltenyi Biotec | 130-052-501 |
| Regulatory T cell Isolation kit | Miltenyi Biotec | 130-091-041 |
| anti-APC beads | Miltenyi Biotec | 130-090-855 |
| MS Columns | Miltenyi Biotec | 130-042-201 |
| LS Columns | Miltenyi Biotec | 130-042-401 |
| LD Columns | Miltenyi Biotec | 130-042-901 |

### 5.1.9 Kits

| **Product** | **Source** | **Cat. No.** |
|---|---|---|
| PE anti-mouse/rat Foxp3 Staining Set | eBioscience | 72-5775 |
| Mouse IFN-γ OptEIA™ Set | BD | 555138 |
| OptEIA™ Reagent Set B | BD | 550534 |
| Mouse IFN-γ *in vivo* capture assay | BD | 558491 |
| Bio-plex cytokine reagent kit | Biorad | 171-304000 |
| Bio-plex cell lysis kit | Biorad | 171-304011 |
| Bio-Plex mouse serum diluent kit | Biorad | 171-305005 |
| Bio-plex mouse IFN-γ assay | Biorad | 171-G11934 |
| Bio-plex mouse IL-1β assay | Biorad | 171-G12819 |
| Bio-plex mouse IL-6 assay | Biorad | 171-G10738 |
| Bio-plex mouse IL-10 assay | Biorad | 171-G11356 |
| Bio-plex mouse IL-13 assay | Biorad | X60-000ZFYB |
| Bio-plex mouse IL-12 (p70) assay | Biorad | 171-G13758 |
| Bio-plex mouse MIP-1α assay | Biorad | 171-G16477 |
| Bio-plex mouse MIP-1β assay | Biorad | X60-005KMTI |
| Bio-plex mouse MIP-2 assay | Biorad | XD0-000001T |
| Bio-plex mouse VEGF assay | Biorad | XD0-000007B |
| BCA™ Protein Assay kit | Pierce | 23227 |

## 5.2 MICE

C57BL/6 wild-type (wt) and C57BL/6-Ly5.1 congenic mice were purchased from Charles River Laboratories (Sulzfeld, Germany and Erembodegem, Belgium). C57BL/6-Ly5.1, IFNAR1$^{-/-}$ and RAG2$^{-/-}$IFNAR1$^{-/-}$ mice were bred in our animal facility. IFN-γ receptor$^{-/-}$ (IFN-γR$^{-/-}$), perforin$^{-/-}$ (*Prf*$^{-/-}$) and inducible Nitric Oxide Synthase$^{-/-}$ (iNOS$^{-/-}$) C57BL/6 mice were purchased from Jackson Laboratory (Bar Harbor, Maine, USA). Mice were housed in specific pathogen-free conditions and used in experiments at 6-8 wk of age. All experiments were performed according to local animal experimental ethics committee guidelines.

## 5.3 METHODS

### 5.3.1 Cell culture methods

#### 5.3.1.1 Determination of cell number

An aliquot of cell suspension was diluted 1:1 with trypan blue solution (0.05 % w/v) to distinguish dead cells and cells were counted with a Neubauer counting chamber (0.1 mm depth). The number of live cells per ml is calculated as following:

average cell number / chamber square (0.1 mm$^3$) x dilution factor x $10^4$

#### 5.3.1.2 Freezing and thawing of cells

For freezing of cells, cell suspensions were centrifuged (1200 rpm, 10 min, RT) and the pellet was resuspended in freezing medium at a concentration of 5 x $10^6$ cells/ml. 2 ml aliquots in freezing tubes were placed in ice-cooled freezing containers and placed for 24 h at -80°C. Frozen cells were subsequently stored in liquid nitrogen.

Cell thawing was performed quickly in a 37°C water bath until ~ 10% of suspension remained frozen. The suspension was immediately diluted into 9 ml of appropriate cold medium and

centrifuged (1200rpm, 10 min, RT). Cells were resuspended in medium and cultured at 37°C, 5 % $CO_2$.

#### 5.3.1.3 Splitting of adherent cells

For the splitting of adherent cells, the culture medium was removed from the flasks, the cells were washed once with pre-warmed PBS, and Trypsin-EDTA or Cell Dissociation Solution was added in sufficient amount to cover the cell layer. Cells were then incubated at 37°C for ~5 min, checking in parallel the progress of detachment under the microscope. After complete detachment, culture medium was added to the flask, cells were collected in Falcon tubes and centrifuged (1200 rpm, 10 min, RT). Cells were subsequently splitted at the appropriate ratio into new flask or used in experiments.

#### 5.3.1.4 Splitting of suspension cells

Cells in suspension reaching an optimal density were split in the appropriate ratio, ranging between 1:5 up to 1:20 by adding the appropriate volume of medium.

### 5.3.2 Mouse tumor model

For the analysis of tumor growth *in vivo*, tumor cell lines were harvested in the exponential growth phase. Tumor cells were washed 3 times with PBS and resuspended in PBS at a concentration of 1 x $10^7$ cells/ml for RMA or RMA-S cells or 1 x $10^6$ cells/ml, primary to injection. Groups of 5-10 mice were injected *s.c.* in the shaved left flank with 100 µl of tumor cell suspension. Tumor growth was assessed 3 times weekly with a caliper measuring along the perpendicular axes of the tumors and expressed as the product of the two diameters. For rechallenge experiments, mice were rested for at least 3 months after primary tumor cell inoculation before secondary challenge.

#### 5.3.2.1 Isolation of organs and preparation of single cell suspensions

##### *5.3.2.1.1 Blood*

For blood isolation, animals were sacrificed using $CO_2$; mouse blood was obtained by puncture of the orbital vein of mice. For FACS staining, 30 µl of heparin were added to 1 ml of blood. For the detection of IFN-γ in the serum or adoptive transfer memory experiments, blood was coagulated in 1.5 ml tubes for 1 h at 4°C. The serum was separated by centrifugation (1500 rpm, 10 min, 4°C).

##### *5.3.2.1.2 Spleen and LN*

Animals were sacrificed by dislocation of the neck; spleen and peripheral LN were excised using sterile forceps and scissors and kept in ice-cold PBS + 5% FCS medium. Single cell suspensions were obtained by mincing the spleen or LN through a 40 µm cell strainer. For the lysis of erythrocytes, splenocytes were treated with buffered ammonium chloride potassium phosphate solution (ACK-buffer) for 1 min at RT and then washed with PBS + 5% FCS (1400 rpm, 10 min, 4°C). Cells were resuspended in PBS + 5% FCS.

##### *5.3.2.1.3 Tumor infiltrating leukocytes*

For the preparation of single cell suspensions from tumors, tumors were excised using sterile forceps, cut into small pieces with a scalpel and digested with 5 mg/ml collagenase type IV and 0.5 mg/ml DNase I for 15 min at 37°C. At the end of the incubation, the digested tumor was smashed through a 70 µm-pore cell strainer, cells were collected in a 50 ml Falcon tube and washed once with PBS + 10% FCS (1400 rpm, 10 min, 4°C).

##### *5.3.2.1.4 Bone marrow (BM) cells*

Animals were sacrificed by dislocation of the neck; hind legs were dissected and bones were freed from all sinews and muscle tissue using sterile forceps and scissors. The femur and tibiae were separated by breaking the knee and the heel, washed briefly in 80 % ethanol and placed in ice-cold PBS. To rinse out the BM cells, the ends of femur and tibiae were cut and 5-10 ml of

ice-cold PBS were forced through the bone cavity with a 27G needle. The isolated BM cells were washed three times with PBS before *i.v.* injection into the mice.

#### 5.3.2.2 *In vivo* depletion and neutralization experiments

For the *in vivo* depletion of Treg, 300 µg of anti-CD25 mAb were injected *i.p.* 2 days before tumor cell inoculation. The depletion efficiency was >95% in blood after 2 days. In some experiments, mice were additionally depleted of $NK1.1^+$ cells or $CD4^+$ T cells by *i.p.* injection of 200 µg anti-NK1.1 or anti-CD4 mAbs, respectively, on days -2, +2, +9, and +16. At day 10 after tumor cell inoculation and at the endpoint, the efficiency of these depletions was >90% in blood, spleen and tumor tissue, as assessed by flow cytometric analysis. For the *in vivo* neutralization of IFN-γ, 300 µg of anti-mouse IFN-γ mAb were injected *i.p.* three times weekly beginning at the day of tumor cell inoculation. For the *in vivo* neutralization of CD95L, 250 µg of anti-mouse CD95L mAb were injected *i.p.* every 3 days beginning from day -1 before tumor inoculation. The anti-apoptotic activity of the anti-CD95L mAb was confirmed *in vitro* by the inhibition of T cell activation-induced cell death, which is known to be mediated via the CD95-CD95L pathway (data not shown). For the *in vivo* neutralization of TGF-β, 2 mg of anti-TGF-β mAb were administered *i.p.* 2 times weekly, starting from day -2 before tumor inoculation. For the *in vivo* blocking of IL-10R, 1 mg of anti-IL-10R mAb was injected *i.p.* once weekly beginning from day -2 before tumor inoculation.

#### 5.3.2.3 Bone marrow transplantation

Wt, $IFNAR1^{-/-}$ or $RAG2^{-/-}IFNAR1^{-/-}$ mice were irradiated with two doses of 450 rad with a 3h interval in between. After 4 hours of rest, irradiated mice were injected with $4 \times 10^6$ bone marrow cells in 200 µl PBS collected from donor wt or $IFNAR1^{-/-}$ mice. Mice were maintained on amoxycilin antibiotic diluted in drinking water for 6 weeks after reconstitution. At 6 weeks after injection, chimeras were analyzed for the reconstitution of immune cell populations by flow cytometry of peripheral blood cells after staining with antibodies to CD45.1 and CD45.2.

#### 5.3.2.4 Memory experiments

##### *5.3.2.4.1 In vivo memory experiments*

Mice which rejected RMA-S tumors after anti-CD25 treatment were rested for at least 3 months after primary tumor cell inoculation. The reconstitution of the Treg compartment at this time was confirmed in the blood of mice by flow cytometric analysis for CD4 and CD25 markers. For rechallenge experiments, mice were injected *s.c.* in the left flank with 1 x $10^6$ RMA-S or RMA cells and tumor growth was monitored. In some experiments, mice were depleted of $CD4^+$ or $CD8^+$ T cells or $NK1.1^+$ cells in combination either with $CD4^+$ or $CD8^+$ T cell depletion. Naïve mice injected for the first time with tumor cells were used as a control.

##### *5.3.2.4.2 Adoptive transfer memory experiments*

In adoptive transfer experiments, $CD4^+$ and $CD8^+$ T cells were isolated by magnetic separation from the spleens and LN of naïve mice or mice which had previously rejected RMA-S tumors and washed 3 times with PBS. The blood serum was also prepared from the same mice. 1 x $10^7$ purified $CD4^+$ T cells or 6 x $10^7$ $CD8^+$ T cells or 250 µl of blood serum were injected *i.v.* to naïve C57BL/6 hosts, one day before *s.c.* RMA-S tumor cell inoculation.

### 5.3.3 Antibody purification

#### 5.3.3.1 Purification of the anti-CD25 mAb

For the purification of the anti-CD25 mAb, PC61 hybridoma cell line was expanded until confluence. Cell cultures were centrifuged (3500 rpm, 7 min, 4°C) and S/N was collected. Total protein was precipitated with ammonium sulfate added at slow rate to the S/N until saturation. The S/N was shaken on a magnetic stirrer for ~1h at RT. After centrifugation (7500 rpm, 30 min, 4°C), pellets were resuspended in 100 ml dd$H_2O$ and dialyzed O/N at 4°C in 1x PBS. The dialyzed mAb was sterile filtered and purified by binding on a protein G column with the means of a peristaltic pump, pre-washed once with ethanol, and once with the binding buffer. The mAb solution was passed through the column twice at a flow rate 4 ml/min. The bound mAb was eluted from the column with 30-50 ml elution buffer and fractions were collected in 15 ml falcon tubes containing 200 µl neutralization buffer. Additional neutralization buffer was added to

adjust the pH to 7. Optical density (O.D.) was measured at 260 nm; the fractions which had an O.D. over 0.6 were pooled. The pooled mAb was dialyzed O/N in 1x PBS and sterile filtered. Protein concentration was analyzed with the BCA kit and purity with a SDS-gel. Aliquots of the mAb were kept at -20$^{o}$C. The protein G column was washed with ethanol and stored at 4$^{o}$C.

#### 5.3.3.2 Purification of the anti- IFN-β mAb

For the purification of the anti-IFN-β mAb, the 7FD3 hybridoma cell line was expanded until confluence. FCS was excluded from the cell culture medium during the last step of culture. Cell cultures were centrifuged (3500 rpm, 7 min, 4$^{o}$C) and S/N was collected. Total protein was precipitated with ammonium sulfate added at slow rate to the S/N until 50% saturation. The S/N was shaken on a magnetic stirrer for ~1h at RT. After centrifugation (7500rpm, 30min, 4$^{o}$C), pellets were resuspended in dd$H_2O$ in a volume corresponding to 0,5% of the starting volume and dialyzed O/N at 4$^{o}$C in 1x PBS. The dialyzed mAb was sterile filtered. Protein concentration was analyzed with the BCA kit and purity with a SDS-gel. Aliquots of the mAb were kept at 4$^{o}$C.

### 5.3.4 Fluorescence-activated cell sorting (FACS)

#### 5.3.4.1 FACS staining and analysis

For staining of cells, 0.5 – 1 x $10^6$ cells were washed once with FACS buffer (1200 rpm, 10 min, 4°C for cell lines or 1400 rpm, 10 min, 4°C for primary mouse cells) and incubated with 10% Fc block (2.4G2 supernatant) for 10 min on ice to block Fc receptors. Subsequently, the primary antibodies were added and cells were further incubated for 30 min at 4°C. For biotinylated antibodies, cells were washed once with FACS buffer and stained with conjugated streptavidin for additional 30 min at 4°C. After staining, cells were washed once, fluorescence was assessed by a FACSCalibur and data were analyzed with the CellQuest software. Peripheral blood leucocytes were stained by adding the primary antibodies directly into the blood samples. At the end of the incubation, erythrocytes were lysed with FACS Lysis Buffer for 1 min at RT, followed by washing with FACS buffer. Streptavidin was added at a second step when necessary. Working concentrations of antibodies are denoted under chapter 5.1.6.1.

#### 5.3.4.2 FACS sorting

For FACS sorting, up to 1 x $10^8$ total tumor cells were washed once with PBS + 0.1% FCS (1400 rpm, 10 min, 4°C,) and incubated with 10% Fc block (2.4G2 supernatant) for 10min on ice to block Fc receptors. Subsequently, the primary antibodies were added and cells were further incubated for 30 min at 4°C. After staining, cells were washed once with PBS + 0.1% FCS, resuspended in PBS + 1% FCS and filtered through a cell strainer to remove cell clusters. Cell sorting was performed with FACSDiva and FACSVantage.

### 5.3.5 MACS sorting

In some cases, primary cell subpopulations were sorted with magnetic beads, according to the manufacturer's protocol.

### 5.3.6 Determination of cytokines

#### 5.3.6.1 Intracellular FACS staining

For the detection of IFN-γ producing cells, single cell suspensions were prepared from tumor tissue of PBS and anti-CD25 treated mice. Cells were stained for extracellular markers and subsequently fixed with 50 µl of 4% PFA for 10 min at RT. Cells were washed once (1400 rpm, 10 min, 4°C,) with cold FACS buffer and permeabilized with 100 µl of 0.5% saponin for 10 min at RT. 10% Fc block and 10 µg/ml rat IgG were added for additional 10 min to block unspecific binding. Cells were subsequently washed once (1400 rpm, 10 min, 4°C) with cold FACS buffer containing 0.5% saponin. Anti-IFN-γ or the appropriate isotype control was added and cells were incubated for 30 min at 4°C. Cells were washed once (1400 rpm, 10 min, 4°C) with cold FACS buffer containing 0.5% saponin and once (1400 rpm, 10 min, 4°C) with cold FACS buffer, before analyzed with the CellQuest software on a FACSCalibur.

#### 5.3.6.2 Enzyme-Linked ImmunoSorbent Assay (ELISA)

$CD8^+$ T cells were purified from spleens and LN by magnetic cell sorting or from tumor tissue of tumor bearing mice by FACS sorting. 1 x $10^5$ $CD8^+$ T cells were cultured either alone or in the presence of RMA-S or EC7.1 cells at a ratio 1:1 for 18h. At the end of the incubation, S/N were

collected and stored at -20$^{o}$C until used. IFN-γ levels were determined by ELISA for murine IFN-γ, according to the manufacturer's instructions.

#### 5.3.6.3 *In vivo* IFN-γ capture assay

For the determination of IFN-γ in the serum of naïve or tumor bearing mice treated with PBS or anti-CD25 mAb, biotinylated anti-IFN-γ mAb was injected *i.v.* into the mice on days 0, 3, 5 and 9 after RMA-S tumor cell inoculation and blood samples were collected after 24 or 48 h. Blood serum was prepared and the levels of IFN-γ were determined according to the manufacturer's instructions.

#### 5.3.6.4 Bio-plex protein array assay for cytokine measurement

For the determination of cytokine and chemokine production by tumor infiltrating macrophages, CD11b$^{+}$F4/80$^{+}$ cells were isolated from tumors of control and Treg depleted mice on day 10 after RMA-S tumor cell inoculation by flow cytometric sorting (purity > 95%). 1 x 10$^{5}$ macrophages were cultured in 200μl primary cell culture medium in a U-bottom 96-well plate and after 12 or 24h supernatants were collected. For the determination of cytokine and chemokine production in tumor tissue, lysates were prepared from total tumor tissue in the presence of PMSF as protease inhibitor. Total protein concentration was calculated with the BCA kit and the concentration of all lysate samples was adjusted optimally to 300 μg/ml with the Bio-plex lysis buffer. All supernatants and lysates were further diluted 1:1 with mouse serum before the assay. Cytokine and chemokine release was determined with the Bio-plex Protein Array system, according to the manufacturer's instructions. The sensitivity of the assay for IFN-γ detection was 2 pg/ml, for MIP-1β 1.5 pg/ml, for MIP-2 3 pg/ml, for IL-6 1 pg/ml, for IL-13 3 pg/ml and for IL-1b 1.6 pg/ml.

### 5.3.7 Proliferation and suppression assays

#### 5.3.7.1 Treg suppression assay

CD4$^{+}$ T cells were isolated from mouse splenocytes based on a negative magnetic selection procedure; Treg (CD4$^{+}$CD25$^{+}$ T cells) and Tcon (CD4$^{+}$CD25$^{-}$ T cells) were subsequently selected

from the pure, untouched $CD4^+$ T cells, based on CD25 magnetic separation. Both populations had a purity of ~90%. To document the suppressive activity of Treg, 1 x $10^5$ Tcon were incubated in U bottom 96-well plates in 200 µl of primary cell culture medium alone or in co-culture with titrating cell numbers of Treg in the following Treg : Tcon ratios: 1:1, 1:2, 1:4, 1:8, 1:16. For the stimulation of proliferation of T cells, 0.5 µg/ml mouse anti-CD3 mAb was added to the culture medium and $1 \times 10^5$ irradiated (30 Gray) CD90-depleted splenocytes served as APC. After 4 days of culture at 37°C in 5% $CO_2$, 1 µCi $^3$H-thymidine, diluted 1:10 in RPMI medium, per well was added for additional 16 h. To control non-specific inhibition due to crowding in the well, 2x Tcon were used as a control. Proliferation was measured using a scintillation counter.

#### 5.3.7.2 Tumor cell growth inhibition assay

$CD11b^+$ cells were isolated with magnetic separation (purity ~50%) or macrophages were purified with FACS sorting (purity > 95% $CD11b^+F4/80^+$) from tumors on d10 after tumor cell inoculation. The purified cell populations were cultured in 96-well plates with 1 x $10^4$ RMA-S cells at the following ratios: $CD11b^+$ cells : RMA-S cells = 5:1, 10:1, 20:1 and 40:1 – depending on the assay – for 24 or 48 h in a U-bottom 96-well plate in 200 µl of primary cell culture medium. RMA-S cells were in parallel cultured in the absence of $CD11b^+$ cells. In some experiments, $CD11b^+$ cells were separated from RMA-S cells by transwell inserts. In some experiments, inhibitors were used to block the activity of iNOS, PGE2 and IDO: 0.5 mM L-NMMA and its stereoisomer D-NMMA as a control, 10µM indomethacin and EtOH diluent control, and 100µM 1MT and HCl diluent control, respectively. Proliferation was assessed by adding 1µCi of $^3$H-thymidine, diluted 1:10 in RPMI medium, to each well, 6h before harvesting. At the end of the incubation, the cells were harvested on filter papers, signal was enhanced by the addition of a scintillator and the radioactivity was quantified by a beta counter. In cases where the plates could not be harvested immediately after the end of the incubation, the plates were placed in -20$^o$C until analyzed for $^3$H-thymidine incorporation. Before harvesting, plates were thawed at 37$^o$C.

#### 5.3.7.3 Documentation of proliferation by CFSE dilution

A total of 1 x $10^7$ RMA-S cells diluted in 1 ml PBS + 5% FCS were labeled with 1 µM CFSE, which was added to the cells while vortexing. After 10 min incubation at RT on shaker, the cells were washed with PBS + 5% FCS three times (1200 rpm, 10 min, 4°C). During the procedure, the cells were protected from the light. 1 x $10^4$ CFSE-labeled RMA-S cells were cultured alone or in the presence of $CD11b^+$ cells at a ratio of $CD11b^+$ cells : RMA-S cells = 40 :1 for 48 h in a U-bottom 96-well plate in 200 µl of primary cell culture medium. At the end of the incubation, cells were harvested from the plate, washed once with FACS buffer (1400 rpm, 10 min, 4°C) and fluorescence was analyzed on a FACSCalibur. Dilution of the CFSE dye corresponded to proliferation of the cells.

### 5.3.8 Killing assays

#### 5.3.8.1 $^{51}$Cr release cytotoxicity assay

RMA-S or YAC-1 tumor cells were labeled with 100µCi $^{51}$Cr for 90min and washed three times with RPMI medium. A total of 1 x $10^3$ $^{51}$Cr-labeled target cells were seeded in each well of a 96-well U-bottom plate. NK cells, purified with $DX5^+$ magnetic cell sorting, were added at different effector to target (E:T) ratios (100:1, 50:1, 25:1, 12.5:1, 6.25:1, 3.125:1, 1.56:1) in a final volume of 200 µl of primary cell culture medium. The plates were centrifuged at 1200 rpm for 3 min and incubated for 6 h at 37°C in 5% $CO_2$. At the end of the incubation, 100 µl of S/N was collected from each well and the radioactivity was counted in a beta counter. The percentage of cytotoxicity in each well was calculated as:

$$\frac{\text{[mean cpm – minimum (spontaneous) mean release]}}{\text{[maximum release (total) – minimum (spontaneous) mean release]}} \times 100$$

Minimum (spontaneous release) corresponds to the amount of radioactivity released by tumor cells cultured in the absence of NK cells. Maximum release relates to the amount of radioactivity released by tumor cells cultured in the presence of 10% Triton X-100.

#### 5.3.8.2 *In vitro* induction of apoptosis by death ligands

RMA-S cells were cultured at a concentration of 1 x $10^5$ cells/ml in the absence or presence of 50 U/ml recombinant mouse IFN-γ for 24h. At the end of the incubation, cells were washed (1200

rpm, 10 min, 4°C) twice and re-plated at a concentration of 1 x $10^6$ cells/ml in a 6-well plate for 6h in the absence or presence of either 0.1 μM TNF-α or 1 μg/ml TRAIL. In parallel, L929 cells were cultured in the absence or presence of TNF-α, and Jurkat cells in the absence or presence of TRAIL, as positive controls to TNF-α- and TRAIL-induced apoptosis *in vitro*. At the end of the incubation, cells were harvested, washed once (1200 rpm, 10 min, 4°C) with FACS buffer and stained with 1μl of PI. Dead cells, defined as $PI^+$ cells, were determined by flow cytometric analysis as percentage of total cells.

### 5.3.9 Visualization of angiogenesis by confocal microscopy

Tumor vasculature was visualized by fluorescent angiography using a FITC-labeled *Lycopersicon esculentum* lectin injected ***i.v.*** (100 μg diluted in 100 μl of PBS) in the tail vein of mice. Two min after lectin injection, mice were sacrificed by cervical dislocation. Tumors were harvested, placed on 0.17 mm thick coverslips and examined unfixed under fluorescent confocal microscopy (Nikon C1Si confocal microscope with a 488-nm argon ion laser). Detection of the *Lycopersicon esculentum* lectin was achieved at 503–537 nm. Datasets typically represented 1 x 1 x 0.1 mm (512 x 512 pixels x 61 planes) with a 1.65 μm step interval. The analysis used the entire z-series of all three channels.

### 5.3.10 Statistical analysis

Differences between groups were calculated using standard Student's *t* test. Differences in tumor growth between groups of mice were calculated using Koziol test. Values of $p < 0.05$ were considered to be statistically significant.

# 6 RESULTS

## 6.1 REGULATORY T CELLS SUPPRESS ANTI-TUMOR IMMUNITY AGAINST A MHC CLASS I DEFICIENT LYMPHOMA

### 6.1.1 Regulatory T cells suppress IFN-γ dependent leukocyte accumulation in lymphoma

#### 6.1.1.1 Accumulation of Treg in RMA-S tumor-bearing mice

RMA-S lymphoma cell line is a MHC class I-deficient variant of the RBL-5 tumor. According to the original characterization by Kärre and colleagues, RMA-S tumor cells are efficiently controlled by NK cells, when injected into mice at relatively low cell numbers [271]. For our study, we used a higher tumor cell number (1 x $10^6$ cells) leading to progressive tumor growth after *s.c.* injection. In order to investigate the role of Treg in the anti-tumor immunity against a MHC class I-deficient tumor, we examined spleens and tumor tissues from RMA-S tumor-bearing mice for the presence of Treg. Flow cytometric analysis revealed that the percentages of $CD4^+CD25^+$ T cells among $CD4^+$ T cells were significantly increased in spleens of tumor-bearing mice (Figure 6.1A). High percentages of $CD4^+CD25^+$ T cells among $CD4^+$ T cells were also observed within the tumor infiltrating leukocytes. Since CD25 expression is also upregulated on $CD4^+CD25^-$ effector T cells after activation, we determined the percentages of $CD4^+$ T cells expressing the Treg specific transcription factor Foxp3. Our results confirmed the significantly increased percentages of Treg in spleens of tumor-bearing mice and high percentages of Treg in the tumor tissue (Figure 6.1B). Interestingly, CD25 expression was not observed in any cell population other than Treg. CD25 expression correlated with suppressive ability, since $CD4^+CD25^+$ T cells were able to suppress the proliferation of $CD4^+CD25^-$ T cells in an *in vitro* co-culture in a dose-dependent manner (Figure 6.1C). Our results demonstrate that in the RMA-S tumor model Treg accumulate in the spleen and are present in high percentages within the tumor tissue.

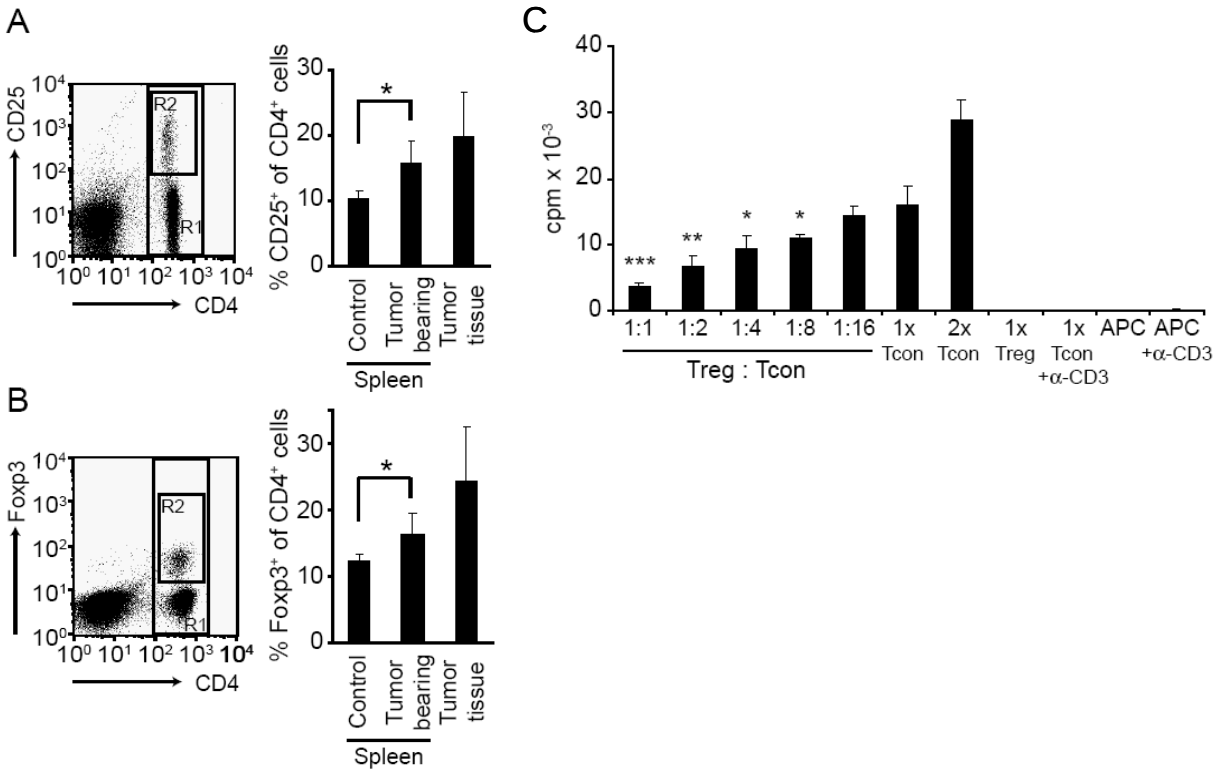


**Figure 6.1. Increased numbers of Treg in mice bearing RMA-S tumors.** (A-B) C57BL/6 mice were injected *s.c.* with RMA-S cells. After 21 days spleens and tumors were removed and analyzed for the presence of $CD4^+CD25^+$ (A) or $CD4^+Foxp3^+$ (B) T cells by flow cytometry. Representative dot plots show CD4 and CD25 staining (A) or CD4 and Foxp3 staining (B) of total splenocytes (left panels). Right panels depict quantification of $CD4^+CD25^+$ (A) or $CD4^+Foxp3^+$ (B) T cells in spleens of control and tumor-bearing mice as well as in tumor tissue. The percentages of $CD25^+$ cells (A, gate R2) or $Foxp3^+$ cells (B, gate R2) among total $CD4^+$ T cells (gate R1) were calculated. Data show the mean ± SD of eight animals per group and are representative of three experiments. *, $p<0.01$ using Student's *t* test. (C) Tcon ($CD4^+CD25^-$ T cells) from C57BL/6 naïve mice were stimulated with anti-CD3 mAb and irradiated syngeneic T cell-depleted splenocytes in the presence of varying numbers of Treg ($CD4^+CD25^+$ T cells). Cells were cultured for 96 h and proliferation was assessed by $^3$H-thymidine-incorporation, added for additional 16 h to the culture. To control for nonspecific inhibition due to crowding in the well, 2x Tcon were used as a control. Data show the mean ± SD of triplicate cultures and are representative of three experiments. *, $p<0.05$, **, $p<0.01$, ***, $p<0.005$, using Student's *t* test.

### 6.1.1.2 Depletion of Treg abrogates RMA-S tumor growth

To examine the impact of Treg on the immune response against RMA-S tumor, Treg were depleted by *i.p.* injection of anti-CD25 mAb 2 days prior to RMA-S tumor cell inoculation. Of note, CD25 expression was not detectable on RMA-S cells cultured *in vitro* or isolated *ex vivo*

from tumor-bearing mice (Figure 6.2). When mice were depleted of Treg, tumor growth initially progressed similar to the control group (Figure 6.3A). However, 10 days after tumor cell injection, tumors started to decrease in size and were eventually rejected in the majority of Treg depleted mice, whereas tumors continued to progressively grow in the PBS-treated control group. Similar results were obtained upon *s.c.* inoculation of RMA cells transduced with RAE-1, a ligand for the NK cell activating receptor NKG2D [69,70] (Figure 6.3B). These results demonstrate that Treg suppress the rejection of NK cell sensitive tumors, like the MHC class I-deficient RMA-S and the RAE-1 expressing RMA tumor cells.

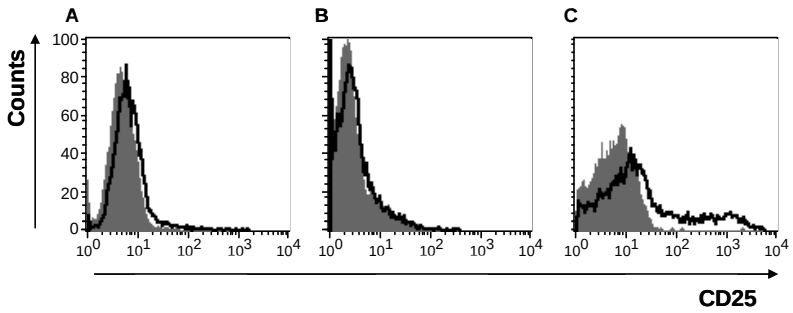


**Figure 6.2. RMA-S cells do not express CD25.** (A-C) Representative histogram plots documenting CD25 expression, as assessed by flow cytometry, on RMA-S cells cultured *in vitro* (A), RMA-S cells isolated from the tumors of RMA-S tumor bearing mice 21 days after *s.c.* tumor cell inoculation (B) and total splenic $CD4^+$ T cells (C). Staining with the specific antibody is indicated by the black line and the corresponding isotype control by the grey filled area. The data are representative of two experiments.

### 6.1.1.3 $NK1.1^+$ cells and $CD4^+CD25^-$ T cells mediate the rejection of RMA-S tumors in the absence of Treg

In order to investigate whether $NK1.1^+$ cells were required for the rejection of RMA-S tumors in the absence of Treg, we depleted $NK1.1^+$ cells alone or in combination with Treg depletion. Depletion of $NK1.1^+$ cells alone led to accelerated tumor growth in comparison to the PBS-treated control group, emphasizing the importance of this cell population for the control of RMA-S tumor growth (Figure 6.3C, left panel). In the absence of Treg, $NK1.1^+$ cell depletion initially resulted in an accelerated tumor growth, followed by a decrease in tumor size after day 10 of tumor inoculation (Figure 6.3C, right panel). This remarkable regression in the absence of $NK1.1^+$ cells, however, did not lead to complete tumor eradication, possibly due to the higher initial tumor load caused by the absence of $NK1.1^+$ cells. In summary, NK1.1 depletion led to enhanced tumor growth at early time points as depicted for day 7, irrespective of the presence or

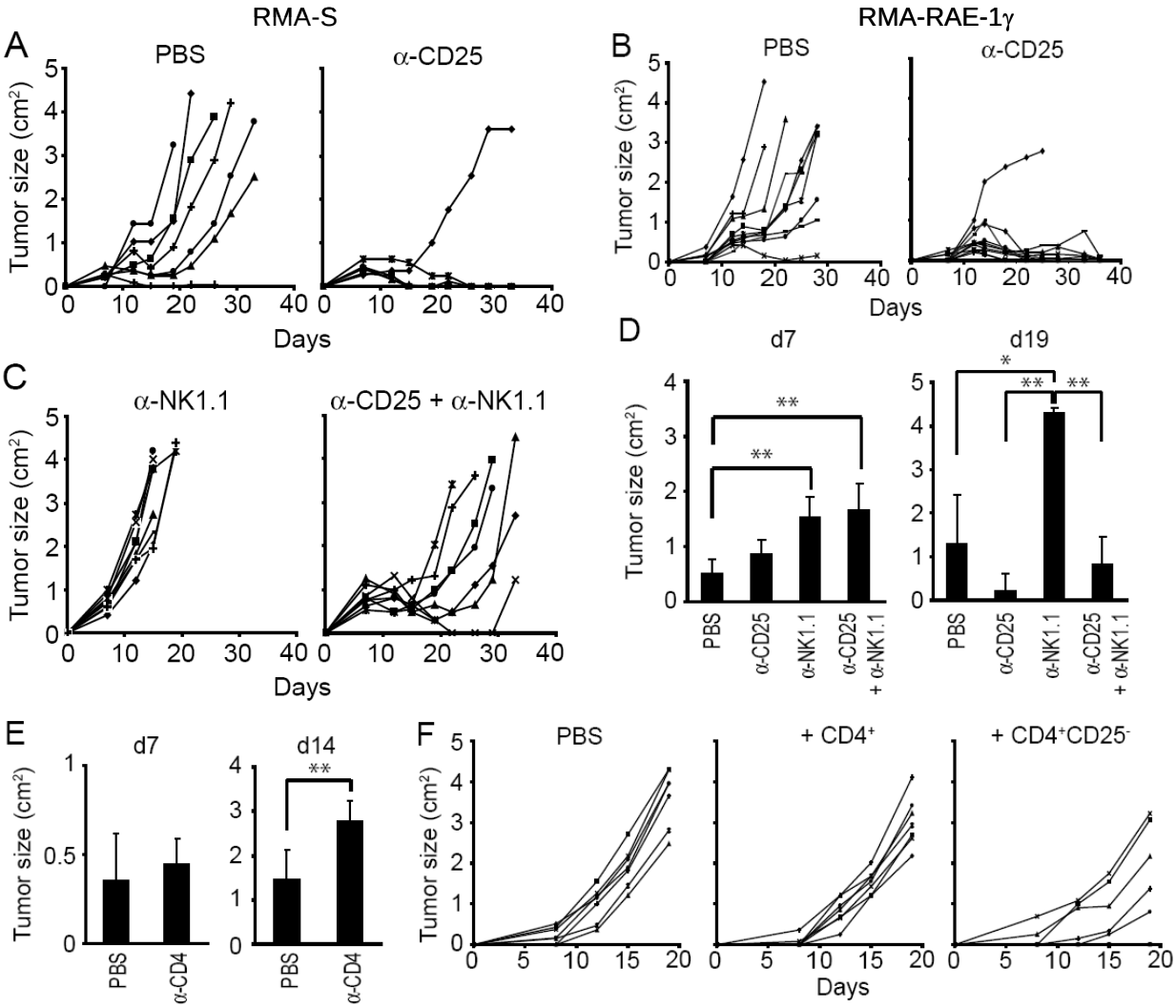


**Figure 6.3. NK1.1$^+$ cells and CD4$^+$CD25$^-$ T cells mediate rejection of RMA-S tumors in the absence of Treg.** (A) C57BL/6 mice were treated with PBS (left panel, n=8) or anti-CD25 mAb (right panel, n=6), before *s.c.* inoculation with RMA-S cells and tumor growth was monitored. (B) C57BL/6 mice were treated with PBS (left panel, n=10) or anti-CD25 mAb (right panel, n=10), before *s.c.* inoculation with RMA-RAE-1g cells and tumor growth was monitored. (C) C57BL/6 mice were treated with anti-NK1.1 (left panel, n=8) or anti-CD25 and anti-NK1.1 mAb (right panel, n=7), inoculated *s.c.* with RMA-S cells and tumor growth was monitored. (D) Bar graphs showing two representative time points of tumor growth as described in panels A and C. (E) Groups of 9 C57BL/6 mice were treated with PBS or anti-CD4 mAb, inoculated *s.c.* with RMA-S cells and tumor growth was monitored. Two representative time points of tumor growth are depicted in bar graphs. (F) C57BL/6 RAG2$^{-/-}$ mice were injected *i.v.* with PBS (left panel, n=7) or 2x10$^6$ CD4$^+$ T cells (middle panel, n=7) or 2x10$^6$ CD4$^+$CD25$^-$ T cells (right panel, n=5), 8 days before *s.c.* inoculation with RMA-S cells, and tumor growth was monitored. (D-E) Error bars depict SD of individual mice in the experiment. (A-C and F) Each line represents one single mouse. The results are representative of four (A), three (C) and two (B, E and F) experiments. *, $p<0.005$, **, $p<0.0005$ using Student's *t* test.

absence of Treg (Figure 6.3D, left panel), whereas Treg depletion had a strong impact on day 19 representing a later time point of tumor growth (Figure 6.3D, right panel). These data suggest that the initial phase of RMA-S tumor growth is controlled by $NK1.1^+$ cells regardless of the presence of Treg.

In several tumor models, depletion of the whole $CD4^+$ T cell compartment, comprising Treg, conventional $CD4^+$ T cells and a subset of NKT cells, had a similar impact on tumor growth as compared to Treg depletion alone [272,273]. Interestingly, in our model, depletion of the whole $CD4^+$ T cell compartment led to progressive tumor growth, which was even enhanced compared to the control group at a later time point, as depicted for day 14 (Figure 6.3E). Therefore, in the absence of Treg, conventional $CD4^+CD25^-$ T cells are important for the rejection of RMA-S tumors. The importance of $CD4^+CD25^-$ T cells in the anti-tumor response against RMA-S cells was analyzed in $RAG2^{-/-}$ mice. Total $CD4^+$ T cells including Treg, or $CD4^+CD25^-$ conventional T cells, isolated from naïve wt mice, were adoptively transferred into $RAG2^{-/-}$ recipients before *s.c.* inoculation of RMA-S tumor cells. Tumor growth in these mice was compared with tumor growth in $RAG2^{-/-}$ mice which did not receive any cells (PBS group). Adoptive transfer of the whole $CD4^+$ T cell compartment hardly affected RMA-S tumor growth when compared to mice which did not receive any cells (Figure 6.3F, left and middle panel). Most importantly, mice which received $CD4^+CD25^-$ T cells exhibited reduced tumor growth compared to mice which received the whole $CD4^+$ T cell compartment (Figure 6.3F, middle and right panel). This observation implies that Treg suppress $CD4^+CD25^-$ T cells during the anti-tumor response against RMA-S cells.

In conclusion, in the absence of Treg, $NK1.1^+$ cells and $CD4^+$ T cells are required for efficient rejection of high numbers of RMA-S tumor cells.

#### 6.1.1.4 Depletion of Treg leads to the generation of anti-tumor memory responses against RMA-S tumor cells

In a further step, we determined whether RMA-S tumor rejection in the absence of Treg also leads to the generation of immunological memory. Mice, which had rejected RMA-S tumors in the absence of Treg, were rechallenged with RMA-S tumor cells after being rested for 3 months. Mice, inoculated with tumor cells for the first time, were used as controls. In mice depleted of $CD25^+$ T cells during the primary response, the Treg compartment had completely recovered on

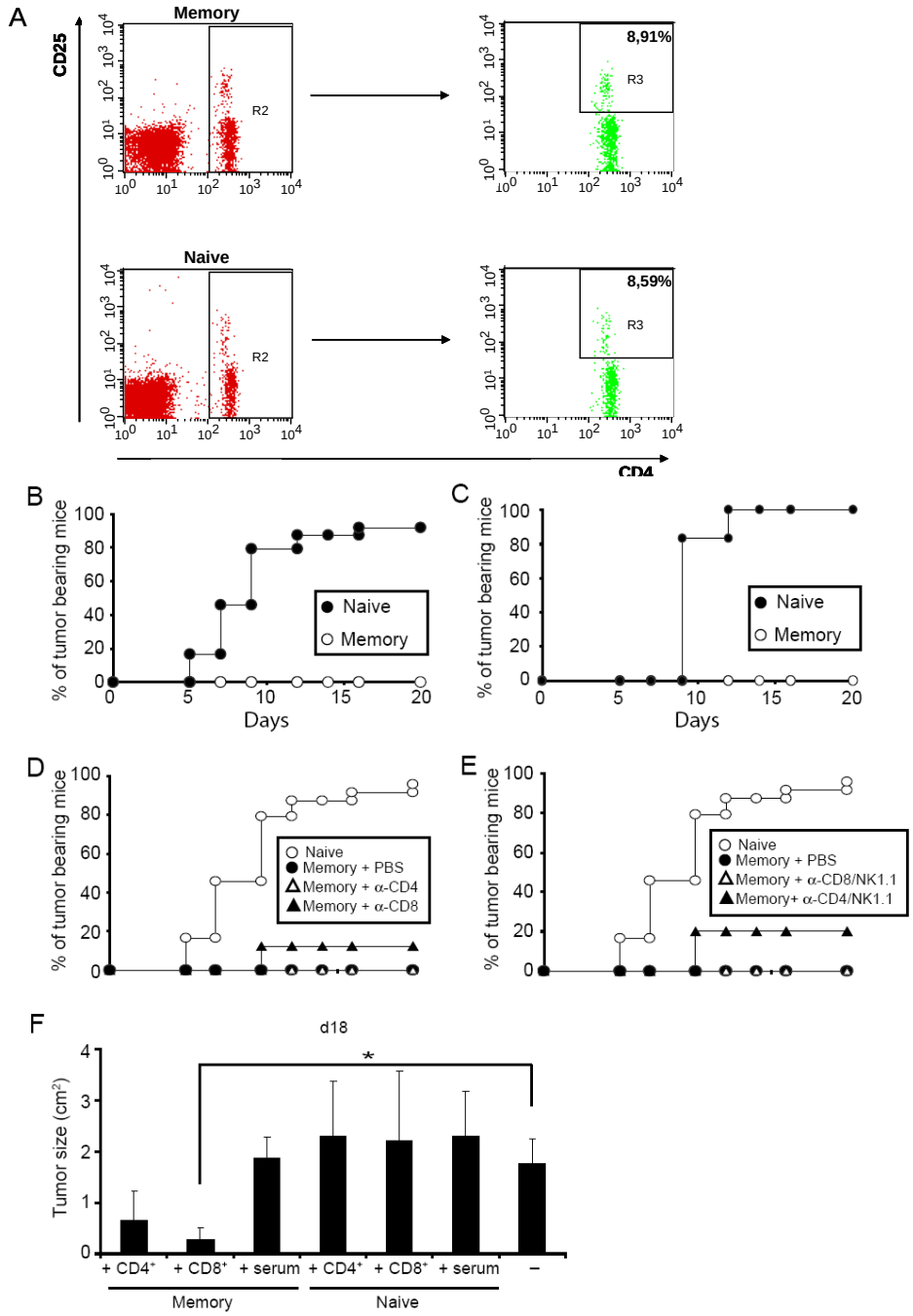


**Figure 6.4. Protective memory is generated in the absence of Treg.** (A-F) C57BL/6 mice were treated with anti-CD25 mAb before *s.c.* inoculation with RMA-S cells, rejected RMA-S tumors and rested for at least 3 months. These mice are designated as memory mice. (A) Three months after RMA-S tumor cell inoculation, the presence of $CD4^+CD25^+$ T cells was assessed by flow cytometry in the blood of memory (upper panels) versus naïve (lower panels) mice. Representative dot plots show CD4 and CD25 staining of PBL (left panels) or gated $CD4^+$ T cells (right panels). The percentages of $CD25^+$ cells (gate R3) among total $CD4^+$ T cells (gate R2) were calculated. (B) Naïve C57BL/6 mice (n=24, closed circles) or memory mice (n=17, open circles) were inoculated *s.c.* with RMA-S cells and tumor growth was monitored. (C) Naïve C57BL/6 mice (n=6) or memory mice (n=4) were inoculated *s.c.*

with RMA cells and tumor growth was monitored. (D) Memory mice were treated with PBS (n=4), anti-CD4 (n=4) or anti-CD8 (n=4) mAb, as designated, and inoculated *s.c.* with 1 x $10^6$ RMA-S cells. Naïve C57BL/6 mice (n=5) were also inoculated with RMA-S cells and tumor growth was monitored. (E) Memory mice were treated with PBS (n=5) or a combination of anti-CD4/NK1.1 (n=5) or anti-CD8/NK1.1 (n=5) mAb, as designated, and inoculated *s.c.* with RMA-S cells. Naïve C57BL/6 mice (n=5) were also inoculated with RMA-S cells and tumor growth was monitored. (F) $CD4^+$ or $CD8^+$ T cells or blood serum were isolated from memory or naïve mice, as designated, and transferred into naïve recipients before *s.c.* inoculation with RMA-S cells. Mice which did not receive any cells or serum were used as a control. A representative time point (day 18) of tumor growth is depicted in bar graphs. *, $p<0.01$ using Student's *t* test. The results are representative of four (B), two (A, D and F) and one (C and E) experiments.

the time of rechallenge, as determined by flow cytometric analysis 3 months after the primary challenge (Figure 6.4A). Thus, Treg were present at normal cell numbers at rechallenge. Upon rechallenge, protective immunity against the RMA-S tumor cells was observed in 100% of mice, whereas progressive tumor growth occurred in almost all of the mice that were injected with RMA-S cells for the first time (Figure 6.4B). Mice that had rejected RMA-S tumors after Treg depletion were also protected against the MHC class I-positive RMA tumor cells (Figure 6.4C).

In order to assess the nature of the memory induced in the absence of Treg, mice were depleted of various cell compartments before rechallenge with RMA-S cells. $CD4^+$ or $CD8^+$ T cell depletion alone was not sufficient to abrogate the memory response observed upon a secondary challenge with RMA-S cells (Figure 6.4D). Interestingly, simultaneous depletion of $NK1.1^+$ and $CD4^+$ cells or $NK1.1^+$ and $CD8^+$ cells only partially abrogated the memory response to a secondary challenge of RMA-S cells (Figure 6.4E). To gain further insight into the cell population(s) which mediate(s) memory responses against RMA-S tumor cells, $CD4^+$ T cells, $CD8^+$ T cells and blood serum were isolated from mice that had previously rejected RMA-S tumors after Treg depletion and were rested for at least 3 months after tumor cell inoculation; these mice are designated as memory mice from hereon. The cells or serum were subsequently transferred into naïve hosts prior to challenge with RMA-S cells. As shown in Figure 6.4F, transfer of $CD4^+$ T cells and, more prominently, of $CD8^+$ T cells isolated from memory mice had a protective effect for the hosts, since it led to reduced tumor growth in comparison to the mice which did not receive any cells or which received $CD4^+$ T cells or $CD8^+$ T cells isolated from naive mice. The role of $CD8^+$ T cells in RMA-S anti-tumor immunity is discussed in paragraph [4.1.3]. Transfer of serum isolated either from memory or naïve mice did not have any influence in tumor growth, excluding a role for humoral immunity in the RMA-S model. In summary our

results demonstrate that immune responses induced during Treg depletion led to the generation of protective cell-mediated immunological memory.

#### 6.1.1.5 Neutralization of IFN-γ abrogates RMA-S tumor rejection mediated by Treg depletion *in vivo*

IFN-γ was shown to mediate anti-tumor immune responses by several mechanisms [2,274]. Therefore, we sought of determining the levels of IFN-γ in the RMA-S model in the presence and absence of Treg. First, we assessed whether depletion of Treg would induce systemically increased levels of IFN-γ. Measurement of *in vivo* cytokine production is problematic owing to the rapid utilization, catabolization, and excretion of the cytokines quickly after secretion. We, therefore, used an *in vivo* IFN-γ capture assay, an adaptation of the standard cytokine ELISA [275]. This assay facilitates the measurement of cytokines in serum by increasing their *in vivo* half lives up to 1000-fold after *in vivo* administration of a biotinylated neutralizing mAb. Thus, we determined the levels of IFN-γ in the blood serum prepared from control or Treg depleted mice, 3, 5 and 9 days after RMA-S tumor inoculation and compared them with those found in the blood serum of naïve mice. No statistically significant difference in the levels of IFN-γ between control and Treg depleted mice or between naïve and tumor bearing mice was found (Figure 6.5A). These data suggest that during the anti-tumor response against RMA-S cells, no systemic IFN-γ production occurs.

In a second step, we determined IFN-γ levels, locally, in the tumor tissue. Significantly increased levels of this cytokine were detected in RMA-S tumors of Treg depleted mice relative to the PBS group (Figure 6.5B). By intracellular staining, we observed that IFN-γ was predominantly produced by $CD8^+$ T cells, NK cells and to a lower extent by $CD4^+$ T cells in the tumor tissue (Figure 6.5C). Most importantly, the percentages of IFN-γ-producing cells were increased in the absence of Treg, suggesting a suppressive effect by Treg. Thus, we studied the contribution of IFN-γ to RMA-S tumor rejection in the absence of Treg. Figure 6.5D shows that, although $CD25^+$ cell depletion alone led to tumor rejection, combined treatment of mice with anti-CD25 and neutralizing anti-IFN-γ mAb abrogated this effect resulting in tumor growth with similar kinetics as in the control mice. The presence of IFN-γ was important during the first week after tumor inoculation, since neutralization of IFN-γ solely after day 7 of tumor inoculation only

minimally affected tumor growth in the absence of Treg (data not shown). These results demonstrate that Treg suppress IFN-γ production and that IFN-γ is crucial for the rejection of RMA-S tumors in the absence of Treg.

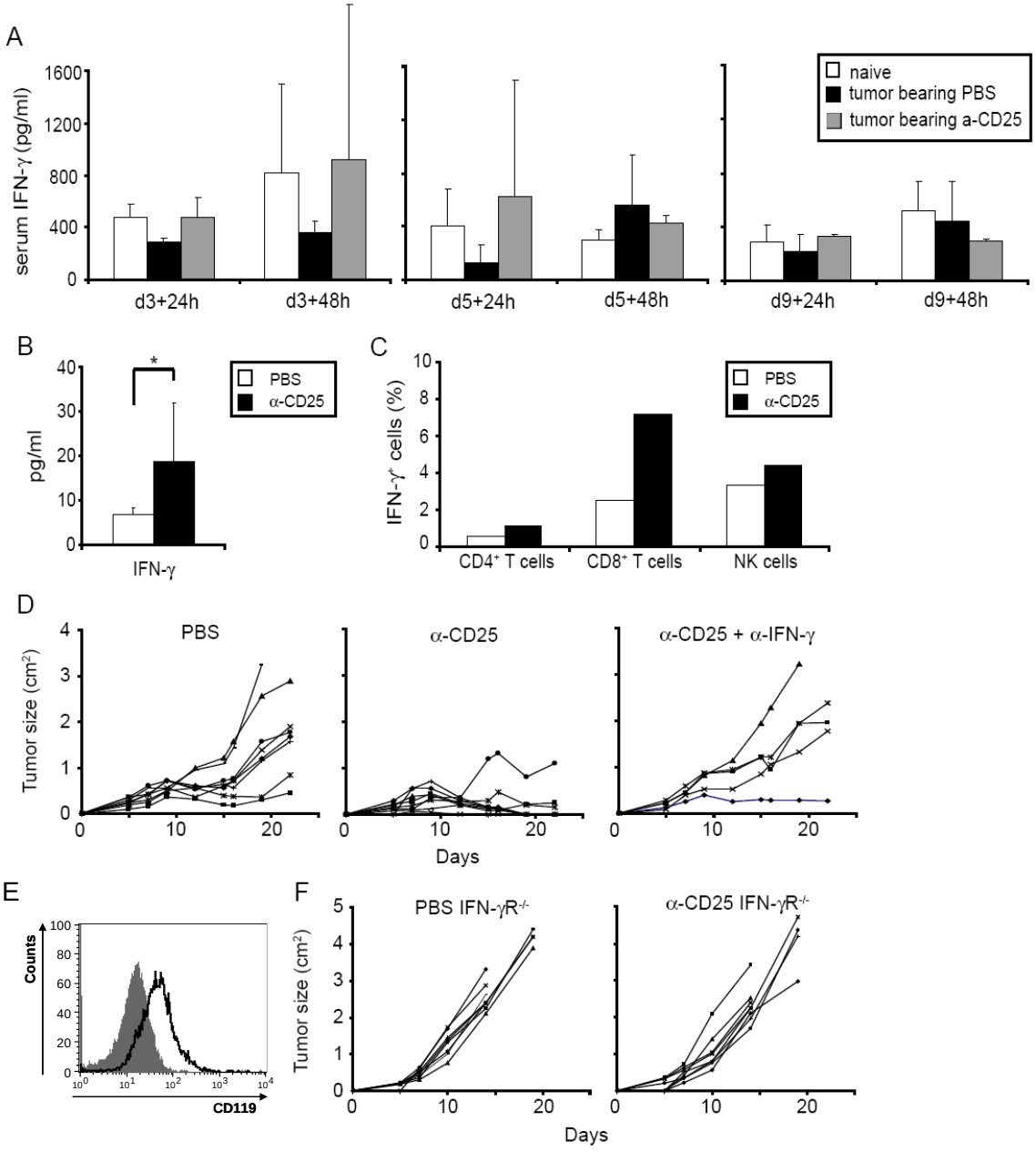


**Figure 6.5. IFN-γ is required for RMA-S tumor rejection in the absence of Treg.** (A) C57BL/6 mice were treated with PBS or anti-CD25 mAb, as indicated, and were inoculated *s.c.* with RMA-S cells. Three, 5 and 9 days after tumor cell inoculation, mice were injected *i.v.* with anti-IFN-γ biotin-conjugated mAb and blood serum was collected 24 or 48h after injections. IFN-γ levels in the serum were subsequently determined with an *in vivo* capture assay. Naïve C57BL/6 mice which were not inoculated with RMA-S cells were used as a control. The data show the mean ± S.D. of 2-3 mice per group and time point. (B) C57BL/6 mice were treated with PBS or anti-CD25 mAb, as

indicated. 10 days later tumors were removed and IFN-γ levels were determined in total tumor lysates by Bioplex analysis. Data show the mean ± SD of lysates from seven animals per group. *, $p<0.05$ using Student's *t* test. (C) C57BL/6 mice were treated with PBS (n=3) or anti-CD25 mAb (n=3), as indicated. 10 days later tumors were removed, pooled single cell suspensions were prepared, and IFN-γ positive $CD4^+$ T cells, $CD8^+$ T cells or NK cells ($NK1.1^+CD3^-$) were determined by intracellular staining. (D) C57BL/6 mice were treated with PBS (left panel, n=8) or anti-CD25 mAb (middle panel, n=8) or anti-CD25 and anti-IFN-γ mAb (right panel, n=5), inoculated *s.c.* with RMA-S cells and tumor growth was monitored. (E) Representative histogram plot documenting CD119 (IFN-gR, a chain) expression on RMA-S cells, as assessed by flow cytometry. Staining with the specific antibody is indicated by the black line and the corresponding isotype control by the grey filled area. (F) C57BL/6 IFN-$\gamma R^{-/-}$ mice were treated with PBS (n=8) or anti-CD25 mAb (n=8), as indicated, before *s.c.* inoculation with RMA-S cells, and tumor growth was monitored. (D and F) Each line represents one single mouse. The results are representative of two (C, D and F) and one (A, B and E) experiments.

Next, we tested whether IFN-γ acted directly on RMA-S cells or on cells of the host to mediate tumor rejection in the absence of Treg. To address this question, we injected RMA-S cells, which express IFN-γR (Figure 6.5E), into IFN-$\gamma R^{-/-}$ mice. In this experimental setup, only the tumor cells responded to IFN-γ. Subsequent monitoring of tumor growth revealed that IFN-$\gamma R^{-/-}$ mice exhibited enhanced tumor growth in comparison to the wt controls, indicating the contribution of IFN-γ signaling on host cells for tumor control in the presence of Treg (Figure 6.5F). More importantly, depletion of Treg had no impact on tumor growth in IFN-$\gamma R^{-/-}$ mice in comparison to IFN-$\gamma R^{-/-}$ mice injected with PBS (Figure 6.5F). This finding suggests that IFN-γ signaling in host cells is essential for tumor rejection in the absence of Treg.

#### 6.1.1.6 Perforin, FasL and inhibition of angiogenesis are not involved in the rejection of RMA-S tumor in the absence of Treg

In order to determine the mechanism leading to RMA-S tumor rejection in the absence of Treg, we investigated the role of perforin and the CD95-CD95L pathway. Perforin-mediated cytotoxicity has been shown to be important for the control of RMA-S tumor growth by NK cells [20]. While perforin$^{-/-}$ mice showed enhanced RMA-S tumor growth in comparison to the wt group in the presence of Treg, reduced tumor growth was observed in these mice after Treg depletion (Figure 6.6A). The CD95-CD95L pathway is known to be important for $CD4^+$ T cell-mediated cytotoxicity [276] and FACS staining revealed that RMA-S cells express CD95 (Figure 6.6B). Nevertheless, neutralization of CD95L *in vivo* by injection of MFL-4 mAb [277] did not

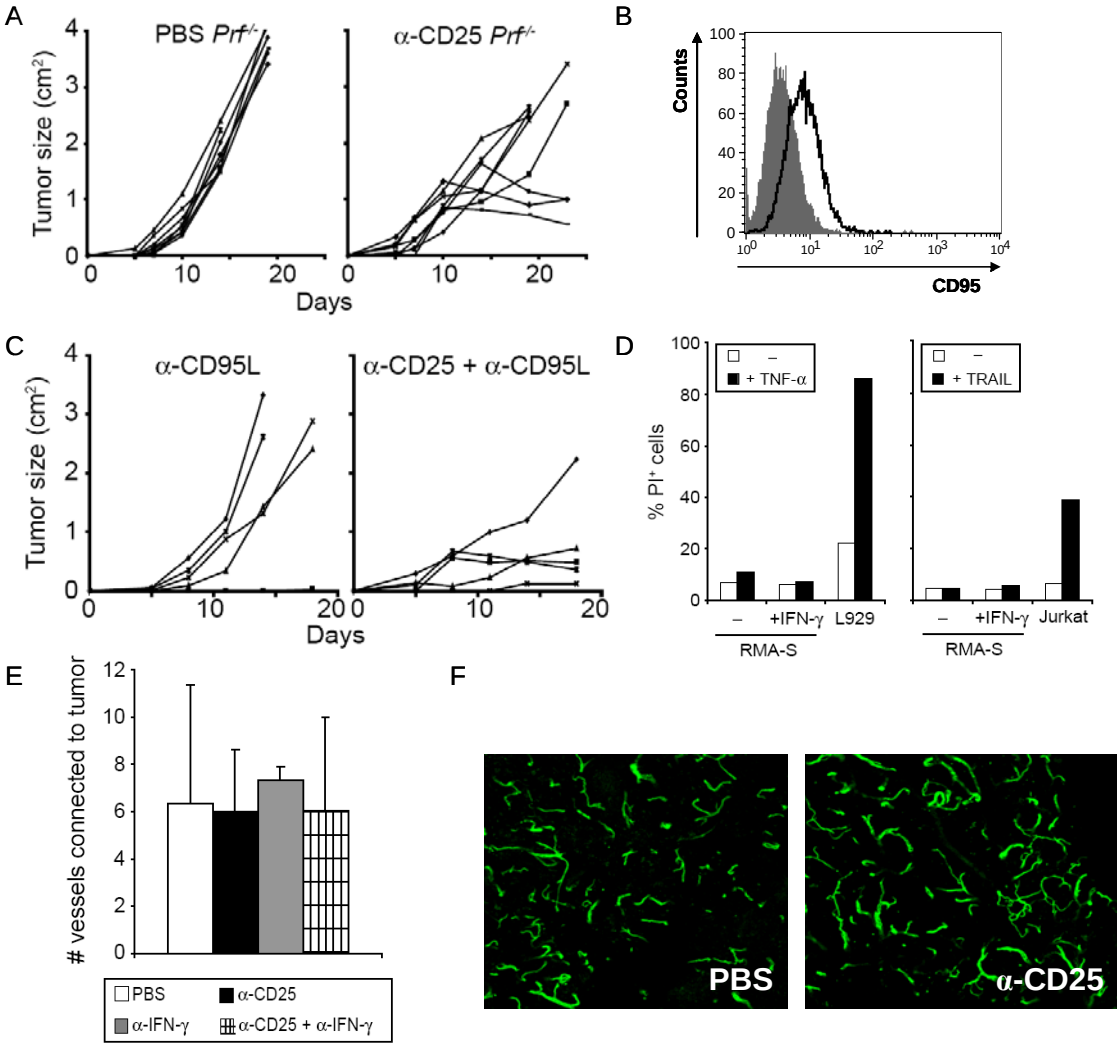


**Figure 6.6. Perforin, CD95L and inhibition of angiogenesis are not involved in the rejection of RMA-S tumors in the absence of Treg.** (A) Groups of 8 perforin$^{-/-}$ (*Prf* $^{-/-}$) mice were treated with PBS or anti-CD25 mAb, as indicated, before *s.c.* inoculation with RMA-S cells, and tumor growth was monitored. The results are representative of two experiments. (B) Representative histogram plot documenting CD95 expression on RMA-S cells, as assessed by flow cytometry. Staining with the specific antibody is indicated by the black line and the corresponding isotype control by the grey filled area. (C) Groups of 5 C57BL/6 wt mice were treated with anti-CD25 and/or anti-CD95L mAb, as indicated, before *s.c.* inoculation with RMA-S cells and tumor growth was monitored. (A and C) Each line represents one single mouse. (D) RMA-S cells cultured in the absence or presence of 50U/ml IFN-γ for 24h were additionally cultured for 6h in the absence or presence of TNF-α or TRAIL and dead cells, defined as PI$^{+}$ cells, were determined at the end of incubation by flow cytometric analysis. L929 and Jurkat cells were used as positive control for TNF-α- or TRAIL-induced *in vitro* apoptosis. (E) Groups of 3 C57BL/6 mice were treated with PBS, anti-CD25 mAb, and/or anti-IFN-γ mAb, as indicated, before *s.c.* inoculation with RMA-S cells. Nine days later, mice were dissected and vessels leading to tumors were enumerated under a dissecting microscope. (F) Groups of 3 C57BL/6 mice were treated with PBS or anti-CD25 mAb, as indicated, before *s.c.* inoculation with RMA-S cells. Ten days

later, FITC-labeled *Lycopersicon esculentum* lectin was injected *i.v.* into mice and the tumor vasculature was observed in unfixed tumors by confocal microscopy.

influence neither tumor growth in the presence of Treg nor tumor rejection observed in the absence of Treg (Figure 6.6C). These data suggest that the anti-tumor effector mechanisms induced in the absence of Treg could still function in the absence of perforin and when CD95L was neutralized. In addition, cell viability of RMA-S cells, which were untreated or sensitized with IFN-γ, was not affected by incubation with TNF-α or TRAIL *in vitro* (Figure 6.6D).

Since IFN-γ was shown to inhibit tumor-induced angiogenesis [278], we determined vessel number and integrity in the presence or absence of Treg on day 10 of tumor growth, because at this time point the mean tumor sizes of control and Treg depleted mice were similar (Figure 6.3A). To address this question, PBS treated and Treg depleted mice, which were in addition neutralized or not for IFN-γ, were dissected on day 9 after tumor cell injection and vessels leading to tumors were enumerated under a dissecting microscope. No difference in the number of vessels connected to the tumor was documented among mice of the different groups (Figure 6.6E). For a more elaborate analysis of the tumor vasculature, FITC-labeled *Lycopersicon esculentum* lectin, an endothelial cell selective reagent, was injected into mice on day 10 of tumor growth and the tumor vasculature was observed by confocal microscopy. No differences regarding vessel number and vessel localization were observed between PBS and anti-CD25 treated mice (Figure 6.6F). In addition, no extravasion of the FITC-lectin was detected in any of the mice of control or Treg depleted groups, indicating that the vessels infiltrating the tumor tissue were functional in both groups. These data render it unlikely that angiogenesis is affected in the absence of Treg.

#### 6.1.1.7 In the absence of Treg, increased numbers of leukocytes accumulate in the RMA-S tumor tissue in an IFN-γ dependent manner

Tumor-infiltrating lymphocytes have been found in many tumors and their numbers have been correlated with control or progression of tumor growth. In a recent study, a high density of immune cells, including T cells, correlated with longer survival in patients with colorectal cancer [279]. Thus, we investigated the accumulation of leukocytes in the RMA-S tumors in the presence or absence of Treg. We determined the quantity of leukocytes as percentages of total live cells in

the tumor in mice treated with PBS or anti-CD25 mAb on days 7-10. To clearly distinguish between tumor cells and infiltrating leukocytes within the tumor tissue, we injected $Ly5.2^+$ RMA-S tumor cells into congenic C57BL/6-$Ly5.1^+$ mice. Flow cytometric analysis revealed that infiltrating $Ly5.1^+$ cells represented higher percentages of total cells in the tumors of Treg depleted mice (Figure 6.7A). There was a significant increase in both the percentages and absolute cell numbers of leukocytes accumulating within the tumor mass, when Treg were depleted ($7.46 \pm 2.46 \times 10^5$ cells in the PBS group versus $14.6 \pm 4.3 \times 10^5$ cells in the anti-CD25 group, $p<0.0005$). Absolute tumor cell numbers and tumor volume were virtually identical between the two groups at the investigated time points (data not shown).

Since we found a requirement of IFN-γ for tumor rejection in the absence of Treg (Figure 6.5D), we asked whether the presence of IFN-γ is required for the accumulation of leukocytes. We neutralized IFN-γ in the presence or absence of Treg and determined percentages of $Ly5.1^+$ leukocytes infiltrating the $Ly5.2^+$ tumors. Interestingly, the enhanced leukocyte accumulation in the absence of Treg was abrogated when IFN-γ was neutralized. IFN-γ neutralization alone did not lead to a reduction in tumor-infiltrating leukocytes in comparison to the control group (Figure 6.7A). In summary, these results indicate that Treg hamper leukocyte accumulation in the tumors, and this accumulation is IFN-γ dependent.

#### 6.1.1.8 Increased numbers of NK cells, conventional $CD4^+$ T cells and macrophages are detected in the RMA-S tumors in the absence of Treg

By analyzing individual leukocyte subpopulations, we observed that $CD11b^+$ cells, NK cells ($NK1.1^+CD3^-$) and conventional $CD4^+$ T cells ($CD4^+CD25^-$) were all increased in the absence of Treg (Figure 6.7B). The overall cellular composition of the infiltrating leukocyte compartment was comparable in both groups, with $CD11b^+$ cells comprising up to 80% of all leukocytes. As observed with the whole $Ly5.1^+$ compartment, the increased $CD11b^+$ and $CD4^+$ T cell accumulation in the absence of Treg was abrogated upon IFN-γ neutralization. Strikingly, almost no NK cells were detected in the tumor after IFN-γ neutralization (Figure 6.7B, insert). Figure 6.7B demonstrates that $CD11b^+$ cells were the most prominent leukocyte subpopulation infiltrating the RMA-S tumor tissue after depletion of Treg. We further characterized the various $CD11b^+$ cell subtypes and determined their accumulation in the absence of Treg. Macrophages, defined as $CD11b^+F4/80^+$ cells, dendritic cells (DC), defined as $CD11b^+CD11c^+$ cells and

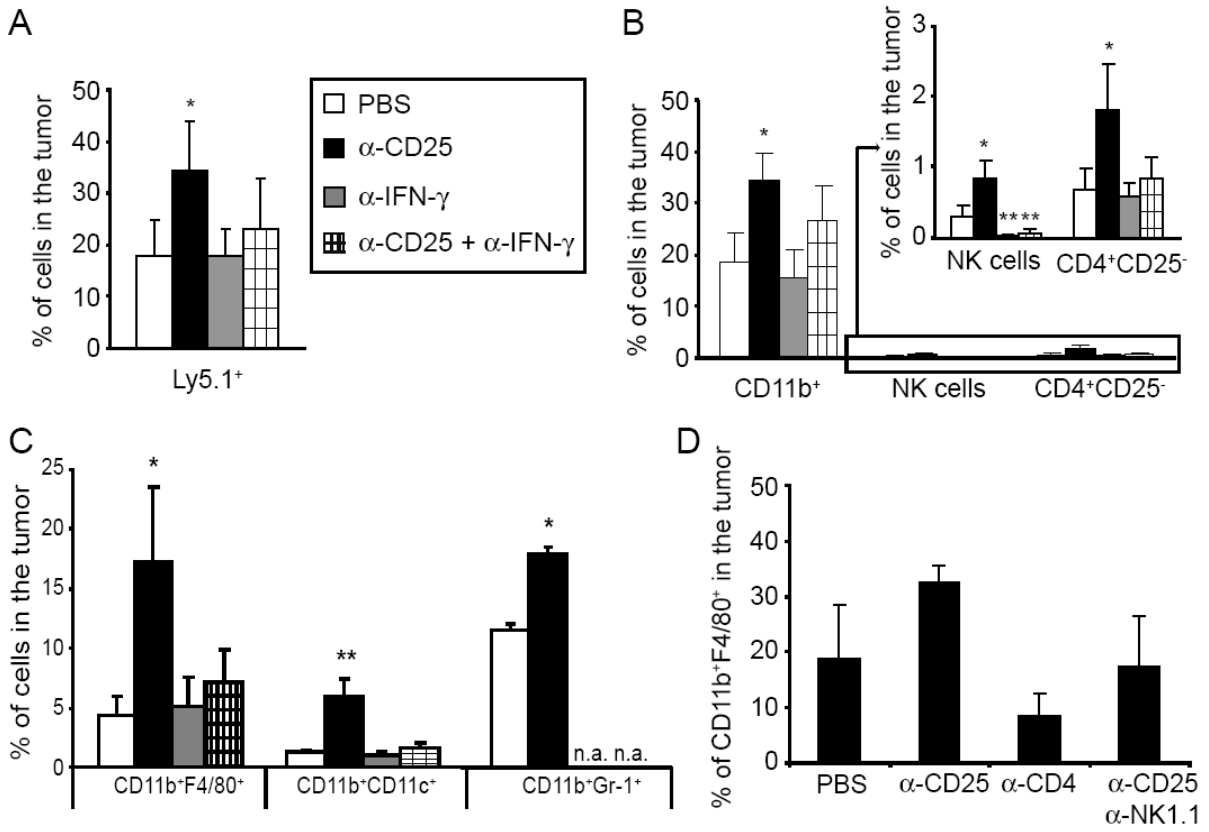


**Figure 6.7. Increased numbers of leukocytes accumulate in the RMA-S tumors in an IFN-γ dependent manner in the absence of Treg.** (A-C) C57BL/6-Ly5.1$^+$ mice were treated with PBS (white bars) or anti-CD25 mAb (black bars) or anti-IFN-γ mAb (grey bars) or anti-CD25 and anti-IFN-γ mAb (checkered bars) and inoculated *s.c.* with Ly5.2$^+$ RMA-S cells. Seven to 10 days later, tumors were removed and infiltrating Ly5.1$^+$ (A), CD11b$^+$, NK (NK1.1$^+$CD3$^-$) and CD4$^+$CD25$^-$ cells (B), or CD11b$^+$F4/80$^+$ cells (C) were determined by flow cytometric analysis and quantified as percentages of total live cells in the tumor. (D) C57BL/6-Ly5.1$^+$ mice were treated with PBS or anti-CD25 mAb or anti-CD4 mAb or anti-CD25 and anti-NK1.1 mAb and inoculated *s.c.* with Ly5.2$^+$ RMA-S cells. Ten days later, tumors were removed and infiltrating CD11b$^+$F4/80$^+$ cells were determined by flow cytometric analysis and quantified as percentages of total live cells in the tumor. (A-B) Data are pooled from 4 independent experiments using 5 animals per group. (C-D) Data show the mean ± SD of 3-5 animals per group and are representative of three (C) and one (D) experiments. *, $p<0.05$, **, $p<0.005$ in comparison to the PBS group, using Student's *t* test. n.a. = not analyzed.

granulocytes, defined as CD11b$^+$Gr-1$^+$ cells, were all detected in significantly higher numbers within the tumor tissue on day 10 of tumor growth (Figure 6.7C). Similar to the whole CD11b$^+$ compartment, the increased accumulation of all these populations in the absence of Treg was dependent on IFN-γ (Figure 6.7C). CD11b is also expressed on NK cells, characterizing their final maturation stage [17]. Approximately 85% of the NK cells infiltrating the tumor tissue on day

10 of tumor growth were positive for the CD11b marker (Figure 6.18). However, the overall NK cell population is only a minor fraction of the whole $CD11b^+$ population (Figure 6.7B). Cell depletion experiments revealed that predominantly $CD4^+$ T cells and NK cells were important for the observed enhanced macrophage accumulation (Figure 6.7D). In summary, our data demonstrate that Treg suppress the accumulation of NK cells, $CD4^+CD25^-$ T cells and $CD11b^+$ cells, including macrophages, in the RMA-S tumors and this accumulation is IFN-γ dependent. In addition, NK cell accumulation in the tumors is absolutely dependent on IFN-γ, irrespective of the presence of Treg.

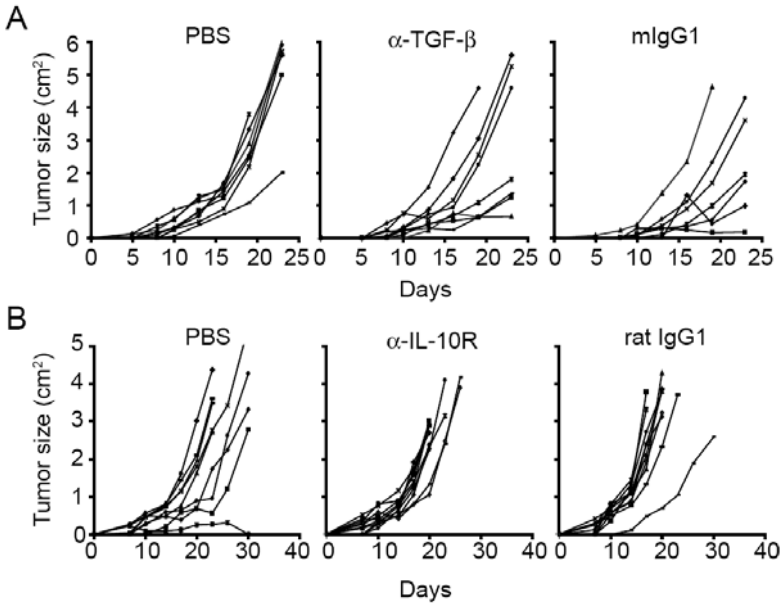


**Figure 6.8. Treg suppress the anti-tumor response against RMA-S independently of TGF-β or IL-10.** (A) Groups of 8 C57BL/6 mice were treated with PBS (left panel) or anti-TGF-b mAb (middle panel) or the appropriate isotype control (mouse IgG1, right panel), were *s.c.* inoculated with RMA-S cells and tumor growth was monitored. Data are representative of two experiments. (B) Groups of 8 C57BL/6 mice were treated with PBS (left panel), anti-IL-10R mAb (middle panel) or the appropriate isotype control (rat IgG1, right panel), were *s.c.* inoculated with RMA-S cells and tumor growth was monitored. (A and B) Each line represents one single mouse.

### 6.1.1.9 Treg suppress RMA-S anti-tumor immunity independently of TGF-β or IL-10

Finally, we wanted to address the question via which mechanism do Treg exert their suppressive effect on the anti-tumor immunity against RMA-S tumor. In certain *in vivo* models, Treg were shown to mediate their suppressive activity via the production of TGF-β [280]. Thus, we examined whether neutralization of TGF-β in mice injected with RMA-S tumor cells would abrogate Treg mediated suppression and thus lead to a similar outcome on tumor growth as Treg depletion.

Figure 6.8A shows that after neutralization of TGF-β, RMA-S cells grew progressively similar to control mice. These data suggest that, in our model, Treg-mediated suppression is independent of TGF-β. Another important Treg-derived factor reported to mediate suppression is IL-10 [281]. *In vivo* administration of a blocking antibody against the IL-10R was not able to affect RMA-S tumor growth, when compared to the administration of an isotype-matched control (Figure 6.8B). In conclusion our data show that in the RMA-S tumor model Treg do not use neither TGF-β nor IL-10 to exert their suppressive function.

## 6.1.2 Regulatory T cells suppress macrophage activation in lymphoma

### 6.1.2.1 Increased amounts of MHC class II on macrophages in the absence of Treg

The observation that $CD11b^+$ cells were the most prominent cell population infiltrating the RMA-S tumors in the absence of Treg, along with the importance of $CD4^+$ T cells for tumor rejection, prompted us to study MHC class II expression on tumor-infiltrating leukocytes on day 10 of tumor growth. Interestingly, as shown in Figure 6.9A and 6.9B, left panel, higher percentages of MHC class II-expressing macrophages ($CD11b^+F4/80^+$) were found in the tumors of Treg depleted mice (49.6 ± 7.9% versus 28.4 ± 6.4% in the PBS group, $p<0.05$). Furthermore, the geometric mean fluorescence intensity (MFI) of MHC class II was also significantly increased on macrophages infiltrating the RMA-S tumors of the Treg depleted mice (Figure 6.9B, right panel). Notably, the MHC class II upregulation in the absence of Treg was abrogated by neutralization of IFN-γ, whereas IFN-γ neutralization alone did not have any significant effect on macrophage MHC class II expression (Figure 6.9B). Expression levels of the costimulatory molecules CD80 (B7-1) and CD86 (B7-2) on tumor-infiltrating macrophages were similar between PBS treated and Treg depleted groups, although – concerning CD80 – the MFI was significantly enhanced when compared to blood monocytes of tumor bearing mice (Figure 6.9C).

B7-H4, an inhibitory member of the B7 family, has been shown to be induced on human monocytes after *in vitro* co-culture with Treg [191]. In addition, B7-H4 expression on macrophages infiltrating ovarian tumors correlated with the patients' survival [192]. Expression levels of B7-H4 were determined on tumor-infiltrating macrophages in the RMA-S model. Increased expression

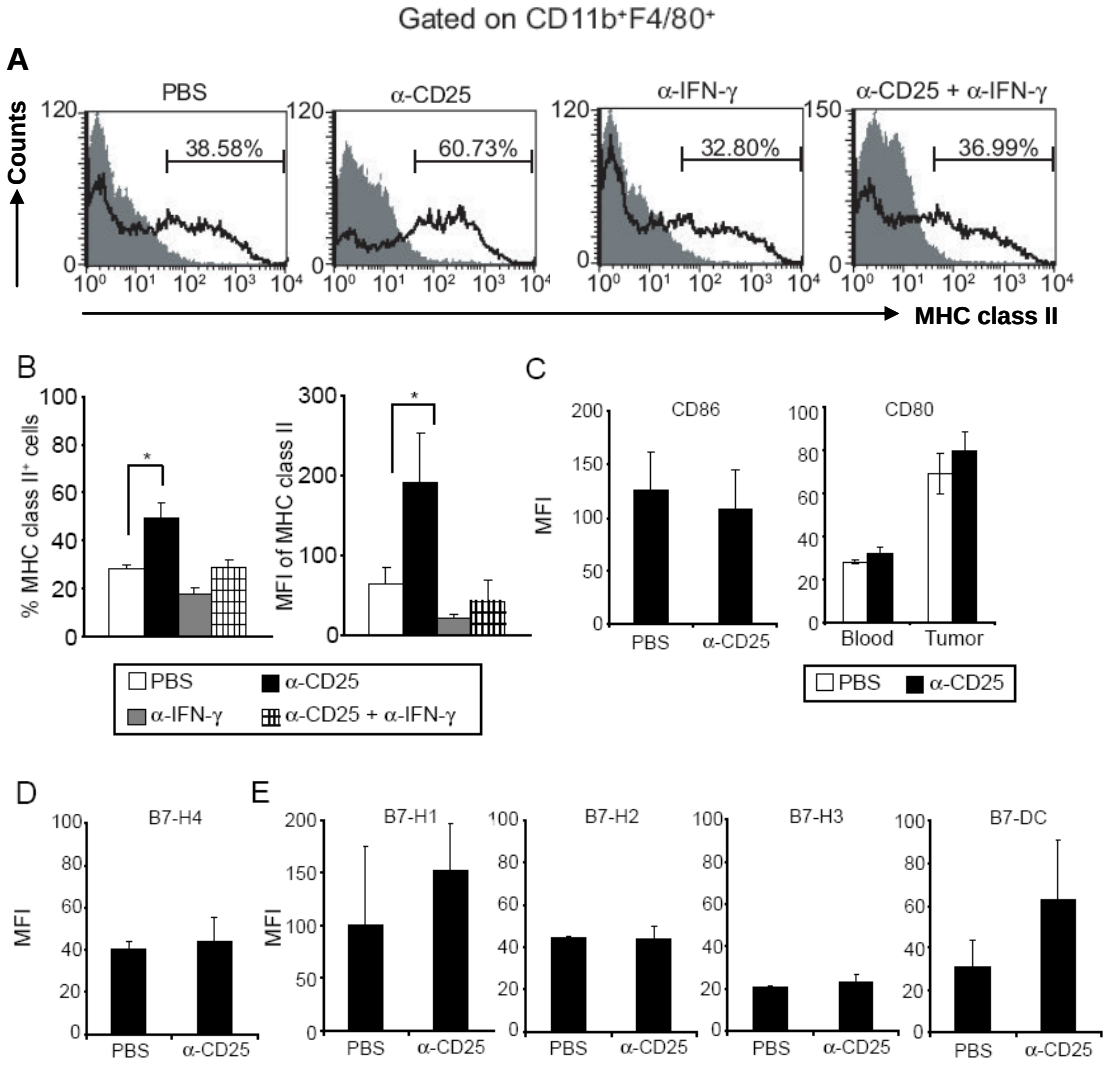


**Figure 6.9. Increased MHC class II expression of tumor-infiltrating macrophages in the absence of Treg.** (A-B) C57BL/6 mice were treated with PBS, anti-CD25 mAb, and/or anti-IFN-γ mAb, as indicated, before *s.c.* inoculation with RMA-S cells and 10 days later tumors were removed. (A) Tumor-infiltrating $CD11b^+F4/80^+$ cells were gated and analyzed for MHC class II expression, as shown in the histograms (one representative analysis out of six mice per group is shown). Staining with the specific antibody is indicated by the black line and the corresponding isotype control by the grey filled area. (B) Percentages of MHC class II-expressing $CD11b^+F4/80^+$ cells (left panel) and MFI of MHC class II of $CD11b^+F4/80^+$ cells (right panel) in the tumor tissue of PBS (white bars) or anti-CD25 mAb (black bars) or anti-IFN-γ mAb (grey bars) or anti-CD25 and anti-IFN-γ mAb (checkered bars) treated mice. Data show the mean ± SD of three animals per group and are representative of two experiments. *, $p< 0.05$, using Student's *t* test. (C-E) C57BL/6 mice were treated with PBS or anti-CD25 mAb, as indicated, before *s.c.* inoculation with RMA-S cells, and 10 days later, tumors (C-E) and blood (C, right panel) were removed. $CD11b^+F4/80^+$ cells were gated and analyzed for CD86 and CD80 (C), B7-H4 (D) B7-H1, B7-H2, B7-H3 and B7-DC (E) expression. (C-E) Data show the mean ± SD of three animals per group.

of cell surface B7-H4 was detected on tumor-infiltrating macrophages as compared to blood monocytes of tumor bearing hosts; however, no differences in B7-H4 expression were observed on tumor-infiltrating macrophages between PBS and anti-CD25 treated mice (Figure 6.9D). When B7-H4 expression was monitored by intracellular staining, high levels of this molecule were detected on both blood and tumor-infiltrating macrophages; however, again, no differences were detected between PBS and anti-CD25 treated mice (data not shown). Finally, we analyzed the tumor-infiltrating macrophages for the expression of other B7 family members, namely B7-H1, B7-H2, B7-H3 and B7-DC. B7-DC, and to a lesser extent B7-H3, expression was induced on tumor-infiltrating macrophages as compared to blood monocytes of tumor bearing hosts (data not shown). However, no difference was observed between PBS and anti-CD25 treated mice (Figure 6.9E). B7-H1 and B7-H2 were highly expressed by both blood and tumor-infiltrating macrophages, but no significant difference could be documented between PBS and anti-CD25 treated groups (Figure 6.9E). In conclusion, our data suggest that in the RMA-S tumor model expression of B7-H1, B7-H2, B7-H3, B7-H4 and B7-DC on tumor-infiltrating macrophages is not controlled by Treg.

#### 6.1.2.2 Enhanced macrophage activity in the absence of Treg

In order to further characterize the macrophages infiltrating the RMA-S tumors in the presence or absence of Treg, cytokine production of freshly isolated tumor-infiltrating macrophages was assessed after 12 h of culture in medium alone (Figure 6.10A, upper panel) or in the presence of RMA-S cells in combination with LPS to induce maximum release of cytokines (Figure 6.10A, lower panel). The results demonstrate consistently higher levels of MIP-1β, MIP-2, MIP-1α, IL-6, IL-13 and IL-1β produced by macrophages isolated from tumors of Treg depleted mice compared to control mice (Figure 6.10A). Similar amounts of cytokines and chemokines were observed in cultures in the absence or presence of RMA-S cells without the addition of LPS, as shown representatively for MIP-2 and IL-6, suggesting that the presence of tumor cells did not influence the amounts of cytokines produced upon LPS stimulation (Figure 6.10B). IL-12 (p70), IFN-γ and VEGF were not detected. Analysis of the macrophage cytokine profile after 24 h of culture revealed a similar pattern (data not shown). *In vivo* IFN-γ neutralization did not affect the production of certain cytokines, such as IL-1β, while it pronouncedly increased the production of IL-6 (Figure 6.10C).

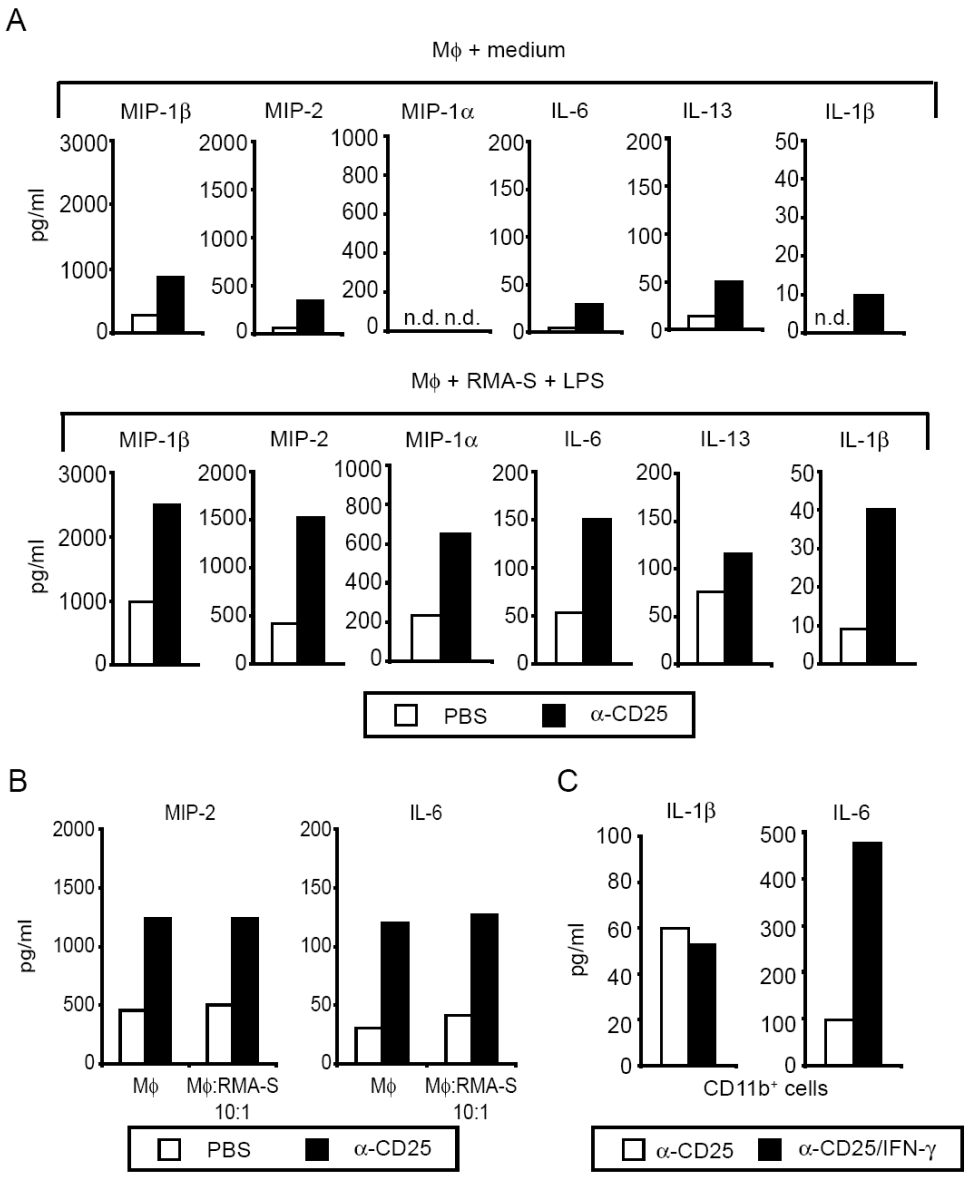


**Figure 6.10. Increased chemokine and cytokine production by tumor-infiltrating macrophages in the absence of Treg.** (A-B) C57BL/6 mice were treated with PBS (white bars) or anti-CD25 mAb (black bars), before *s.c.* inoculation with RMA-S cells, and 10 days later, tumors were removed. Tumor-infiltrating $CD11b^+F4/80^+$ cells were purified and cultured *in vitro* either with medium (A, upper panel) or RMA-S cells in a 5:1 ratio in combination with LPS (A, lower panel) or RMA-S cells in a 5:1 ratio alone (B) for 12 h and analyzed for chemokine and cytokine production by Bioplex. (C) C57BL/6 mice were treated with anti-CD25 mAb (white bars) or anti-CD25 and anti-IFN-γ mAb (black bars), before *s.c.* inoculation with RMA-S cells and 10 days later tumors were removed. Tumor-infiltrating $CD11b^+$ cells were purified and cultured *in vitro* either with medium for 24 h and analyzed for cytokine production by Bioplex. (A-C) Data are representative of three (A and B) and one (C) experiments. n.d. = not detectable.

Next, we examined whether macrophages, found in tumors of Treg depleted mice, could directly inhibit RMA-S tumor growth. For this purpose, $CD11b^+$ cells were enriched from tumors of control or Treg depleted mice; alternatively macrophages ($CD11b^+$ $F4/80^+$) were isolated by flow cytometric sorting (purity > 95%). These cells were cultured for 48 h with RMA-S cells and proliferation was monitored. Enriched $CD11b^+$ cells (Figure 6.11A, left panel) as well as macrophages purified by flow cytometric sorting (Figure 6.11A, right panel) suppressed RMA-S tumor cell growth at similar levels at a 10:1 ratio. In addition, they were significantly more potent when isolated from tumors of Treg depleted mice compared to cells from the control group (Figure 6.11A). Similar results were obtained after 24 h of co-culture, as shown representatively for enriched $CD11b^+$ cells (Figure 6.11B). No proliferation was detected when macrophages were cultured in the absence of tumor cells. $CD11b^+F4/80^-$ cells isolated from Treg depleted mice also suppressed RMA-S proliferation, in contrast to $CD11b^+F4/80^-$ cells isolated from PBS treated mice (Figure 6.11C). Treg were not present during the tumor cell growth inhibition assay indicating that the difference in the suppression between the two groups was not due to Treg contaminating the culture of macrophages derived from PBS treated mice (data not shown). Interestingly, RMA-S cell growth suppression by $CD11b^+$ cells was completely abrogated when IFN-γ was neutralized both in the presence and to a lesser extent – which was not statistically significant – in the absence of Treg, pinpointing a role for IFN-γ in enhancing the tumoristatic function of macrophages (Figure 6.11D).

#### 6.1.2.3 Macrophages kill RMA-S cells independently of the enzymatic activity of iNOS, PGE2 and IDO

In order to examine the mechanism of suppression of RMA-S proliferation by macrophages, we used a trans-well system to separate the macrophages from the RMA-S tumor cells during a 48h co-culture. Interestingly, the suppression of RMA-S proliferation was still observed when the cells were not in contact (Figure 6.12A), suggesting that a soluble factor was responsible for the effect. The suppression of RMA-S proliferation was not due to cell cycle arrest, since the presence of macrophages did not have any influence on the CFSE dilution of labeled RMA-S cells (Figure 6.12B). Interestingly, dead RMA-S cells, as documented by PI staining, could not be detected in the co-culture of macrophages and RMA-S cells, unless the two populations were separated with a trans-well insert (Figure 6.12C). At the same time, macrophages became $CFSE^+$

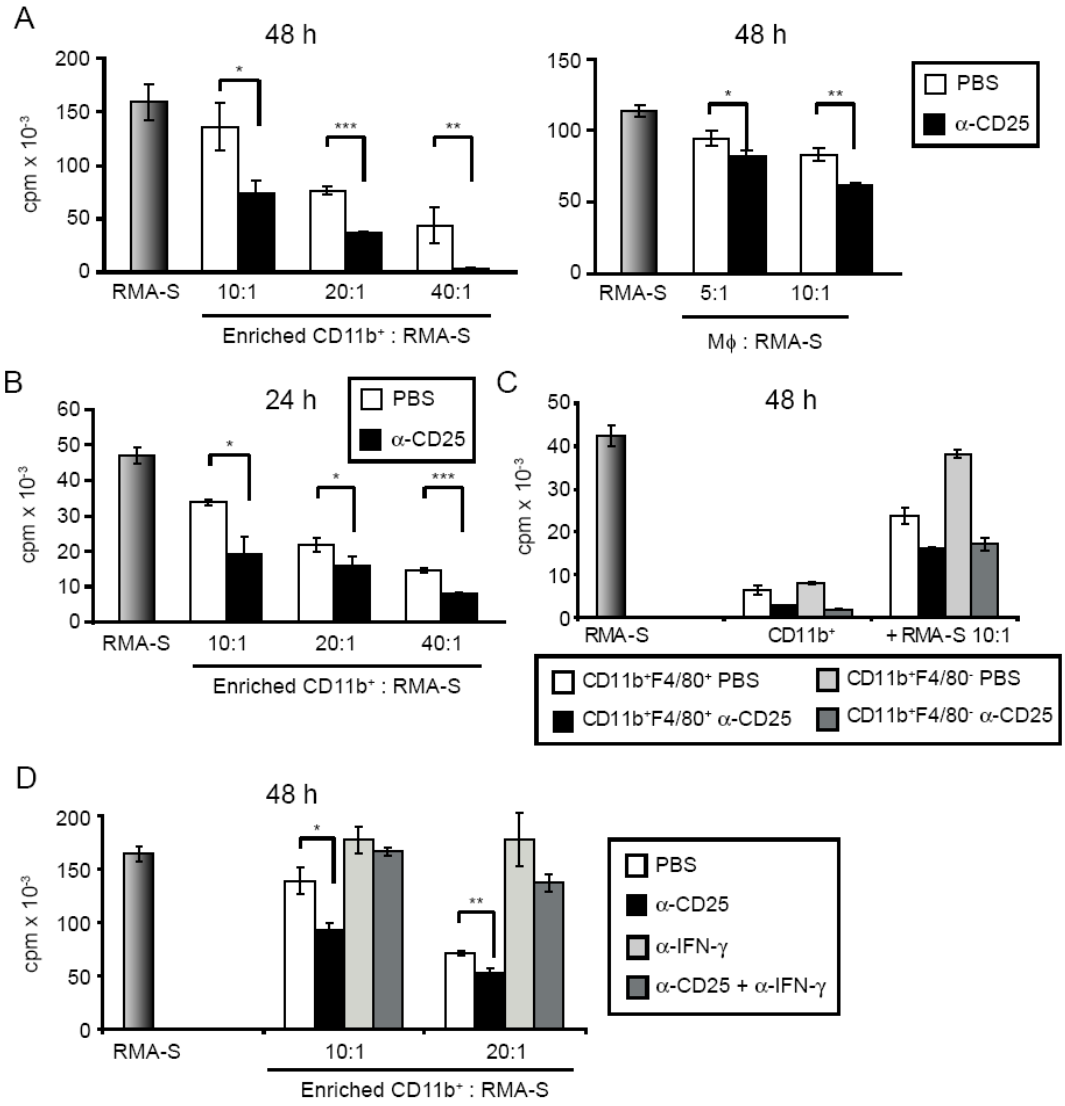


**Figure 6.11. Enhanced macrophage activity in the absence of Treg.** (A-D) C57BL/6 mice were treated with PBS or anti-CD25 and/or anti-IFN-γ mAb, as indicated, before *s.c.* inoculation with RMA-S cells and 10 days later, tumors were removed. (A) Enriched $CD11b^+$ cells (left panel) or purified macrophages ($CD11b^+F4/80^+$, >95% pure) (right panel) were isolated from tumors and co-cultured *in vitro* with RMA-S cells at the indicated ratios. After 48h of co-culture, tumor cell proliferation was monitored by $^3$H-thymidine incorporation assay. (B) Enriched $CD11b^+$ cells were isolated from tumors and co-cultured *in vitro* with RMA-S cells at the indicated ratios. After 24h of co-culture, tumor cell proliferation was monitored by $^3$H-thymidine incorporation assay. (C) Purified $CD11b^+F4/80^+$ or $CD11b^+F4/80^-$ cells were isolated from tumors (>95% pure) and co-cultured *in vitro* with RMA-S cells at a 10:1 ratio. After 48h of co-culture, tumor cell proliferation was monitored by $^3$H-thymidine incorporation assay. (D) Enriched $CD11b^+$ cells were isolated from tumors and co-cultured *in vitro* with RMA-S cells at the indicated ratios. After 48h of co-culture, tumor cell proliferation was monitored by $^3$H-thymidine incorporation assay. (A-D) Data represent mean ± SD of triplicate cultures and are representative of three (A and B) and one (C and D) experiments. *, $p<0.05$, **, $p<0.005$, ***, $p<0.0001$ using Student's *t* test.

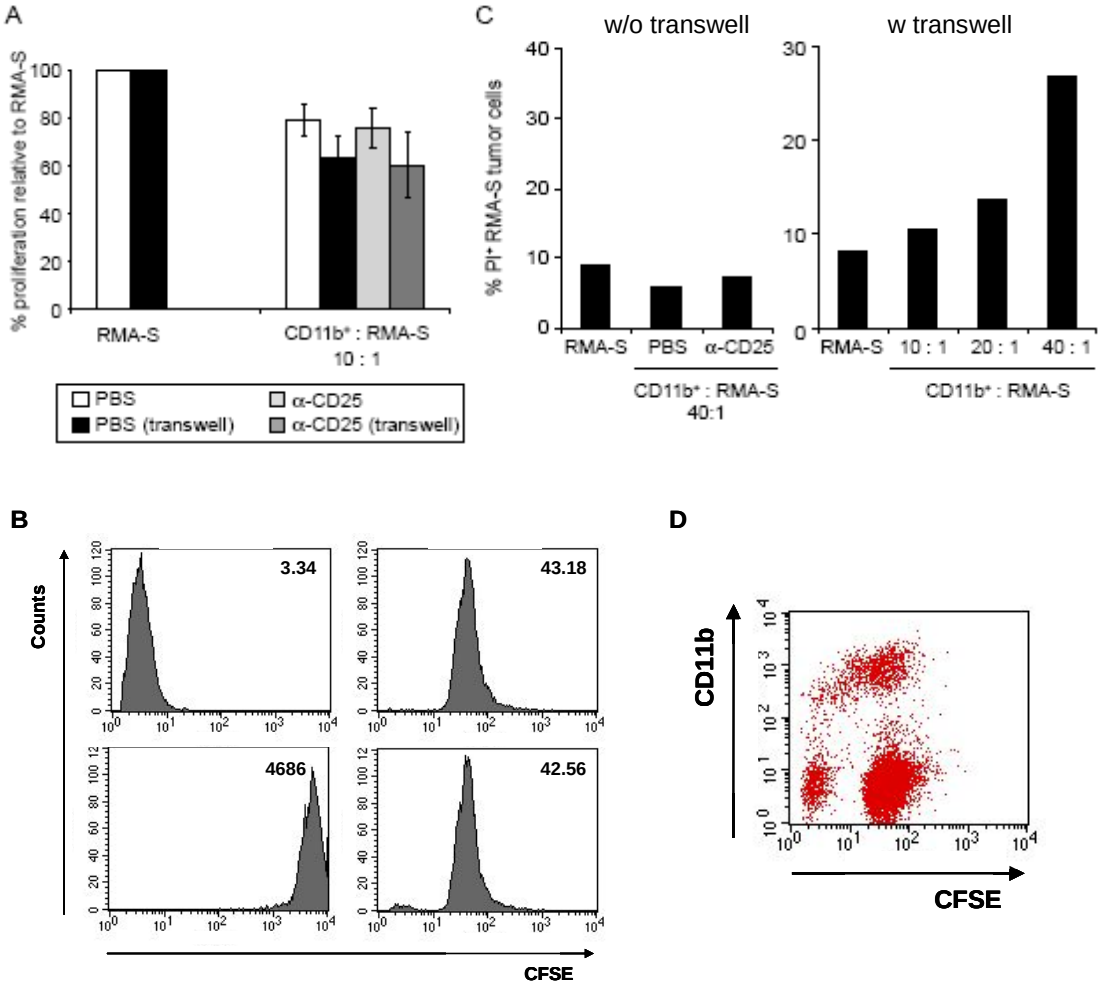


**Figure 6.12. Macrophages kill and phagocytose RMA-S cells *in vitro*.** (A-D) C57BL/6 mice were treated with PBS or anti-CD25 mAb, as indicated, before *s.c.* inoculation with RMA-S cells and 10 days later tumors were removed. (A) Enriched $CD11b^+$ cells were isolated from tumors and co-cultured *in vitro* with RMA-S cells in the absence or presence of a transwell insert at a 10:1 ratio. After 48h of co-culture, tumor cell proliferation was monitored by $^3$H-thymidine incorporation assay. The data represent mean ± SD of triplicate cultures. (B) RMA-S cells (unstained, upper left panel) were labeled with CFSE (t = 0, lower left panel) and cultured in the absence (upper right panel) or presence (lower right panel) of $CD11b^+$ cells originating from PBS treated mice. After 48h of co-culture, CFSE dilution was detected by flow cytometric analysis. The data originate from pooled triplicate cultures. (C) Enriched $CD11b^+$ cells were isolated from tumors of PBS treated mice and co-cultured *in vitro* with RMA-S cells, in the absence (left panel) or presence (right panel) of a transwell insert, at the indicated ratios. After 48h of co-culture, dead RMA-S cells were determined as $PI^+$ cells by flow cytometric analysis. (D) Enriched $CD11b^+$ cells were isolated from tumors of PBS treated mice and co-cultured *in vitro* with CFSE-labeled RMA-S cells at a 40:1 ratio. After 48h of co-culture, CFSE staining on $CD11b^+$ cells was documented by flow cytometric analysis.

when they were in the same chamber with CFSE-labeled RMA-S cells (Figure 6.12D). The same results were observed when macrophages were isolated either from PBS or anti-CD25 treated mice. In summary, our results suggest that the macrophages induce RMA-S cell death *in vitro* via a soluble factor and then uptake RMA-S cells by phagocytosis.

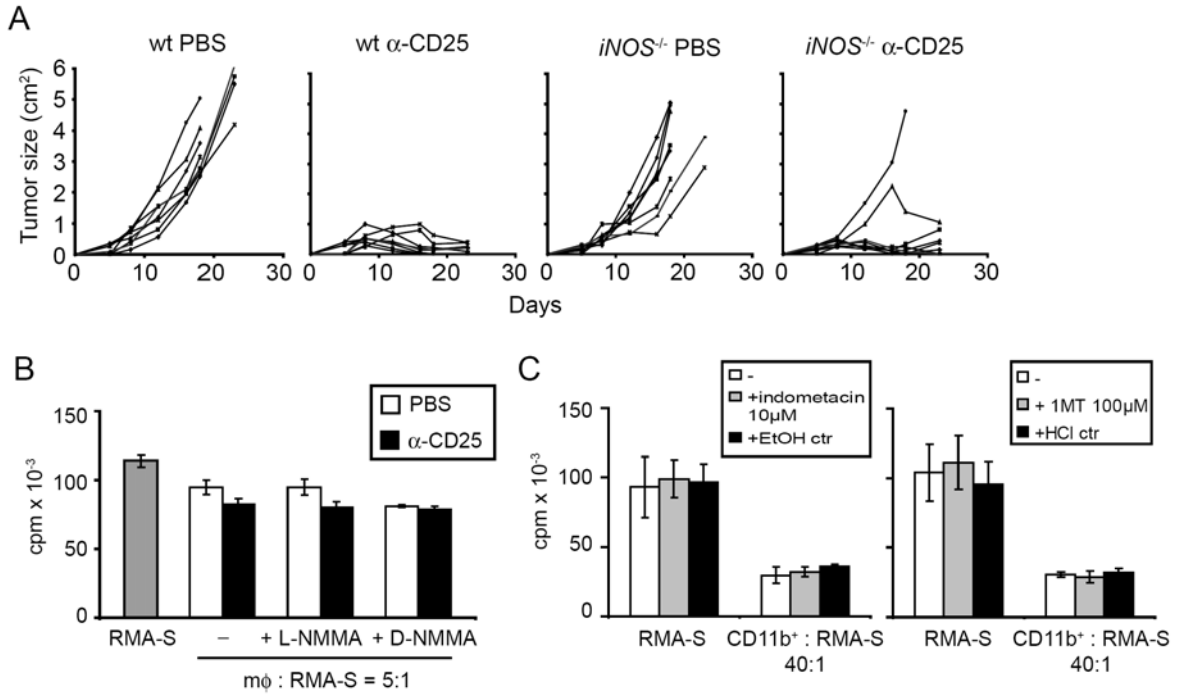


**Figure 6.13. iNOS, PGE2 and IDO are not involved in the suppression of RMA-S tumor growth by macrophages.** (A) Groups of 8 wt or inducible Nitric Oxide Synthase$^{-/-}$ (*iNOS* $^{-/-}$) mice were treated with PBS or anti-CD25 mAb, as indicated, before *s.c.* inoculation with RMA-S cells, and tumor growth was monitored. Each line represents one single mouse. (B-C) C57BL/6 mice were treated with PBS or anti-CD25 mAb, as indicated, before *s.c.* inoculation with RMA-S cells, and 10 days later, tumors were removed. Enriched CD11b$^{+}$ cells were isolated from tumors and co-cultured *in vitro* with RMA-S cells at the indicated ratios in the presence of L-NMMA (B), indomethacin (C, left panel), 1MT (C, right panel) or the appropriate controls, as indicated. After 48h of co-culture, tumor cell proliferation was monitored by $^{3}$H-thymidine incorporation assay. Data represent mean ± SD of triplicate cultures.

One effector molecule of activated macrophages is nitric oxide (NO) produced by the enzyme inducible nitric oxide synthase (iNOS), which has been shown to have tumor-suppressing or tumor-promoting functions [282]. In the presence and absence of Treg, tumor growth in *iNOS*$^{-/-}$ mice progressed similarly to the wt controls (Figure 6.13A). In addition, the presence of a NO inhibitor, NG-monomethyl-L-arginine (L-NMMA), did not affect macrophage-mediated inhibition of tumor cell proliferation *in vitro* (Figure 6.13B), arguing against a role of NO in the

RMA-S model. Prostaglandin E synthase 2 (PGE2) and indoleamine-pyrrole 2,3-dioxygenase (IDO) had been initially described as tumor-derived factors involved in immune suppression; however, many publications have identified these enzymes in various APC populations, including macrophages [283]. We addressed the role of these two enzymes by the addition of the specific inhibitors indomethacin, to block the activity of PGE2, and 1MT, which blocks IDO activity, during the 48h co-culture of RMA-S cells with macrophages. The addition of inhibitors for either of these molecules was not able to reverse the suppressive effect of macrophages (Figure 6.13C). In summary, macrophages induce RMA-S cell death during their *in vitro* co-culture via a soluble factor, which is independent of the enzymatic activity of iNOS, PGE2 and IDO.

### 6.1.3 Regulatory T cells suppress CD8$^+$ T cell recognition of TAP-deficient tumors

#### 6.1.3.1 CD8$^+$ T cells contribute to RMA-S tumor rejection in the absence of Treg by direct recognition of RMA-S cells

Our depletion experiments implied a role of CD8$^+$ T cells in the memory response against RMA-S tumors (Figure 6.4D-F). In addition, CD8$^+$ T cells were the most prominent IFN-γ producing cell population in the tumor tissue on day 10 after tumor cell inoculation (Figure 6.5C). These findings prompted us to further investigate the role of CD8$^+$ T cells in the primary anti-tumor response against RMA-S. Interestingly, depletion of the CD8$^+$ T cell compartment abrogated RMA-S tumor rejection in the absence of Treg, suggesting that, together with NK cells and CD4$^+$ T cells (Figure 6.3C-F), CD8$^+$ T cells also contribute to RMA-S tumor eradication during the primary anti-tumor response (Figure 6.14A). In addition, when we analyzed RMA-S tumor infiltrates on day 10 after tumor cell inoculation, in the presence or absence of Treg, we found increased accumulation of CD8$^+$ T cells in the absence of Treg (Figure 6.14B), as shown for other leukocyte populations in our model (Figure 6.7B-C). These data suggest that Treg suppress CD8$^+$ T cell accumulation in the tumor, as well as CD8$^+$ T cell mediated anti-tumor activity against RMA-S tumor.

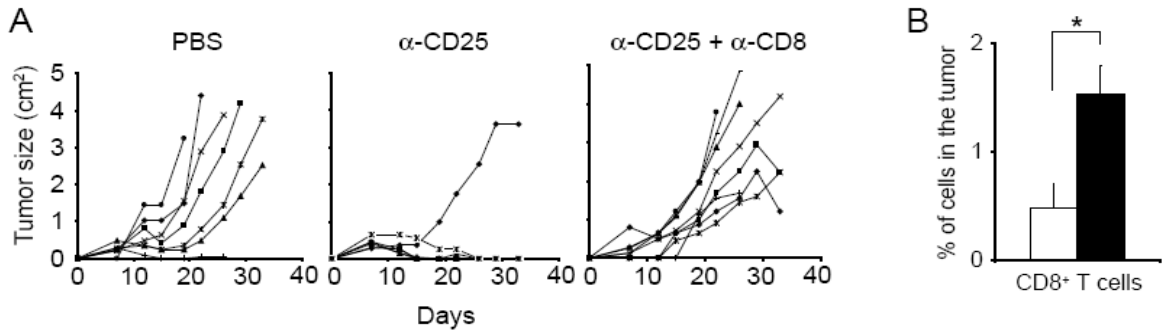


**Figure 6.14. CD8$^+$ T cells contribute to the rejection of RMA-S tumors in the absence of Treg.** (A) C57BL/6 mice were treated with PBS (left panel, n=8) or anti-CD25 mAb (middle panel, n=6), or anti-CD25 and anti-CD8 mAb (right panel, n=7) before *s.c.* inoculation with RMA-S cells and tumor growth was monitored. Each line represents one single mouse. (B) C57BL/6-Ly5.1$^+$ mice were treated with PBS (white bars) or anti-CD25 mAb (black bars) and inoculated *s.c.* with Ly5.2$^+$ RMA-S cells. Ten days later, tumors were removed and infiltrating CD8$^+$ T cells, determined by flow cytometric analysis, were quantified as percentages of total live cells in the tumor. *, $p<0.05$, using Student's *t* test.

The recognition of tumor cells by CD8$^+$ T cells *in vivo* can be either a direct process, by the presentation of tumor peptides on the surface of tumor cells in the context of MHC class I molecules or an indirect process, by the presentation of tumor antigens on the surface of APC, via a mechanism known as cross-presentation [284]. In the first case, a mechanism of direct recognition of TAP$^{-/-}$ tumors by CD8$^+$ T cells has been recently described [267,285]. This recognition is possible due to the fact that cells with an impairment in the antigen processing pathway – as is the case for RMA-S cells – are not completely negative for MHC class I expression (Figure 6.15, left panel), but can present a variety of peptides originating within the endoplasmic reticulum [267]. Thus, we addressed the question whether CD8$^+$ T cells in our model can directly recognize RMA-S tumor cells. For this purpose, we isolated highly purified CD8$^+$ T cells from the LN, DLN and tumor tissue of PBS and anti-CD25 treated mice 10 days after RMA-S tumor cell inoculation and co-cultured them *in vitro* with fresh RMA-S cells. Supernatants were collected after 18h of culture and levels of IFN-γ were determined by ELISA, as a readout for CD8$^+$ T cell activation. Figure 6.16A, left panel shows that CD8$^+$ T cells isolated from the DLN of Treg depleted mice produced IFN-γ *in vitro* in the presence of RMA-S cells. This was not the case for CD8$^+$ T cells isolated from the DLN of PBS treated mice or CD8$^+$ T cells isolated from the non-DLN (LN) either of tumor bearing or naïve mice. Most interestingly, CD8$^+$ T cells infiltrating the RMA-S tumors of both PBS and anti-CD25 treated mice potently produced IFN-γ *in vitro* in the presence of RMA-S

cells and this production was significantly higher when $CD8^+$ T cells were isolated from the tumors of Treg depleted animals (Figure 6.16A, right panel). IFN-γ production by $CD8^+$ T cells in this *in vitro* set-up was absolutely dependent on MHC class I, since co-culture of $CD8^+$ T cells with EC7.1 cells, the MHC class I-negative variant of RMA-S (Figure 6.15, right panel), abrogated IFN-γ production (Figure 6.16A). Finally, no IFN-γ production was detected when $CD8^+$ T cells were cultured alone (Figure 6.16A). In conclusion, our data show that $CD8^+$ T cells isolated from RMA-S tumor bearing mice can directly recognize RMA-S cells, via a MHC class I dependent manner and this recognition is enhanced in the absence of Treg.

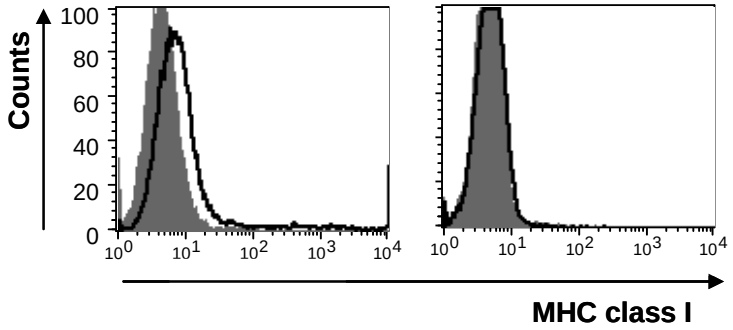


**Figure 6.15. RMA-S cells express low levels of MHC class I.** Representative histogram plots documenting MHC class I expression, as assessed by flow cytometry, on RMA-S (left panel) and EC7.1 cells (right panel) . Staining with the specific antibody is indicated by the black line and the corresponding isotype control by the grey filled area.

In a second set of experiments, we isolated $CD8^+$ T cells from spleens and LN of mice which had rejected RMA-S tumors after Treg depletion and were then rested for at least three months to allow the recovery of the Treg compartment. These mice are designated as memory mice. In parallel, $CD8^+$ T cells from spleens and LN of naïve mice were also isolated. In both cases, $CD8^+$ T cells were co-cultured with RMA-S cells *in vitro*, and IFN-γ production was determined in the supernatants after 18h of co-culture. As shown in Figure 6.16B, $CD8^+$ T cells isolated from spleens or LN of naïve mice did not produce any detectable amounts of IFN-γ upon co-culture with RMA-S cells. In contrast, $CD8^+$ T cells isolated from spleens or, most prominently, from LN of memory mice produced significant amounts of IFN-γ. This production was dependent on MHC class I, because when $CD8^+$ T cells were co-cultured with EC7.1 cells, IFN-γ production was not observed (Figure 6.16B). These data indicate that $CD8^+$ T cells isolated from secondary lymphoid organs of mice, which had rejected RMA-S tumors after Treg depletion, can directly recognize RMA-S cells.

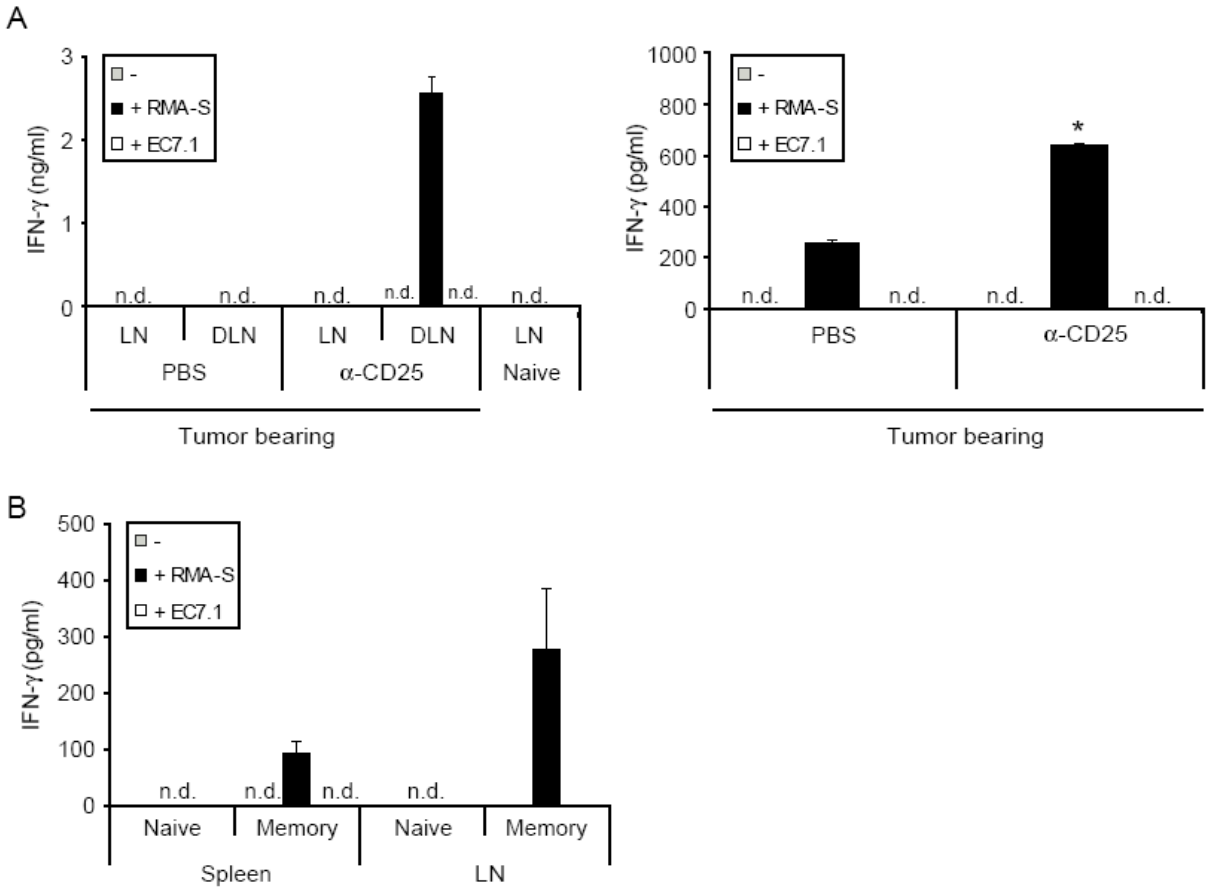


**Figure 6.16. Enhanced direct recognition of RMA-S tumor cells by CD8$^+$ T cells in the absence of Treg.** (A) C57BL/6 mice were treated with PBS or anti-CD25 mAb, as indicated, and inoculated *s.c.* with RMA-S cells. Mice which were not inoculated with RMA-S cells are designated as naive. Ten days later, draining LN (DLN), non-draining LN (LN) and tumors were removed. CD8$^+$ T cells were purified from LN and DLN by MACS sorting (purity > 80%) or from tumors by FACS sorting (purity > 95%) and cultured alone or in the presence of RMA-S or EC7.1 tumor cells for 18h. IFN-γ production was measured in the S/N by ELISA. (B) C57BL/6 mice were treated with anti-CD25 mAb before *s.c.* inoculation with RMA-S cells, rejected RMA-S tumors and rested for at least 3 months. These mice are designated as memory mice. Mice which were not inoculated with RMA-S cells are designated as naïve. CD8$^+$ T cells were isolated from the spleens or LN of naïve or memory mice, and co-cultured for 18h alone or in the presence of RMA-S or EC7.1 tumor cells. (A-B) Data represent the mean of duplicates in ELISA ± SD and are representative of one (A) and three (B) experiments. *. $p < 0{,}001$ in comparison to the PBS group, using Student's *t* test. n.d. = not detectable.

### 6.1.4 Immune intervention in established RMA-S tumors

#### 6.1.4.1 Depletion of Treg in established RMA-S tumors

We showed that Treg depletion before RMA-S tumor cell inoculation led to tumor rejection (Figure 6.3A). Furthermore, we addressed the question whether Treg depletion could enhance anti-tumor immunity to mediate the rejection of already established RMA-S tumors. For this purpose, we injected mice *s.c.* with RMA-S cells and allowed the tumors to grow. 10 days after tumor cell inoculation, 200μg of anti-CD25 depleting mAb or PBS as a control were injected intra- and peritumorally, and tumor growth was observed. Figure 6.17A shows that RMA-S tumor growth could be efficiently controlled when the anti-CD25 mAb was administered 2 days prior to tumor cell inoculation, while late Treg depletion was not able to influence RMA-S tumor growth, when compared to the control group that was treated with PBS. These data suggest that depletion of Treg is not by itself sufficient to influence tumor growth of established RMA-S tumors.

#### 6.1.4.2 Depletion of NK cells in established RMA-S tumors

NK cells are absolutely required for RMA-S tumor eradication (Figure 6.3C). Their absence led to enhanced tumor growth already in early time points after RMA-S tumor inoculation (Figure 6.3D, left panel) and this enhanced tumor growth was still present in later time points (Figure 6.3D, right panel). In later time points of tumor growth, however, it is not obvious whether this increased tumor growth is due to the absence of NK cells or to the initial tumor load, which is higher when NK cells are not present. In order to investigate the contribution of NK cells in later time points of RMA-S tumor growth in the presence or absence of Treg, mice were treated with PBS or anti-CD25 mAb before *s.c.* injection with RMA-S cells; 10 days after tumor cell inoculation, anti-NK1.1 depleting mAb or PBS as a control was administered *i.p.* and tumor growth was monitored. Depletion of NK cells 2 days prior to tumor cell inoculation led to enhanced tumor growth either in the presence or absence of Treg (Figure 6.17B). Interestingly, late depletion of NK cells had only a minor effect on RMA-S tumor growth, in the presence (Figure 6.17B, upper panel) or in the absence of Treg (Figure 6.17B, lower panel). These data

suggest that NK cells have only a minor contribution to the anti-RMA-S tumor immune response in later time points of tumor growth.

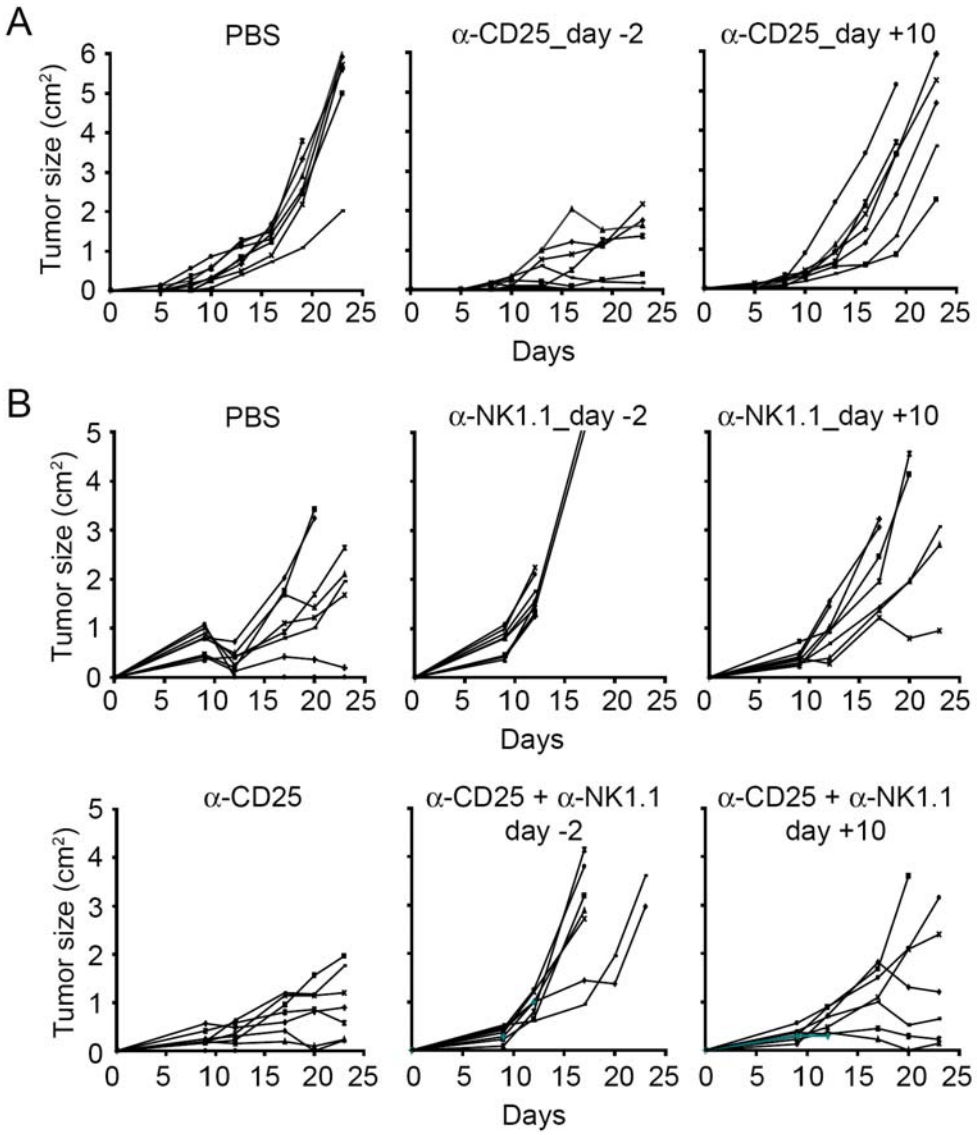


**Figure 6.17. Depletion of Treg or NK cells in established RMA-S tumors does not affect tumor growth.** (A) Groups of 8 C57BL/6 mice were treated with PBS (left panel) or anti-CD25 mAb administered either on day -2 (middle panel) or on day +10 (right panel), *s.c.* inoculated with RMA-S cells and tumor growth was monitored. (B) Groups of 7 C57BL/6 mice were treated with PBS or anti-CD25 mAb on day -2 and/or NK1.1 mAb administered starting either from day -2 or day +10, as indicated, *s.c.* inoculated with RMA-S cells and tumor growth was monitored. (A-B) Each line represents one single mouse.

Acquisition of NK cell function during development correlates with high expression of the CD11b marker by NK cells [17]. In addition, it was reported that various lineages of tumors

interfere with NK cell functions, by interrupting their maturation in the bone-marrow [286]. To address the question whether RMA-S tumor impedes the functional maturation of NK cells, we monitored CD11b expression on NK cells in various organs during RMA-S tumor progression. Figure 6.18 shows that CD11b expression on NK cells was reduced in the BM, blood, spleen and tumor tissue, starting from day 10 after RMA-S tumor cell inoculation, while this reduction became more prominent at later time points of tumor growth, as representatively shown for days 17 and 21 after tumor cell inoculation. Similar results were found when CD43 was used as a maturation marker for NK cells (data not shown). These data correlate late NK cell dysfunction with reduced CD11b expression in RMA-S tumor bearing mice, without excluding, however, that alternative mechanisms may be involved.

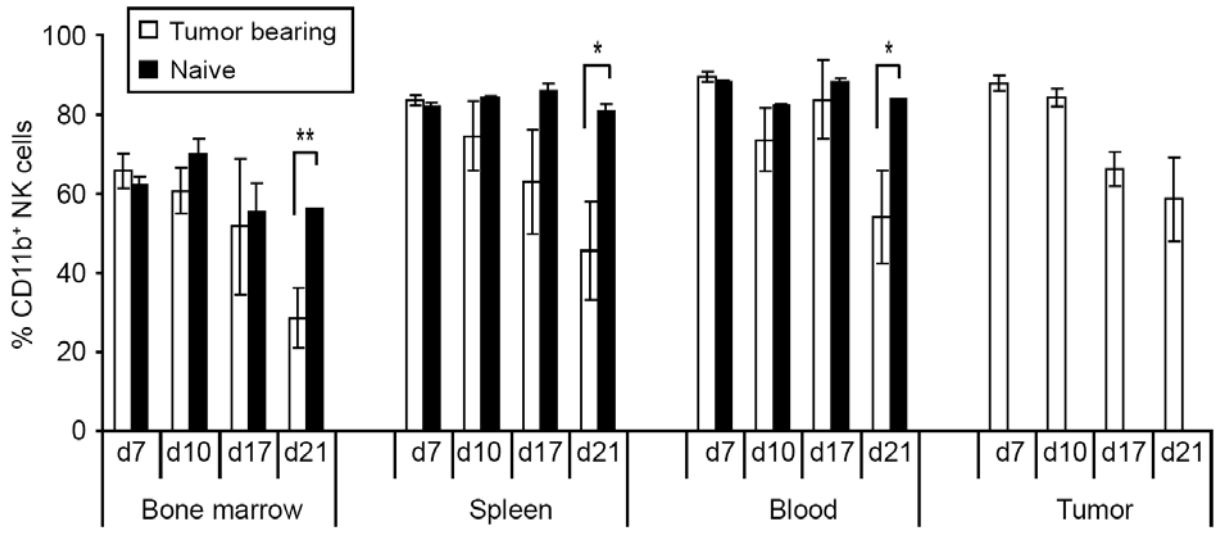


**Figure 6.18. Decreased CD11b expression on NK cells during RMA-S tumor progression.** C57BL/6 mice were injected *s.c.* with RMA-S cells. After 7, 10, 17 and 21 days, bone marrow, spleens, blood and tumors were removed and analyzed for CD11b expression on NK cells by flow cytometry. Data show the mean ± SD of four tumor bearing and two naïve animals per time point and are representative of two experiments. *, $p<0.05$, **, $p<0.01$ using Student's *t* test.

## 6.2 Control of anti-tumor immunity by type I IFN

### 6.2.1 Enhanced RMA-S tumor growth in the absence of type I IFN signaling

In order to assess the role of type I IFN in the anti-tumor immunity against RMA-S, we *s.c.* injected $1x10^6$ RMA-S tumor cells in wt or IFNAR1$^{-/-}$ mice, which lack the IFNAR1 subunit of the IFN-α/β receptor complex [287]. Interestingly, we found that mice which could not respond to type I IFN exhibited enhanced RMA-S tumor growth, which was statistically significant (Figure 6.19A). This phenotype could also be observed in wt mice when injected with a neutralizing anti-IFN-β mAb (Figure 6.19B). These data show that RMA-S tumor growth is under the control of endogenously produced type I IFN.

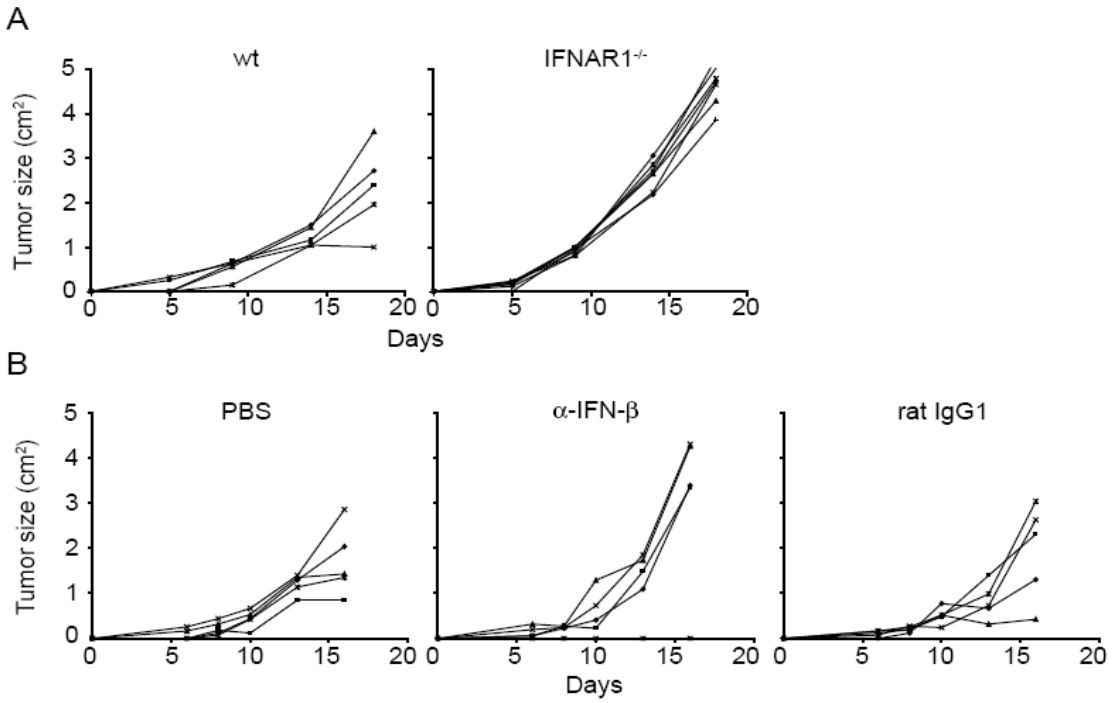


**Figure 6.19. IFNAR1$^{-/-}$ mice exhibit enhanced RMA-S tumor growth.** (A) C57BL/6 wt (left panel, n=5) or IFNAR1$^{-/-}$ (right panel, n=7) mice were *s.c.* inoculated with RMA-S cells and tumor growth was monitored. wt versus IFNAR1$^{-/-}$, $p > 0.01$, using Koziol test. (B) C57BL/6 wt mice were treated with PBS (left panel, n=5) or anti-IFN-β mAb (middle panel, n=5) or rat IgG1 mAb (right panel, n=5), inoculated *s.c.* with RMA-S cells and tumor growth was monitored. (A-B) Each line represents one single mouse. The results are representative of two independent experiments.

### 6.2.2 Requirement of hematopoietic and non-hematopoietic compartment for responsiveness to type I IFN

We next addressed the question whether the cell targets of type I IFN in our model were derived from the hematopoietic or non-hematopoietic compartment of the host. For this purpose, we reconstituted lethally irradiated wt and RAG2$^{-/-}$IFNAR1$^{-/-}$ mice with BM cells isolated from wt or IFNAR1$^{-/-}$ mice. Thus, we created the following BM chimeras: wt → wt, in which reconstitution leads to type I IFN responsiveness in both the hematopoietic and non-hematopoietic compartments, wt → RAG2$^{-/-}$IFNAR1$^{-/-}$ mice, in which type I IFN responsiveness is reconstituted only in the hematopoietic cells, and IFNAR1$^{-/-}$ → wt, in which type I IFN responsiveness is present only in the non-hematopoietic compartment. The use of congenic markers (Ly5.1/Ly5.2) was employed for the discrimination of host versus donor cells (Table 6.1). Five weeks after BM reconstitution, the efficiency of the reconstitution was assessed in the blood of mice by flow cytometric analysis and varied between 60 and 90% in individual mice (data not shown). Six weeks after BM reconstitution, RMA-S tumor growth was assessed in the chimeric mice, in comparison to non-reconstituted IFNAR1$^{-/-}$ mice. Figure 6.20 shows that reconstitution of the type I IFN responsiveness in either the hematopoietic or non-hematopoietic compartment of the host only partially restored the enhanced RMA-S tumor growth observed in the IFNAR1$^{-/-}$ mice. These results show that type I IFN sensitivity within both hematopoietic and non-hematopoietic cells is required for RMA-S tumor growth control.

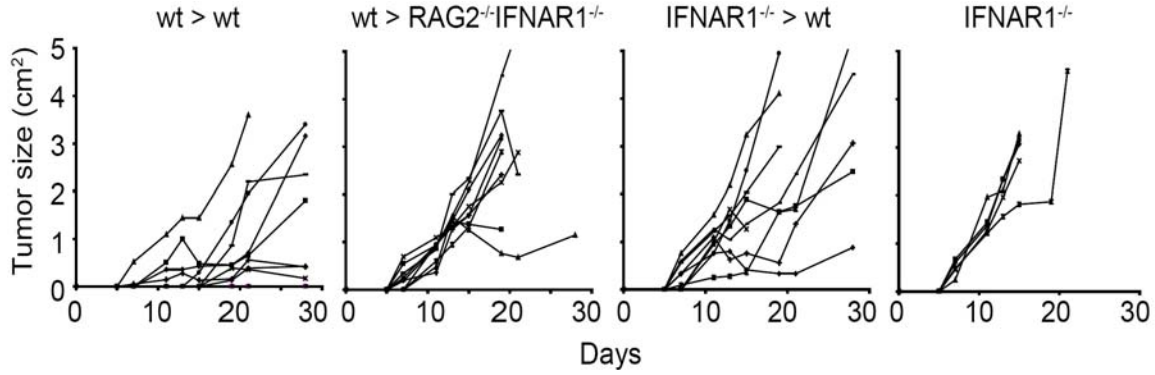


**Figure 6.20. IFNAR1 signaling on both hematopoietic and non-hematopoietic cells is important in RMA-S anti-tumor response.** Groups of 9 C57BL/6 wt or RAG2$^{-/-}$IFNAR1$^{-/-}$ mice were lethally irradiated and reconstituted with BM derived either from wt or IFNAR1$^{-/-}$ mice, as indicated. Six weeks after BM reconstitution, chimeric mice, as well as IFNAR1$^{-/-}$ mice (n=5) were *s.c.* injected with RMA-S cells and tumor growth was monitored. Each line represents one single mouse. The results are representative of two experiments.

| GROUP | BM DONOR | HOST | IFNAR1 DEFICIENCY |
|---|---|---|---|
| 1 | Ly5.1$^{+}$ wt | Ly5.2$^{+}$ wt | — |
| 2 | Ly5.1$^{+}$ wt | Ly5.2$^{+}$RAG2$^{-/-}$ IFNAR1$^{-/-}$ | Non-hematopoietic cells |
| 3 | Ly5.2$^{+}$ IFNAR1$^{-/-}$ | Ly5.1$^{+}$ wt | Hematopoietic cells |
| 4 | — | Ly5.2$^{+}$ IFNAR1$^{-/-}$ | Both |

**Table 6.1.** Generation of BM chimeras with differential defect in IFNAR1 signaling either on hematopoietic or non-hematopoietic cells.

### 6.2.3 Contribution of the hematopoietic compartment for responsiveness to type I IFN

#### 6.2.3.1 NK cell cytotoxicity is impaired in IFNAR1$^{-/-}$ mice

NK cells are absolutely required for the control of RMA-S tumor growth (Figure 6.3C-D). Therefore, we addressed the question whether NK cell function is impaired in IFNAR1$^{-/-}$ mice. For this purpose, NK cells were isolated from the spleens of wt or IFNAR1$^{-/-}$ mice by magnetic separation and their cytotoxic ability was tested against the NK cell sensitive tumor cell line YAC-1 or against RMA-S cells in a standard *in vitro* 6h $^{51}$Cr release assay. Interestingly, NK cells isolated from the spleens of IFNAR1$^{-/-}$ mice had significantly reduced ability to kill YAC-1 or RMA-S targets when compared to NK cells from wt mice (Figure 6.21A). Thus, NK cell cytotoxicity is impaired in IFNAR1$^{-/-}$ mice.

#### 6.2.3.2 Macrophage tumoristatic activity is not impaired in IFNAR1$^{-/-}$ mice

Another important effector cell population identified in the RMA-S tumor model is macrophages, which can suppress RMA-S proliferation *in vitro* (Figure 6.11). Macrophage tumoristatic activity against RMA-S tumor cells was assessed in the IFNAR1$^{-/-}$ mice. Tumor infiltrating CD11b$^{+}$ cells isolated from RMA-S tumors grown in wt or IFNAR1$^{-/-}$ mice were enriched with magnetic cell sorting 10 days after tumor cell inoculation and co-cultured *in vitro* with RMA-S tumor cells. RMA-S tumor cell proliferation was assessed after 48h using $^{3}$H-thymidine incorporation assay. As shown in Figure 6.21B, CD11b$^{+}$ cells from IFNAR1$^{-/-}$ mice were equally efficient to suppress

RMA-S tumor cell growth *in vitro* as CD11b$^+$ cells isolated from wt mice. These finding suggests that macrophage tumoristatic function is not impaired in IFNAR1$^{-/-}$ mice.

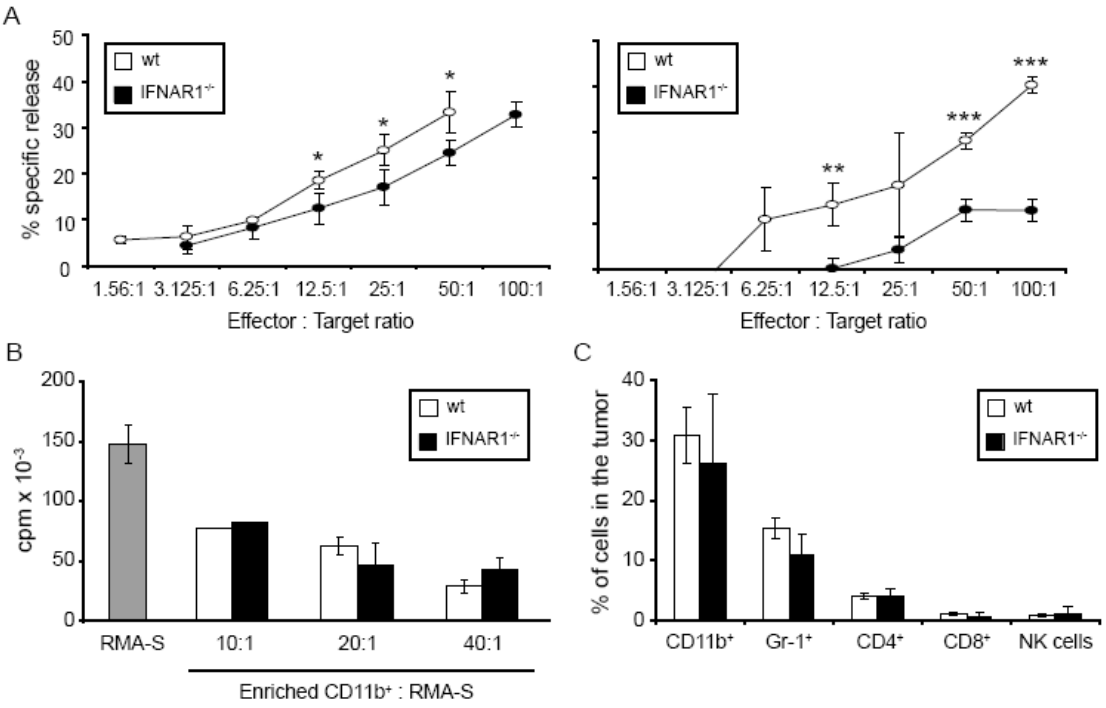


**Figure 6.21. Impaired NK cell but normal macrophage function in the IFNAR1$^{-/-}$ mice.** (A) NK cells were isolated from spleens of wt (white points) or IFNAR1$^{-/-}$ (black points) mice and co-cultured *in vitro* with $^{51}$Cr-labelled YAC-1 (left panel) or RMA-S (right panel) target cells at the indicated ratios. After 6h of co-culture, $^{51}$Cr release was measured in the S/N. Data represent mean ± SD of triplicate cultures. *, $p<0.05$, **, $p<0.001$, ***, $p<0.0001$ using Student's *t* test. (B) C57BL/6 wt (white bars) or IFNAR1$^{-/-}$ (black bars) mice were *s.c.* inoculated with RMA-S cells and 10 days later tumors were removed. CD11b$^+$ cells were isolated from the tumors and co-cultured *in vitro* with RMA-S cells at the indicated ratios. After 48h of co-culture, tumor cell proliferation was monitored by $^3$H-thymidine incorporation assay. Data represent mean ± SD of triplicate cultures. (C) C57BL/6 wt (white bars) or IFNAR1$^{-/-}$ (black bars) mice were *s.c.* inoculated with RMA-S cells and 10 days later tumors were removed and infiltrating CD11b$^+$, Gr-1$^+$, CD4$^+$, CD8$^+$ and NK (NK1.1$^+$CD3$^-$) cells were determined by flow cytometric analysis and quantified as percentages of total live cells in the tumor. Data show the mean ± SD of 3 animals per group.

### 6.2.3.3 Intratumoral leukocyte accumulation is not impaired in IFNAR1$^{-/-}$ mice

Increased numbers of myeloid cells [287] and reduced numbers of NK cells [259] have been reported in the blood of IFNAR1$^{-/-}$ mice. We addressed the question whether leukocyte accumulation in

the RMA-S tumors is impaired in IFNAR1$^{-/-}$ mice. For this purpose, we determined the quantity of various tumor infiltrating leukocyte subpopulations as percentages of total live cells in the tumor in wt and IFNAR1$^{-/-}$ mice on day 10 after RMA-S tumor cell inoculation. The mean tumor size of the two groups was comparable at this time point. Flow cytometric analysis revealed that CD11b$^{+}$ cells, Gr-1$^{+}$ cells, CD4$^{+}$ T cells, CD8$^{+}$ T cells and NK cells were infiltrating the tumors of wt and IFNAR1$^{-/-}$ mice in similar amounts (Figure 6.21C). These data indicate that, although the numbers of some cell populations are misbalanced in the blood of IFNAR1$^{-/-}$ mice, the leukocyte accumulation in the RMA-S tumors is not impaired and is comparable to the wt situation.

## 6.2.4 Contribution of the non-hematopoietic compartment for responsiveness to type I IFN

### 6.2.4.1 Angiogenesis is impaired in IFNAR1$^{-/-}$ mice

Figure 6.20 shows that type I IFN responsiveness is required in the non-hematopoietic compartment. To address the importance of this finding, angiogenesis pattern and vessel functionality were observed in RMA-S tumors of wt and IFNAR1$^{-/-}$ mice. For this purpose, wt or IFNAR1$^{-/-}$ mice were injected with FITC-labeled *Lycopersicon esculentum* lectin on day 10 of tumor growth and the tumor vasculature was observed by confocal microscopy. Long vessels with normal branching were commonly present within the tumors of wt mice, and no extravasated FITC-lectin could be detected (Figure 6.22A, left panel). On the other hand, structural irregularity, heterogeneity and leakiness were common features of the vessels in the RMA-S tumors of IFNAR1$^{-/-}$ mice (Figure 6.22A, right panel).

| GROUP | BM DONOR | HOST | IFNAR1 DEFICIENCY |
|---|---|---|---|
| 1 | — | Ly5.2$^{+}$ wt | — |
| 2 | Ly5.1$^{+}$ wt | Ly5.2$^{+}$ IFNAR1$^{-/-}$ | Non-hematopoietic cells |
| 3 | Ly5.2$^{+}$ IFNAR1$^{-/-}$ | Ly5.1$^{+}$ wt | Hematopoietic cells |
| 4 | Ly5.2$^{+}$ IFNAR1$^{-/-}$ | Ly5.2$^{+}$ IFNAR1$^{-/-}$ | Both |

**Table 6.2.** Generation of BM chimeras with differential defect in IFNAR1 signaling either on hematopoietic or non-hematopoietic cells.

In a further step, we wanted to address the question whether the observed defect in angiogenesis depends solely on IFNAR1 signaling on non-hematopoietic cells or factors produced by infiltrating leukocytes are also involved. For this purpose, we created BM chimeras, where either the hematopoietic or non-hematopoietic system was impaired in IFNAR1 signaling (Table 2). As expected, normal vessel pattern was observed in the wt tumors, while disoriented vessel formation and destroyed vessels, as documented by the presence of extravasated FITC-lectin, were observed in the tumors of IFNAR1$^{-/-}$ mice (Figure 6.22B). Interestingly, most vessels infiltrating the tumors of either wt → IFNAR1$^{-/-}$ or IFNAR1$^{-/-}$ → wt chimeric mice exhibited an abnormal branching pattern, quite similar to the one observed in the tumors of IFNAR1$^{-/-}$ mice (Figure 6.22B). In summary, these data support that angiogenesis is impaired in the RMA-S tumors of IFNAR1$^{-/-}$ mice and both hematopoietic and non-hematopoietic cells are responsible for this impairment.

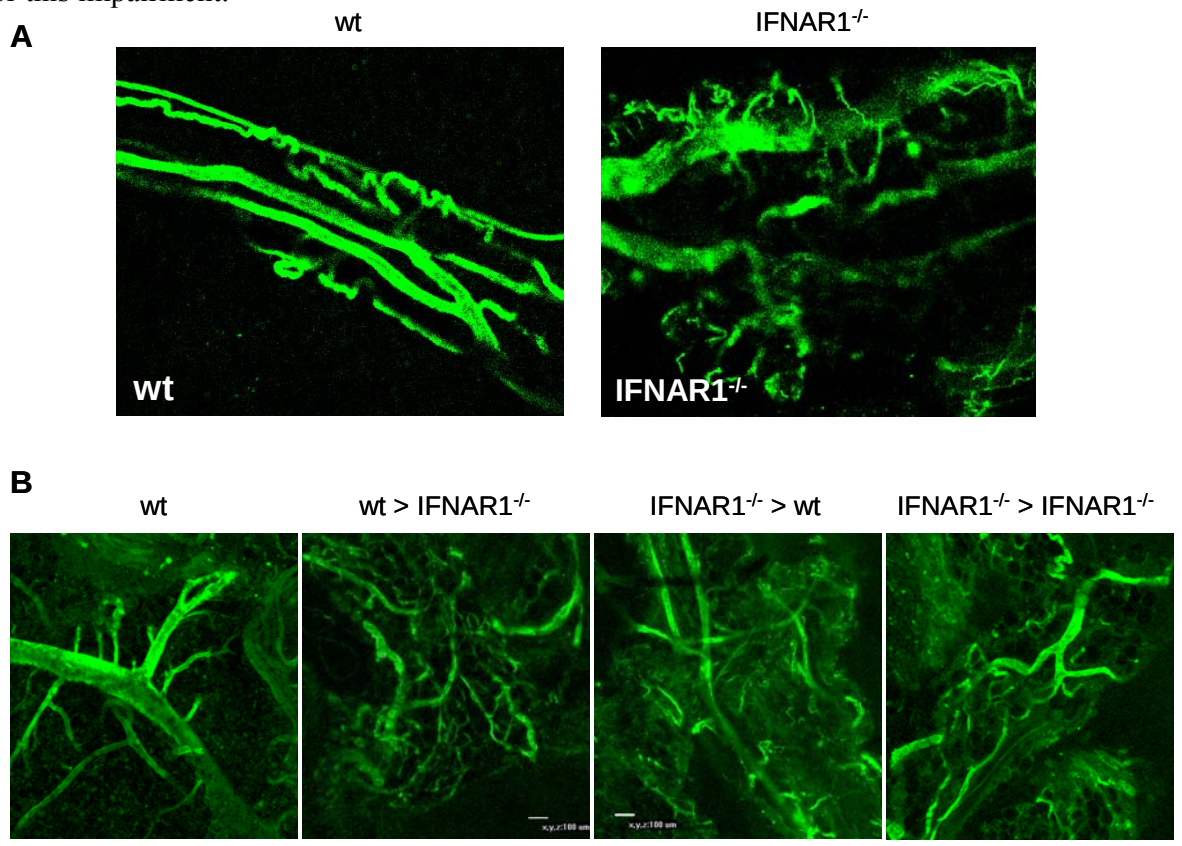


**Figure 6.22. Impaired angiogenesis in the IFNAR1$^{-/-}$ mice.** Groups of 3 C57BL/6 wt or IFNAR1-/- mice (A) or groups of 3 C57BL/6 wt mice or wt > IFNAR1$^{-/-}$ or IFNAR1$^{-/-}$ > wt or IFNAR1$^{-/-}$ > IFNAR1$^{-/-}$ BM chimeras (B) were *s.c.* inoculated with RMA-S cells. (A-B) Ten days later, FITC-labeled *Lycopersicon esculentum* lectin was injected into the mice and tumor vasculature was observed in unfixed tumors by confocal microscopy.

# 7 DISCUSSION

## 7.1 Suppression of innate immune cells by Treg

In the first part of this study, we investigated the role of Treg on the innate immune response against the lymphoma RMA-S. Our study revealed that Treg suppress RMA-S tumor rejection by inhibiting the IFN-γ-mediated accumulation of leukocytes, including macrophages at the tumor site. Most importantly, we demonstrated that highly activated, tumoristatic macrophages accumulated in the tumor tissue in the absence of Treg, unraveling a novel aspect of Treg-mediated suppression of anti-tumor immune responses *in vivo*.

During the last years, the role of Treg as professional suppressive cells has been confirmed by several studies [288]. Treg were shown to exert an immunosuppressive role in multiple disease settings, including anti-tumor responses. Indeed, Treg were shown to accumulate in high numbers in both murine and human tumors, as well as in secondary lymphoid organs [180,181,289]. This increased accumulation can be due either to proliferation of preexisting Treg [290] or to the conversion of $CD4^+CD25^-$ T cells into Treg, which has been described to take place in the periphery under certain conditions [291]. In the *s.c.* RMA-S mouse lymphoma model, we detected high percentages of $CD4^+Foxp3^+$ Treg among $CD4^+$ T cells in secondary lymphoid organs, as well as infiltrating the tumor tissue. Foxp3 expression coincided with CD25 expression on $CD4^+$ T cells, which in turn correlated with suppressive activity in an *in vitro* assay. Most importantly, *in vivo* depletion of $CD25^+$ cells led to RMA-S tumor rejection, pinpointing the suppressive role of the $CD4^+CD25^+Foxp3^+$ Treg in the control of the MHC class I-deficient RMA-S tumor.

There have been many reports addressing the suppressive effect of Treg on T cells in the context of autoimmune diseases, infectious models and tumor immunity. It has been suggested that human Treg have overlapping TCR specificities as Tcon and would be able to suppress in an antigen-specific manner [292]. Thus, the concept that Treg would suppress innate immune cell functions, which are not antigen specific, is intriguing. Nevertheless, there have been some reports which documented the suppressive effect of Treg on cells of the innate immune system [185-194]. Previous studies showed that Treg inhibited NK cell effector functions in both mouse and human systems [185,186,293-295]. In the absence of Treg, 3LL Lewis Lung carcinoma cells, RAE-1-

transfected B16 melanoma, and RAE-1-transfected RMA-S lymphoma cells, all of which express high levels of the NKG2D ligand RAE-1, were more efficiently controlled *in vivo* [185,186]. These data suggest that Treg can directly inhibit NK cell activation towards NKG2D ligand-expressing tumor cells *in vivo*. Our depletion experiments indicated that $NK1.1^+$ cells are necessary but not sufficient for tumor rejection in the absence of Treg. Notably, in our experiments, the early growth of RMA-S tumors, which do not express NKG2D-ligands, was retarded by NK cells, irrespective of whether Treg were present or absent. Our data indicate that the early NK cell-mediated tumor control, most likely due to direct tumor cell killing, was not hampered by Treg. This suggests that distinct NK cell activation pathways might be differentially controlled by Treg.

We discovered that IFN-γ, produced by NK cells, $CD8^+$ T cells and to a lesser extent by $CD4^+$ T cells, was absolutely required for the eradication of RMA-S cells in Treg depleted mice. In addition, our data revealed that high amounts of IFN-γ were detected in the tumor and that these levels were significantly elevated in the absence of Treg. IFN-γ can exert anti-tumor immunity by various mechanisms. First, IFN-γ can directly suppress tumor growth. Nevertheless, IFN-γ did not influence RMA-S cell proliferation *in vitro* (data not shown). IFN-γ has also been shown to inhibit angiogenesis in some tumors [278,296]. In our tumor model, CD31 or MECA-1 staining of tumor sections obtained at day 10 did not show any significant difference in vessel number or localization in the presence or absence of Treg (data not shown). In addition, vessel integrity remained unchanged in the absence or presence of Treg, suggesting that angiogenesis was not altered in Treg depleted mice.

IFN-γ has been shown to facilitate leukocyte migration into tumors, directly or indirectly, by the modulation of certain chemokines and chemokine receptors [297]. In order to gain insight into the immune response within the tumor, we analyzed tumor-infiltrating cells at day 10, before RMA-S tumors were rejected in Treg depleted mice. At this time point, the tumor size between control and Treg depleted mice was similar. We detected that mostly $CD11b^+$ cells −consisting of macrophages, dendritic cells and granulocytes− and comparably lower amounts of NK cells, $CD4^+$ and $CD8^+$ T cells accumulated in the tumor tissue. Importantly, all these cell populations were significantly increased in mice depleted of Treg. In this context, it has also been shown that Treg inhibited tissue infiltration of conventional $CD4^+$ T cells in a diabetes model [298]. In addition, injection of Treg into nude mice inhibited accumulation of NK cells to RMA-S cells injected into the peritoneum [186]. In these studies, the Treg mediated mechanisms responsible for the inhibition of cell accumulation were not defined. In a recent study, it was reported that Treg could induce

NK and $CD8^+$ T cell death in a granzyme B- and perforin-dependent fashion [187], suggesting that this may be the mechanism via which Treg control NK cell numbers also in our tumor model. In a study involving large cohorts of human colorectal cancers, a high density of immune cells, including T cells, correlated with longer survival in patients, suggesting that *in situ* analysis of tumor infiltrating immune cells may be a valuable prognostic tool in the treatment of some types of malignancies [279]. In the RMA-S *s.c.* tumor model, higher density of infiltrating cells also correlated positively with tumor regression in the absence of Treg. Our experiments further show that the increased $CD11b^+$ and $CD4^+$ T and $CD8^+$ T cell accumulation in the tumors of Treg depleted mice was dependent on IFN-γ. Furthermore, the presence of IFN-γ was absolutely required for NK cell accumulation in the tumor tissue.

Finally, IFN-γ is involved in macrophage activation [299]. Indeed, in the absence of Treg, we did not only find high numbers of macrophages in the tumor tissue but these cells also displayed increased MHC class II expression. The upregulation of MHC class II was dependent on IFN-γ. These data suggest that increased IFN-γ levels in the absence of Treg lead to enhanced macrophage activation. We assume that these macrophages, due to enhanced levels of MHC class II, have the potential to induce efficient activation of $CD4^+$ T cells at the tumor site. In addition, increased numbers of MHC class $II^{high}$ DC accumulated in the tumor in the absence of Treg. Taken together, this increase of antigen-presenting cells with high MHC class II expression may be instrumental for efficient presentation of tumor antigens to $CD4^+$ T cells in the absence of Treg. Indeed, $CD4^+$ T cells are absolutely required for tumor rejection in these mice. Moreover, the absence of Treg led to the generation of immunological memory.

Tumor-associated macrophages represent the major infiltrating component of many tumors and can have multi-faceted functions depending on the tumor microenvironment [103]. In several experimental tumor models, activation of an inflammatory response mediated by macrophages promoted tumor progression [300]. In addition, a subpopulation of myeloid cells, designated as MDSC (myeloid-derived suppressor cells), expressing the markers Gr-1 and CD11b, was shown to suppress T cell responses [301]. We have evidence that the tumor-infiltrating macrophages in our model did not suppress, but rather activated T cell proliferation (data not shown). Therefore, our data suggest that in our model, tumor-infiltrating macrophages are distinct from myeloid-derived suppressor cells. Studies have shown that macrophages produce inflammatory chemokines and cytokines, which recruit and activate other cell types [103]. In addition, tumor-infiltrating macrophages have the potential to directly control tumor cell

proliferation when appropriately stimulated, *e.g.* by potently activated T cells in the presence of IFN-γ or after CpG treatment [109,110]. Our experiments showed that, in the absence of Treg, macrophages isolated from tumors produced higher amounts of chemokines and inflammatory cytokines, which could lead to efficient cell recruitment and activation. Most importantly, enriched $CD11b^+$ cells and macrophages isolated from tumors in the absence of Treg inhibited tumor cell growth more potently, as compared to cells isolated from control tumors. The suppressive effect of macrophages on the growth of RMA-S cells *in vitro* was abrogated when IFN-γ was neutralized *in vivo* during the anti-tumor immune response. One effector molecule expressed by activated macrophages is nitric oxide (NO) produced by the enzyme inducible nitric oxide synthase (iNOS), which has tumor-suppressing or tumor-promoting functions. In the presence and absence of Treg, tumor growth in $iNOS^{-/-}$ mice progressed similarly to the wt controls. In addition, the presence of a NO inhibitor did not affect macrophage-mediated inhibition of tumor cell proliferation *in vitro*. Similarly, the addition of inhibitors against the activity of PGE-2 and IDO did not affect RMA-S tumor growth in the presence of macrophages *in vitro*. These data argue against a role of the enzymes NO, PGE-2 and IDO in our model.

Of note, IFN-γ neutralization had a diverse effect on the pro-inflammatory cytokine profile in the absence of Treg; while it did not affect IL-1β production by $CD11b^+$ cells, it strongly enhanced IL-6 production. This is of importance, since IL-6 in combination with TGF-β has been shown to be necessary for the differentiation of naïve T cells into Th17 cells [302]. It is also reported that IFN-γ can negatively regulate Th17 cell differentiation and *vice versa* [303]. It is possible that the presence of IFN-γ in the absence of Treg suppresses Th17 polarization and protects the host from autoimmune reactions, which have often been linked to Th17 cells [304]. Of note, IL-17 was detected in low amounts in tumor lysates from both control and Treg depleted animals 10 days after RMA-S tumor inoculation (data not shown). It will be of interest to quantify Th17 levels in the RMA-S tumor tissue after IFN-γ neutralization.

It has been reported that Treg suppress macrophage activation and effector function directly *in vitro* [190,193]. *In vivo*, Kim *et al.* documented that macrophage expansion was under the control of Treg under steady state conditions in adult mice [195]. Kryczek *et al.* showed upregulation of the B7 family member B7-H4 (B7S1, B7-S1, B7x) on isolated human monocytes by Treg after direct contact in an *in vitro* co-culture [191]. In mice, B7-H4 is expressed upon activation on B cells, T cells and monocytes and was shown to negatively regulate T cell

responses [305]. Its ligand remains to be identified, but evidence support that it is expressed on activated T cells. In addition, B7-H4 expression on macrophages infiltrating ovarian tumors correlated with the patients' survival [192]. In our tumor model, no difference in the expression of B7-H4 was observed on tumor-infiltrating macrophages between control and Treg depleted mice. Our study reveals a novel role of Treg mediated suppression of macrophage function in a tumor model *in vivo*. Whether the suppression of macrophages requires a direct Treg/macrophage interaction, as observed for Treg/DC interaction *in vivo* [197], or is rather due to indirect effects *via* inhibition of other immune cells, requires further investigation. Kryczek *et al* showed that Treg directly suppressed macrophages in an *in vitro* co-culture [191]. Our experiments demonstrate that *in vivo* macrophage accumulation at the tumor site was absolutely dependent on $CD4^+$ T cells and to a lesser extent on NK cells. In addition, increased macrophage accumulation in the absence of Treg, MHC class II upregulation and tumoristatic activity of macrophages were all dependent on IFN-γ, which in turn Treg suppressed its production. We assume that, in our model, Treg suppressed IFN-γ production by lymphocytes, which in a second step interfered with macrophage activation and accumulation at the tumor site.

The mechanism that Treg use to exert their suppressive function in the RMA-S model is still under investigation. Neutralization of TGF-β or blocking IL-10R by specific mAbs, two pathways that have been linked to Treg-mediated suppression [281], did not influence tumor growth and did not lead to tumor rejection in our model, suggesting that neither TGF-β nor IL-10 are required for Treg mediated suppression *in vivo*. Recently, it was reported that IL-35 is specifically produced by Treg and not effector T cells and can mediate suppression [306]. So far, reagents to block this cytokine *in vivo* are not available.

Unexpectedly, we discovered an important contribution of $CD8^+$ T cells in the rejection of the MHC class I-deficient RMA-S tumor in the absence of Treg, as well as during the memory response against a secondary challenge to RMA-S cells. In this context, Kelly *at al*. reported that $CD8^+$ T cells mediated memory responses after rejection of RMA-S cells transfected with CD70 or CD80. The mechanism, however, via which $CD8^+$ T cells would recognize RMA-S cells was not addressed in this studies [20,307]. In our model, $CD8^+$ T cells isolated from RMA-S tumor tissue during the primary anti-tumor response or from the secondary lymphoid organs of mice which had previously rejected RMA-S tumors after Treg depletion were able to directly recognize RMA-S cells in an *in vitro* co-culture. It has been reported that the TAP-negative RMA-S cells, which express only very low amounts of MHC class I on their surface, present a range of

antigens – referred to as TEIPP – which are TAP-independent and can be recognized by $CD8^+$ T cells [267,285]. It is possible that Treg depletion increases the potential recognition of such peptides by $CD8^+$ T cells, allowing potent antigen-specific responses to take place even against targets which express very low amounts of MHC class I. This observation might offer new therapeutic approaches against human cancers, which often have low MHC class I expression.

The manipulation of Treg is currently evaluated in clinical trials in tumor patients [209,210]. It will be informative to monitor numbers and activation status of tumor-infiltrating macrophages in patients undergoing Treg depletion or treated with other immunotherapeutic protocols and to correlate these data with the clinical outcome. The results of our study may have substantial impact on the design of novel strategies in anti-cancer therapy to strengthen both the innate and adaptive immune responses against cancer.

## 7.2 The role of endogenous type I IFN in the anti-tumor response

In the second part of this study, we addressed the role of endogenously produced type I IFN in the anti-tumor response against the MHC class I-deficient lymphoma RMA-S. We showed that RMA-S tumor growth is accelerated in mice, which are non-responsive to type I IFN. Our data demonstrate that this acceleration in tumor growth correlates with defects in NK cell activity and vessel network formation at the tumor site.

Type I IFN have been extensively used in the treatment of various types of cancer, although their mechanism of action is not completely clear [252]. *In vitro* high doses of type I IFN promote cell cycle arrest in various cell types [248,249]. It is believed that this may be their mechanism of action after exogenous administration in cancer patients. The study of RMA-S tumor growth in the $IFNAR1^{-/-}$ mice allows dissecting the effect of type I IFN on the host and on the tumor cells. The accelerated tumor growth observed in these mice after *s.c.* RMA-S inoculation showed that type I IFN need to signal to the host's cells for an efficient anti-tumor response. Our findings are in concordance with other reports, which demonstrated a role for type I IFN in tumor immunosurveillance using $IFNAR1^{-/-}$ 129/Sv mice [258]. In this study, transplanted tumors originating from MCA-induced fibrosarcomas were under the control of type I IFN-responsive hematopoietic cells. In the RMA-S model, by the generation of BM chimeras, we

showed that cells of both the hematopoietic and non-hematopoietic system responded to type I IFN and were required for an efficient anti-tumor response. The different tumor origin in these models may account for this difference in the immune response. In addition, it was reported that IFN-α did not affect the proliferation of RMA-S cells *in vitro* [259]. Our results pinpoint a role for endogenously produced type I IFN in the anti-tumor response against the RMA-S tumor, and in addition suggest a mechanism of action, which is dependent on the host's response to type I IFN.

Type I IFN can exert multi-faceted functions in the hematopoietic system. Type I IFN can promote $CD8^+$ T cell-mediated responses, induce the maturation of DC and indirectly enhance NK cell cytotoxicity [87,231,232]. We addressed the question which cell population was impaired during the anti-tumor response in the IFNAR1$^{-/-}$ mice. MHC class I-deficient RMA-S tumor growth is under the control of NK cells. Indeed, we found that NK cells derived from IFNAR1$^{-/-}$ mice exhibited impaired cytotoxicity against two different tumor targets *in vitro*. This finding is in corcondance with a report from another group, which in addition observed reduced NK cell numbers in the spleens of IFNAR1$^{-/-}$ mice [259]. This observation pinpoints to a role for type I IFN in the homeostasis of NK cells, and not only in their function during an immune response. It is known that IFN-β, binding to the IFNAR1, is constitutively produced by fibroblasts and macrophages [287], so it is possible that these constant levels of IFN-β contribute to NK cell homeostasis. Interestingly, despite the reduced occurrence of NK cells in the spleens of IFNAR1$^{-/-}$ mice, we observed that the accumulation of NK cells – as well as other leukocyte populations – at the tumor site was not impaired. This observation suggests that the factors responsible for the recruitment of leukocytes at the tumor tissue during the anti-tumor response to RMA-S cells are not under the control of endogenous type I IFN. We showed that, in addition to NK cells, in the RMA-S model macrophages are important effector cells, which mediate a tumoristatic effect. It was reported that the response of macrophages to CSF-1 and LPS was impaired in IFNAR1$^{-/-}$ mice [287]. In a co-culture of macrophages and RMA-S cells, the suppressive effect of macrophages on RMA-S tumor growth was indistinguishable between macrophages originating from wt and IFNAR1$^{-/-}$ mice, suggesting that the anti-tumor response of macrophages might not be tightly regulated by type I IFN. Our study correlated the acceleration in tumor growth in IFNAR1$^{-/-}$ mice with an impaired function of NK cells, without excluding, nevertheless, that other cell populations might be affected.

An effect of type I IFN on non-hematopoietic cells has been documented. Treatment with type I IFN caused damage on endothelial cells, which led to tumor necrosis [250]. Anti-angiogenesis

factors which inhibit blood vessel growth are commonly used in cancer immunotherapy based on the notion that angiogenesis is absolutely required for tumor growth [308]. IFN-α has been introduced into clinical applications as an anti-angiogenic factor to treat haemangiomas [309,310]. In IFNAR1$^{-/-}$ mice, we observed increased vascularization, albeit deregulated. The use of *in vivo* fluorescent angiography revealed a difference in vascular architecture of the tumors of IFNAR1$^{-/-}$ versus wt mice, and namely a less organized blood vessel network in the IFNAR1$^{-/-}$ mice. In addition, extravasated FITC-lectin was detected. The latter finding pinpoints to the lack of sufficient pericyte recruitment, which form a layer around the endothelial cells. Stainings of tumor sections for pericyte markers should address these questions. It is suggested that angiogenic factors, such as basic fibroblast growth factor (bFGF), downregulate adhesion molecules on endothelial cells, which are involved in leukocyte-vessel wall interactions, such as intercellular adhesion molecule (ICAM)-1 [311].This correlated with decreased leukocyte infiltration of the tumors and thus to reduced immune surveillance. We found that leukocyte accumulation in the tumors of IFNAR1$^{-/-}$ mice, as assessed by flow cytometry, was similar to the wt levels, suggesting that this mechanism might not be impaired in IFNAR1$^{-/-}$ mice. Nevertheless, it is possible that leukocyte localization within the tumor tissue is different between wt and IFNAR1$^{-/-}$ mice. Analysis of tumor tissue sections can address the question whether leukocytes are uniformely distributed throughout the tumor mass in wt and IFNAR1$^{-/-}$ mice. In summary, our findings show that endogenous type I IFN are important for the architecture of tumor vasculature and the formation of mature blood vessels; the contribution of an organized vessel network to tumor growth control needs to be elucidated.

The phenotype of impaired anti-tumor response in the IFNAR1$^{-/-}$ mice could be mimicked by the administration of an anti-IFN-β neutralizing mAb *in vivo*. This result implicates IFN-β production during the anti-tumor response, without excluding a role also for the different subtypes of IFN-α. During an anti-viral response, IFN-β and/or IFN-α4 genes are readily induced and subsequently induce the production of the other subtypes of IFN-α [224,230]. A similar mechanism may as well take place during the anti-tumor response. We were able to detect both IFN-β and IFN-α mRNA in leukocytes infiltrating the RMA-S tumors 10 days after tumor inoculation (data not shown), showing that at least some subtype of IFN-α is produced during the anti-tumor response. Due to the lack of efficiently neutralizing anti-IFN-α mAb, we were not able to address the importance of IFN-α *in vivo*. The use of an anti-IFN-β neutralizing mAb also

excluded a possible developmental defect in the IFNAR1$^{-/-}$ mice which could be responsible for the observed phenotype. The identification of the type I IFN-producing cell population during the anti-tumor response remains still unclear. In principle, all cells are capable of producing type I IFN during a viral infection, although pDC are specialized IFN-producing cells producing high amounts of type I IFN after TLR stimulation [229]. We could detect IFN-β and IFN-α mRNA on leukocytes of both myeloid and non-myeloid lineage based on CD11b marker discrimination, and in addition IFN-β mRNA on non-hematopoietic cells (data not shown), suggesting that – similar to an anti-viral response – the production of type I IFN during the anti-tumor response can have multiple sources. Nevertheless, the stimuli which can induce the production of type I IFN during the tumor growth remain unknown.

Further investigations on the source and function of endogenous type I IFN during the anti-tumor response will help to identify new therapeutic targets for cancer immunotherapy, and assist the efficacy of the presently applied clinical treatments which are based on the use of type I IFN.

# 8 References


1. Dunn, G.P., Bruce, A.T., Ikeda, H., Old, L.J. & Schreiber, R.D. Cancer immunoediting: from immunosurveillance to tumor escape. *Nat Immunol* **3**, 991-8 (2002).
2. Dunn, G.P. et al. Interferon-gamma and cancer immunoediting. *Immunol Res* **32**, 231-45 (2005).
3. Dunn, G.P., Old, L.J. & Schreiber, R.D. The three Es of cancer immunoediting. *Annu Rev Immunol* **22**, 329-60 (2004).
4. Dunn, G.P., Old, L.J. & Schreiber, R.D. The immunobiology of cancer immunosurveillance and immunoediting. *Immunity* **21**, 137-48 (2004).
5. Smyth, M.J., Dunn, G.P. & Schreiber, R.D. Cancer immunosurveillance and immunoediting: the roles of immunity in suppressing tumor development and shaping tumor immunogenicity. *Adv Immunol* **90**, 1-50 (2006).
6. MacKie, R.M., Reid, R. & Junor, B. Fatal melanoma transferred in a donated kidney 16 years after melanoma surgery. *N Engl J Med* **348**, 567-8 (2003).
7. Medzhitov, R. Recognition of microorganisms and activation of the immune response. *Nature* **449**, 819-26 (2007).
8. Akira, S., Uematsu, S. & Takeuchi, O. Pathogen recognition and innate immunity. *Cell* **124**, 783-801 (2006).
9. Kiessling, R., Klein, E. & Wigzell, H. "Natural" killer cells in the mouse. I. Cytotoxic cells with specificity for mouse Moloney leukemia cells. Specificity and distribution according to genotype. *Eur J Immunol* **5**, 112-7 (1975).
10. Kiessling, R., Klein, E., Pross, H. & Wigzell, H. "Natural" killer cells in the mouse. II. Cytotoxic cells with specificity for mouse Moloney leukemia cells. Characteristics of the killer cell. *Eur J Immunol* **5**, 117-21 (1975).
11. Herberman, R.B., Nunn, M.E. & Lavrin, D.H. Natural cytotoxic reactivity of mouse lymphoid cells against syngeneic acid allogeneic tumors. I. Distribution of reactivity and specificity. *Int J Cancer* **16**, 216-29 (1975).
12. Herberman, R.B., Nunn, M.E., Holden, H.T. & Lavrin, D.H. Natural cytotoxic reactivity of mouse lymphoid cells against syngeneic and allogeneic tumors. II. Characterization of effector cells. *Int J Cancer* **16**, 230-9 (1975).
13. Barlozzari, T., Reynolds, C.W. & Herberman, R.B. In vivo role of natural killer cells: involvement of large granular lymphocytes in the clearance of tumor cells in anti-asialo GM1-treated rats. *J Immunol* **131**, 1024-7 (1983).
14. Moretta, L. et al. Human natural killer cells: their origin, receptors and function. *Eur J Immunol* **32**, 1205-11 (2002).
15. Andre, P. et al. Modification of P-selectin glycoprotein ligand-1 with a natural killer cell-restricted sulfated lactosamine creates an alternate ligand for L-selectin. *Proc Natl Acad Sci U S A* **97**, 3400-5 (2000).
16. Walzer, T. et al. Identification, activation, and selective in vivo ablation of mouse NK cells via NKp46. *Proc Natl Acad Sci U S A* **104**, 3384-9 (2007).
17. Kim, S. et al. In vivo developmental stages in murine natural killer cell maturation. *Nat Immunol* **3**, 523-8 (2002).
18. Hayakawa, Y. & Smyth, M.J. CD27 dissects mature NK cells into two subsets with distinct responsiveness and migratory capacity. *J Immunol* **176**, 1517-24 (2006).

19. Vossen, M.T. et al. CD27 Defines Phenotypically and Functionally Different Human NK Cell Subsets. *J Immunol* **180**, 3739-45 (2008).
20. Kelly, J.M. et al. Induction of tumor-specific T cell memory by NK cell-mediated tumor rejection. *Nat Immunol* **3**, 83-90 (2002).
21. Haller, O., Kiessling, R., Orn, A. & Wigzell, H. Generation of natural killer cells: an autonomous function of the bone marrow. *J Exp Med* **145**, 1411-6 (1977).
22. Kumar, V., Ben-Ezra, J., Bennett, M. & Sonnenfeld, G. Natural killer cells in mice treated with 89strontium: normal target-binding cell numbers but inability to kill even after interferon administration. *J Immunol* **123**, 1832-8 (1979).
23. Sanchez, M.J., Muench, M.O., Roncarolo, M.G., Lanier, L.L. & Phillips, J.H. Identification of a common T/natural killer cell progenitor in human fetal thymus. *J Exp Med* **180**, 569-76 (1994).
24. Spits, H. et al. Early stages in the development of human T, natural killer and thymic dendritic cells. *Immunol Rev* **165**, 75-86 (1998).
25. Michie, A.M. et al. Clonal characterization of a bipotent T cell and NK cell progenitor in the mouse fetal thymus. *J Immunol* **164**, 1730-3 (2000).
26. Vosshenrich, C.A. et al. A thymic pathway of mouse natural killer cell development characterized by expression of GATA-3 and CD127. *Nat Immunol* **7**, 1217-24 (2006).
27. Takeda, K. et al. TRAIL identifies immature natural killer cells in newborn mice and adult mouse liver. *Blood* **105**, 2082-9 (2005).
28. Freud, A.G. et al. A human CD34(+) subset resides in lymph nodes and differentiates into CD56bright natural killer cells. *Immunity* **22**, 295-304 (2005).
29. Georgopoulos, K. et al. The Ikaros gene is required for the development of all lymphoid lineages. *Cell* **79**, 143-56 (1994).
30. Wang, J.H. et al. Selective defects in the development of the fetal and adult lymphoid system in mice with an Ikaros null mutation. *Immunity* **5**, 537-49 (1996).
31. Colucci, F. et al. Differential requirement for the transcription factor PU.1 in the generation of natural killer cells versus B and T cells. *Blood* **97**, 2625-32 (2001).
32. Wang, D. et al. Ets-1 deficiency leads to altered B cell differentiation, hyperresponsiveness to TLR9 and autoimmune disease. *Int Immunol* **17**, 1179-91 (2005).
33. Yokota, Y. et al. Development of peripheral lymphoid organs and natural killer cells depends on the helix-loop-helix inhibitor Id2. *Nature* **397**, 702-6 (1999).
34. Ikawa, T., Fujimoto, S., Kawamoto, H., Katsura, Y. & Yokota, Y. Commitment to natural killer cells requires the helix-loop-helix inhibitor Id2. *Proc Natl Acad Sci U S A* **98**, 5164-9 (2001).
35. Held, W., Kunz, B., Lowin-Kropf, B., van de Wetering, M. & Clevers, H. Clonal acquisition of the Ly49A NK cell receptor is dependent on the trans-acting factor TCF-1. *Immunity* **11**, 433-42 (1999).
36. Duncan, G.S., Mittrucker, H.W., Kagi, D., Matsuyama, T. & Mak, T.W. The transcription factor interferon regulatory factor-1 is essential for natural killer cell function in vivo. *J Exp Med* **184**, 2043-8 (1996).
37. Ogasawara, K. et al. Requirement for IRF-1 in the microenvironment supporting development of natural killer cells. *Nature* **391**, 700-3 (1998).
38. Lohoff, M. et al. Deficiency in the transcription factor interferon regulatory factor (IRF)-2 leads to severely compromised development of natural killer and T helper type 1 cells. *J Exp Med* **192**, 325-36 (2000).
39. Wu, Q. et al. Signal via lymphotoxin-beta R on bone marrow stromal cells is required for an early checkpoint of NK cell development. *J Immunol* **166**, 1684-9 (2001).

40. Iizuka, K. et al. Requirement for membrane lymphotoxin in natural killer cell development. *Proc Natl Acad Sci U S A* **96**, 6336-40 (1999).
41. Smyth, M.J. et al. Multiple deficiencies underlie NK cell inactivity in lymphotoxin-alpha gene-targeted mice. *J Immunol* **163**, 1350-3 (1999).
42. Ito, D., Back, T.C., Shakhov, A.N., Wiltrout, R.H. & Nedospasov, S.A. Mice with a targeted mutation in lymphotoxin-alpha exhibit enhanced tumor growth and metastasis: impaired NK cell development and recruitment. *J Immunol* **163**, 2809-15 (1999).
43. Lodolce, J.P. et al. IL-15 receptor maintains lymphoid homeostasis by supporting lymphocyte homing and proliferation. *Immunity* **9**, 669-76 (1998).
44. Gilmour, K.C. et al. Defective expression of the interleukin-2/interleukin-15 receptor beta subunit leads to a natural killer cell-deficient form of severe combined immunodeficiency. *Blood* **98**, 877-9 (2001).
45. Suzuki, H., Duncan, G.S., Takimoto, H. & Mak, T.W. Abnormal development of intestinal intraepithelial lymphocytes and peripheral natural killer cells in mice lacking the IL-2 receptor beta chain. *J Exp Med* **185**, 499-505 (1997).
46. Colucci, F. & Di Santo, J.P. The receptor tyrosine kinase c-kit provides a critical signal for survival, expansion, and maturation of mouse natural killer cells. *Blood* **95**, 984-91 (2000).
47. Puzanov, I.J., Bennett, M. & Kumar, V. IL-15 can substitute for the marrow microenvironment in the differentiation of natural killer cells. *J Immunol* **157**, 4282-5 (1996).
48. Kennedy, M.K. et al. Reversible defects in natural killer and memory CD8 T cell lineages in interleukin 15-deficient mice. *J Exp Med* **191**, 771-80 (2000).
49. McKenna, H.J. et al. Mice lacking flt3 ligand have deficient hematopoiesis affecting hematopoietic progenitor cells, dendritic cells, and natural killer cells. *Blood* **95**, 3489-97 (2000).
50. Riccardi, C., Santoni, A., Barlozzari, T., Puccetti, P. & Herberman, R.B. In vivo natural reactivity of mice against tumor cells. *Int J Cancer* **25**, 475-86 (1980).
51. Gorelik, E., Rosen, B., Copeland, D., Weatherly, B. & Herberman, R.B. Evaluation of role of natural killer cells in radiation-induced leukemogenesis in mice. *J Natl Cancer Inst* **72**, 1397-403 (1984).
52. Haliotis, T., Ball, J.K., Dexter, D. & Roder, J.C. Spontaneous and induced primary oncogenesis in natural killer (NK)-cell-deficient beige mutant mice. *Int J Cancer* **35**, 505-13 (1985).
53. Argyle, J.C., Kjeldsberg, C.R., Marty, J., Shigeoka, A.O. & Hill, H.R. T-cell lymphoma and the Chediak-Higashi syndrome. *Blood* **60**, 672-6 (1982).
54. Ljunggren, H.G. & Karre, K. In search of the 'missing self': MHC molecules and NK cell recognition. *Immunol Today* **11**, 237-44 (1990).
55. Arase, H., Mocarski, E.S., Campbell, A.E., Hill, A.B. & Lanier, L.L. Direct recognition of cytomegalovirus by activating and inhibitory NK cell receptors. *Science* **296**, 1323-6 (2002).
56. Ravetch, J.V. & Lanier, L.L. Immune inhibitory receptors. *Science* **290**, 84-9 (2000).
57. van den Broek, M.F., Kagi, D., Zinkernagel, R.M. & Hengartner, H. Perforin dependence of natural killer cell-mediated tumor control in vivo. *Eur J Immunol* **25**, 3514-6 (1995).
58. Smyth, M.J., Kelly, J.M., Baxter, A.G., Korner, H. & Sedgwick, J.D. An essential role for tumor necrosis factor in natural killer cell-mediated tumor rejection in the peritoneum. *J Exp Med* **188**, 1611-9 (1998).

59. Smyth, M.J. et al. Perforin is a major contributor to NK cell control of tumor metastasis. *J Immunol* **162**, 6658-62 (1999).
60. Rosen, D. et al. Tumor immunity in perforin-deficient mice: a role for CD95 (Fas/APO-1). *J Immunol* **164**, 3229-35 (2000).
61. Kashii, Y., Giorda, R., Herberman, R.B., Whiteside, T.L. & Vujanovic, N.L. Constitutive expression and role of the TNF family ligands in apoptotic killing of tumor cells by human NK cells. *J Immunol* **163**, 5358-66 (1999).
62. Takeda, K. et al. Involvement of tumor necrosis factor-related apoptosis-inducing ligand in NK cell-mediated and IFN-gamma-dependent suppression of subcutaneous tumor growth. *Cell Immunol* **214**, 194-200 (2001).
63. Karre, K. NK cells, MHC class I molecules and the missing self. *Scand J Immunol* **55**, 221-8 (2002).
64. Moretta, L., Biassoni, R., Bottino, C., Mingari, M.C. & Moretta, A. Natural killer cells: a mystery no more. *Scand J Immunol* **55**, 229-32 (2002).
65. Cerwenka, A. & Lanier, L.L. Ligands for natural killer cell receptors: redundancy or specificity. *Immunol Rev* **181**, 158-69 (2001).
66. Raulet, D.H. Roles of the NKG2D immunoreceptor and its ligands. *Nat Rev Immunol* **3**, 781-90 (2003).
67. Gasser, S., Orsulic, S., Brown, E.J. & Raulet, D.H. The DNA damage pathway regulates innate immune system ligands of the NKG2D receptor. *Nature* **436**, 1186-90 (2005).
68. Routes, J.M. et al. Adenovirus serotype 5 E1A sensitizes tumor cells to NKG2D-dependent NK cell lysis and tumor rejection. *J Exp Med* **202**, 1477-82 (2005).
69. Cerwenka, A., Baron, J.L. & Lanier, L.L. Ectopic expression of retinoic acid early inducible-1 gene (RAE-1) permits natural killer cell-mediated rejection of a MHC class I-bearing tumor in vivo. *Proc Natl Acad Sci U S A* **98**, 11521-6 (2001).
70. Diefenbach, A., Jensen, E.R., Jamieson, A.M. & Raulet, D.H. Rae1 and H60 ligands of the NKG2D receptor stimulate tumour immunity. *Nature* **413**, 165-71 (2001).
71. Smyth, M.J. et al. NKG2D function protects the host from tumor initiation. *J Exp Med* **202**, 583-8 (2005).
72. Guerra, N. et al. NKG2D-deficient mice are defective in tumor surveillance in models of spontaneous malignancy. *Immunity* **28**, 571-80 (2008).
73. Groh, V., Wu, J., Yee, C. & Spies, T. Tumour-derived soluble MIC ligands impair expression of NKG2D and T-cell activation. *Nature* **419**, 734-8 (2002).
74. Whiteside, T.L. & Herberman, R.B. Role of human natural killer cells in health and disease. *Clin Diagn Lab Immunol* **1**, 125-33 (1994).
75. Whiteside, T.L., Vujanovic, N.L. & Herberman, R.B. Natural killer cells and tumor therapy. *Curr Top Microbiol Immunol* **230**, 221-44 (1998).
76. Imai, K., Matsuyama, S., Miyake, S., Suga, K. & Nakachi, K. Natural cytotoxic activity of peripheral-blood lymphocytes and cancer incidence: an 11-year follow-up study of a general population. *Lancet* **356**, 1795-9 (2000).
77. Maraninchi, D. et al. A phase II study of interleukin-2 in 49 patients with relapsed or refractory acute leukemia. *Leuk Lymphoma* **31**, 343-9 (1998).
78. Chang, E. & Rosenberg, S.A. Patients with melanoma metastases at cutaneous and subcutaneous sites are highly susceptible to interleukin-2-based therapy. *J Immunother* **24**, 88-90 (2001).
79. Mulatero, C.W. et al. A phase II study of combined intravenous and subcutaneous interleukin-2 in malignant pleural mesothelioma. *Lung Cancer* **31**, 67-72 (2001).

80. Benyunes, M.C. et al. Interleukin-2 with or without lymphokine-activated killer cells as consolidative immunotherapy after autologous bone marrow transplantation for acute myelogenous leukemia. *Bone Marrow Transplant* **12**, 159-63 (1993).
81. Rosenberg, S.A. et al. Prospective randomized trial of high-dose interleukin-2 alone or in conjunction with lymphokine-activated killer cells for the treatment of patients with advanced cancer. *J Natl Cancer Inst* **85**, 622-32 (1993).
82. Fernandez, N.C. et al. Dendritic cells directly trigger NK cell functions: cross-talk relevant in innate anti-tumor immune responses in vivo. *Nat Med* **5**, 405-11 (1999).
83. Ferlazzo, G. et al. Human dendritic cells activate resting natural killer (NK) cells and are recognized via the NKp30 receptor by activated NK cells. *J Exp Med* **195**, 343-51 (2002).
84. Piccioli, D., Sbrana, S., Melandri, E. & Valiante, N.M. Contact-dependent stimulation and inhibition of dendritic cells by natural killer cells. *J Exp Med* **195**, 335-41 (2002).
85. Gerosa, F. et al. The reciprocal interaction of NK cells with plasmacytoid or myeloid dendritic cells profoundly affects innate resistance functions. *J Immunol* **174**, 727-34 (2005).
86. Martin-Fontecha, A. et al. Induced recruitment of NK cells to lymph nodes provides IFN-gamma for T(H)1 priming. *Nat Immunol* **5**, 1260-5 (2004).
87. Lucas, M., Schachterle, W., Oberle, K., Aichele, P. & Diefenbach, A. Dendritic cells prime natural killer cells by trans-presenting interleukin 15. *Immunity* **26**, 503-17 (2007).
88. Ebata, K. et al. Immature NK cells suppress dendritic cell functions during the development of leukemia in a mouse model. *J Immunol* **176**, 4113-24 (2006).
89. Nishikawa, K. et al. Accumulation of CD16-CD56+ natural killer cells with high affinity interleukin 2 receptors in human early pregnancy decidua. *Int Immunol* **3**, 743-50 (1991).
90. Liu, C.C. & Young, J.D. Uterine natural killer cells in the pregnant uterus. *Adv Immunol* **79**, 297-329 (2001).
91. Hanna, J. et al. Decidual NK cells regulate key developmental processes at the human fetal-maternal interface. *Nat Med* **12**, 1065-74 (2006).
92. Manaster, I. & Mandelboim, O. The unique properties of human NK cells in the uterine mucosa. *Placenta* (2007).
93. Hanna, J. & Mandelboim, O. When killers become helpers. *Trends Immunol* **28**, 201-6 (2007).
94. Baxter, A.G. & Smyth, M.J. The role of NK cells in autoimmune disease. *Autoimmunity* **35**, 1-14 (2002).
95. Martinez, F.O., Sica, A., Mantovani, A. & Locati, M. Macrophage activation and polarization. *Front Biosci* **13**, 453-61 (2008).
96. Rabinowitz, S.S. & Gordon, S. Macrosialin, a macrophage-restricted membrane sialoprotein differentially glycosylated in response to inflammatory stimuli. *J Exp Med* **174**, 827-36 (1991).
97. Geissmann, F., Jung, S. & Littman, D.R. Blood monocytes consist of two principal subsets with distinct migratory properties. *Immunity* **19**, 71-82 (2003).
98. Dalton, D.K. et al. Multiple defects of immune cell function in mice with disrupted interferon-gamma genes. *Science* **259**, 1739-42 (1993).
99. Gordon, S. Alternative activation of macrophages. *Nat Rev Immunol* **3**, 23-35 (2003).
100. Wiktor-Jedrzejczak, W. & Gordon, S. Cytokine regulation of the macrophage (M phi) system studied using the colony stimulating factor-1-deficient op/op mouse. *Physiol Rev* **76**, 927-47 (1996).
101. Scott, E.W., Simon, M.C., Anastasi, J. & Singh, H. Requirement of transcription factor PU.1 in the development of multiple hematopoietic lineages. *Science* **265**, 1573-7 (1994).

102. van Rooijen, N. & van Nieuwmegen, R. Elimination of phagocytic cells in the spleen after intravenous injection of liposome-encapsulated dichloromethylene diphosphonate. An enzyme-histochemical study. *Cell Tissue Res* **238**, 355-8 (1984).
103. Mantovani, A., Sozzani, S., Locati, M., Allavena, P. & Sica, A. Macrophage polarization: tumor-associated macrophages as a paradigm for polarized M2 mononuclear phagocytes. *Trends Immunol* **23**, 549-55 (2002).
104. Dinapoli, M.R., Calderon, C.L. & Lopez, D.M. The altered tumoricidal capacity of macrophages isolated from tumor-bearing mice is related to reduce expression of the inducible nitric oxide synthase gene. *J Exp Med* **183**, 1323-9 (1996).
105. Klimp, A.H. et al. Expression of cyclooxygenase-2 and inducible nitric oxide synthase in human ovarian tumors and tumor-associated macrophages. *Cancer Res* **61**, 7305-9 (2001).
106. Tsutsui, S. et al. Macrophage infiltration and its prognostic implications in breast cancer: the relationship with VEGF expression and microvessel density. *Oncol Rep* **14**, 425-31 (2005).
107. Biswas, S.K. et al. A distinct and unique transcriptional program expressed by tumor-associated macrophages (defective NF-kappaB and enhanced IRF-3/STAT1 activation). *Blood* **107**, 2112-22 (2006).
108. Dong, Z., Yoneda, J., Kumar, R. & Fidler, I.J. Angiostatin-mediated suppression of cancer metastases by primary neoplasms engineered to produce granulocyte/macrophage colony-stimulating factor. *J Exp Med* **188**, 755-63 (1998).
109. Corthay, A. et al. Primary antitumor immune response mediated by CD4+ T cells. *Immunity* **22**, 371-83 (2005).
110. Buhtoiarov, I.N., Sondel, P.M., Eickhoff, J.C. & Rakhmilevich, A.L. Macrophages are essential for antitumour effects against weakly immunogenic murine tumours induced by class B CpG-oligodeoxynucleotides. *Immunology* **120**, 412-23 (2007).
111. Serafini, P., Borrello, I. & Bronte, V. Myeloid suppressor cells in cancer: recruitment, phenotype, properties, and mechanisms of immune suppression. *Semin Cancer Biol* **16**, 53-65 (2006).
112. Kusmartsev, S. & Gabrilovich, D.I. Role of immature myeloid cells in mechanisms of immune evasion in cancer. *Cancer Immunol Immunother* **55**, 237-45 (2006).
113. Bronte, V. et al. Identification of a CD11b(+)/Gr-1(+)/CD31(+) myeloid progenitor capable of activating or suppressing CD8(+) T cells. *Blood* **96**, 3838-46 (2000).
114. Huang, B. et al. Gr-1+CD115+ immature myeloid suppressor cells mediate the development of tumor-induced T regulatory cells and T-cell anergy in tumor-bearing host. *Cancer Res* **66**, 1123-31 (2006).
115. Pak, A.S. et al. Mechanisms of immune suppression in patients with head and neck cancer: presence of CD34(+) cells which suppress immune functions within cancers that secrete granulocyte-macrophage colony-stimulating factor. *Clin Cancer Res* **1**, 95-103 (1995).
116. Almand, B. et al. Clinical significance of defective dendritic cell differentiation in cancer. *Clin Cancer Res* **6**, 1755-66 (2000).
117. Gabrilovich, D.I. et al. Production of vascular endothelial growth factor by human tumors inhibits the functional maturation of dendritic cells. *Nat Med* **2**, 1096-103 (1996).
118. Young, M.R., Young, M.E. & Wright, M.A. Myelopoiesis-associated suppressor-cell activity in mice with Lewis lung carcinoma tumors: interferon-gamma plus tumor necrosis factor-alpha synergistically reduce suppressor cell activity. *Int J Cancer* **46**, 245-50 (1990).

119. Otsuji, M., Kimura, Y., Aoe, T., Okamoto, Y. & Saito, T. Oxidative stress by tumor-derived macrophages suppresses the expression of CD3 zeta chain of T-cell receptor complex and antigen-specific T-cell responses. *Proc Natl Acad Sci U S A* **93**, 13119-24 (1996).
120. Kusmartsev, S.A., Li, Y. & Chen, S.H. Gr-1+ myeloid cells derived from tumor-bearing mice inhibit primary T cell activation induced through CD3/CD28 costimulation. *J Immunol* **165**, 779-85 (2000).
121. Gabrilovich, D.I., Velders, M.P., Sotomayor, E.M. & Kast, W.M. Mechanism of immune dysfunction in cancer mediated by immature Gr-1+ myeloid cells. *J Immunol* **166**, 5398-406 (2001).
122. Liu, C. et al. Expansion of spleen myeloid suppressor cells represses NK cell cytotoxicity in tumor-bearing host. *Blood* **109**, 4336-42 (2007).
123. Terabe, M. et al. Transforming growth factor-beta production and myeloid cells are an effector mechanism through which CD1d-restricted T cells block cytotoxic T lymphocyte-mediated tumor immunosurveillance: abrogation prevents tumor recurrence. *J Exp Med* **198**, 1741-52 (2003).
124. Bendelac, A., Bonneville, M. & Kearney, J.F. Autoreactivity by design: innate B and T lymphocytes. *Nat Rev Immunol* **1**, 177-86 (2001).
125. Lohmann, T., Leslie, R.D. & Londei, M. T cell clones to epitopes of glutamic acid decarboxylase 65 raised from normal subjects and patients with insulin-dependent diabetes. *J Autoimmun* **9**, 385-9 (1996).
126. Semana, G., Gausling, R., Jackson, R.A. & Hafler, D.A. T cell autoreactivity to proinsulin epitopes in diabetic patients and healthy subjects. *J Autoimmun* **12**, 259-67 (1999).
127. Kyewski, B. & Klein, L. A central role for central tolerance. *Annu Rev Immunol* **24**, 571-606 (2006).
128. Derbinski, J., Schulte, A., Kyewski, B. & Klein, L. Promiscuous gene expression in medullary thymic epithelial cells mirrors the peripheral self. *Nat Immunol* **2**, 1032-9 (2001).
129. Bouneaud, C., Kourilsky, P. & Bousso, P. Impact of negative selection on the T cell repertoire reactive to a self-peptide: a large fraction of T cell clones escapes clonal deletion. *Immunity* **13**, 829-40 (2000).
130. Jenkins, M.K. & Schwartz, R.H. Antigen presentation by chemically modified splenocytes induces antigen-specific T cell unresponsiveness in vitro and in vivo. *J Exp Med* **165**, 302-19 (1987).
131. Lane, P., Haller, C. & McConnell, F. Evidence that induction of tolerance in vivo involves active signaling via a B7 ligand-dependent mechanism: CTLA4-Ig protects V beta 8+ T cells from tolerance induction by the superantigen staphylococcal enterotoxin B. *Eur J Immunol* **26**, 858-62 (1996).
132. Steinman, R.M., Hawiger, D. & Nussenzweig, M.C. Tolerogenic dendritic cells. *Annu Rev Immunol* **21**, 685-711 (2003).
133. Schwartz, R.H. T cell anergy. *Annu Rev Immunol* **21**, 305-34 (2003).
134. Fathman, C.G. & Lineberry, N.B. Molecular mechanisms of CD4+ T-cell anergy. *Nat Rev Immunol* **7**, 599-609 (2007).
135. Walker, L.S. & Abbas, A.K. The enemy within: keeping self-reactive T cells at bay in the periphery. *Nat Rev Immunol* **2**, 11-9 (2002).
136. Young, D.A. et al. IL-4, IL-10, IL-13, and TGF-beta from an altered peptide ligand-specific Th2 cell clone down-regulate adoptive transfer of experimental autoimmune encephalomyelitis. *J Immunol* **164**, 3563-72 (2000).

137. Bradley, L.M. et al. Islet-specific Th1, but not Th2, cells secrete multiple chemokines and promote rapid induction of autoimmune diabetes. *J Immunol* **162**, 2511-20 (1999).
138. Sakaguchi, S. Naturally arising CD4+ regulatory t cells for immunologic self-tolerance and negative control of immune responses. *Annu Rev Immunol* **22**, 531-62 (2004).
139. Shevach, E.M. Regulatory T cells in autoimmmunity*. *Annu Rev Immunol* **18**, 423-49 (2000).
140. Maloy, K.J. & Powrie, F. Regulatory T cells in the control of immune pathology. *Nat Immunol* **2**, 816-22 (2001).
141. Itoh, M. et al. Thymus and autoimmunity: production of CD25+CD4+ naturally anergic and suppressive T cells as a key function of the thymus in maintaining immunologic self-tolerance. *J Immunol* **162**, 5317-26 (1999).
142. Seddon, B. & Mason, D. The third function of the thymus. *Immunol Today* **21**, 95-9 (2000).
143. Apostolou, I. & von Boehmer, H. In vivo instruction of suppressor commitment in naive T cells. *J Exp Med* **199**, 1401-8 (2004).
144. Chen, W. et al. Conversion of peripheral CD4+CD25- naive T cells to CD4+CD25+ regulatory T cells by TGF-beta induction of transcription factor Foxp3. *J Exp Med* **198**, 1875-86 (2003).
145. Hsieh, C.S., Zheng, Y., Liang, Y., Fontenot, J.D. & Rudensky, A.Y. An intersection between the self-reactive regulatory and nonregulatory T cell receptor repertoires. *Nat Immunol* **7**, 401-10 (2006).
146. Jordan, M.S. et al. Thymic selection of CD4+CD25+ regulatory T cells induced by an agonist self-peptide. *Nat Immunol* **2**, 301-6 (2001).
147. Fisson, S. et al. Continuous activation of autoreactive CD4+ CD25+ regulatory T cells in the steady state. *J Exp Med* **198**, 737-46 (2003).
148. Thornton, A.M. & Shevach, E.M. CD4+CD25+ immunoregulatory T cells suppress polyclonal T cell activation in vitro by inhibiting interleukin 2 production. *J Exp Med* **188**, 287-96 (1998).
149. Takahashi, T. et al. Immunologic self-tolerance maintained by CD25+CD4+ naturally anergic and suppressive T cells: induction of autoimmune disease by breaking their anergic/suppressive state. *Int Immunol* **10**, 1969-80 (1998).
150. Suri-Payer, E. & Cantor, H. Differential cytokine requirements for regulation of autoimmune gastritis and colitis by CD4(+)CD25(+) T cells. *J Autoimmun* **16**, 115-23 (2001).
151. Asseman, C., Mauze, S., Leach, M.W., Coffman, R.L. & Powrie, F. An essential role for interleukin 10 in the function of regulatory T cells that inhibit intestinal inflammation. *J Exp Med* **190**, 995-1004 (1999).
152. Belkaid, Y., Piccirillo, C.A., Mendez, S., Shevach, E.M. & Sacks, D.L. CD4+CD25+ regulatory T cells control Leishmania major persistence and immunity. *Nature* **420**, 502-7 (2002).
153. Hori, S., Nomura, T. & Sakaguchi, S. Control of regulatory T cell development by the transcription factor Foxp3. *Science* **299**, 1057-61 (2003).
154. Fontenot, J.D., Gavin, M.A. & Rudensky, A.Y. Foxp3 programs the development and function of CD4+CD25+ regulatory T cells. *Nat Immunol* **4**, 330-6 (2003).
155. Khattri, R., Cox, T., Yasayko, S.A. & Ramsdell, F. An essential role for Scurfin in CD4+CD25+ T regulatory cells. *Nat Immunol* **4**, 337-42 (2003).
156. Walker, M.R. et al. Induction of FoxP3 and acquisition of T regulatory activity by stimulated human CD4+CD25- T cells. *J Clin Invest* **112**, 1437-43 (2003).

157. Morgan, M.E. et al. Expression of FOXP3 mRNA is not confined to CD4+CD25+ T regulatory cells in humans. *Hum Immunol* **66**, 13-20 (2005).
158. Roncador, G. et al. Analysis of FOXP3 protein expression in human CD4+CD25+ regulatory T cells at the single-cell level. *Eur J Immunol* **35**, 1681-91 (2005).
159. Gavin, M.A. et al. Single-cell analysis of normal and FOXP3-mutant human T cells: FOXP3 expression without regulatory T cell development. *Proc Natl Acad Sci U S A* **103**, 6659-64 (2006).
160. Pillai, V., Ortega, S.B., Wang, C.K. & Karandikar, N.J. Transient regulatory T-cells: a state attained by all activated human T-cells. *Clin Immunol* **123**, 18-29 (2007).
161. Wang, J., Ioan-Facsinay, A., van der Voort, E.I., Huizinga, T.W. & Toes, R.E. Transient expression of FOXP3 in human activated nonregulatory CD4+ T cells. *Eur J Immunol* **37**, 129-38 (2007).
162. Allan, S.E. et al. Activation-induced FOXP3 in human T effector cells does not suppress proliferation or cytokine production. *Int Immunol* **19**, 345-54 (2007).
163. Allan, S.E. et al. The role of 2 FOXP3 isoforms in the generation of human CD4+ Tregs. *J Clin Invest* **115**, 3276-84 (2005).
164. Brunkow, M.E. et al. Disruption of a new forkhead/winged-helix protein, scurfin, results in the fatal lymphoproliferative disorder of the scurfy mouse. *Nat Genet* **27**, 68-73 (2001).
165. Wildin, R.S. et al. X-linked neonatal diabetes mellitus, enteropathy and endocrinopathy syndrome is the human equivalent of mouse scurfy. *Nat Genet* **27**, 18-20 (2001).
166. Bennett, C.L. et al. The immune dysregulation, polyendocrinopathy, enteropathy, X-linked syndrome (IPEX) is caused by mutations of FOXP3. *Nat Genet* **27**, 20-1 (2001).
167. Fontenot, J.D., Dooley, J.L., Farr, A.G. & Rudensky, A.Y. Developmental regulation of Foxp3 expression during ontogeny. *J Exp Med* **202**, 901-6 (2005).
168. Asano, M., Toda, M., Sakaguchi, N. & Sakaguchi, S. Autoimmune disease as a consequence of developmental abnormality of a T cell subpopulation. *J Exp Med* **184**, 387-96 (1996).
169. Schorle, H., Holtschke, T., Hunig, T., Schimpl, A. & Horak, I. Development and function of T cells in mice rendered interleukin-2 deficient by gene targeting. *Nature* **352**, 621-4 (1991).
170. Horak, I., Lohler, J., Ma, A. & Smith, K.A. Interleukin-2 deficient mice: a new model to study autoimmunity and self-tolerance. *Immunol Rev* **148**, 35-44 (1995).
171. Willerford, D.M. et al. Interleukin-2 receptor alpha chain regulates the size and content of the peripheral lymphoid compartment. *Immunity* **3**, 521-30 (1995).
172. Suzuki, H., Zhou, Y.W., Kato, M., Mak, T.W. & Nakashima, I. Normal regulatory alpha/beta T cells effectively eliminate abnormally activated T cells lacking the interleukin 2 receptor beta in vivo. *J Exp Med* **190**, 1561-72 (1999).
173. Sharfe, N., Dadi, H.K., Shahar, M. & Roifman, C.M. Human immune disorder arising from mutation of the alpha chain of the interleukin-2 receptor. *Proc Natl Acad Sci U S A* **94**, 3168-71 (1997).
174. Sakaguchi, S., Sakaguchi, N., Asano, M., Itoh, M. & Toda, M. Immunologic self-tolerance maintained by activated T cells expressing IL-2 receptor alpha-chains (CD25). Breakdown of a single mechanism of self-tolerance causes various autoimmune diseases. *J Immunol* **155**, 1151-64 (1995).
175. Singh, B. et al. Control of intestinal inflammation by regulatory T cells. *Immunol Rev* **182**, 190-200 (2001).
176. Ochs, H.D., Ziegler, S.F. & Torgerson, T.R. FOXP3 acts as a rheostat of the immune response. *Immunol Rev* **203**, 156-64 (2005).

177. Shimizu, J., Yamazaki, S. & Sakaguchi, S. Induction of tumor immunity by removing CD25+CD4+ T cells: a common basis between tumor immunity and autoimmunity. *J Immunol* **163**, 5211-8 (1999).
178. Woo, E.Y. et al. Regulatory CD4(+)CD25(+) T cells in tumors from patients with early-stage non-small cell lung cancer and late-stage ovarian cancer. *Cancer Res* **61**, 4766-72 (2001).
179. Liyanage, U.K. et al. Prevalence of regulatory T cells is increased in peripheral blood and tumor microenvironment of patients with pancreas or breast adenocarcinoma. *J Immunol* **169**, 2756-61 (2002).
180. Curiel, T.J. et al. Specific recruitment of regulatory T cells in ovarian carcinoma fosters immune privilege and predicts reduced survival. *Nat Med* **10**, 942-9 (2004).
181. Viguier, M. et al. Foxp3 expressing CD4+CD25(high) regulatory T cells are overrepresented in human metastatic melanoma lymph nodes and inhibit the function of infiltrating T cells. *J Immunol* **173**, 1444-53 (2004).
182. Ormandy, L.A. et al. Increased populations of regulatory T cells in peripheral blood of patients with hepatocellular carcinoma. *Cancer Res* **65**, 2457-64 (2005).
183. Kawaida, H. et al. Distribution of CD4+CD25high regulatory T-cells in tumor-draining lymph nodes in patients with gastric cancer. *J Surg Res* **124**, 151-7 (2005).
184. Yang, Z.Z., Novak, A.J., Stenson, M.J., Witzig, T.E. & Ansell, S.M. Intratumoral CD4+CD25+ regulatory T-cell-mediated suppression of infiltrating CD4+ T cells in B-cell non-Hodgkin lymphoma. *Blood* **107**, 3639-46 (2006).
185. Smyth, M.J. et al. CD4+CD25+ T regulatory cells suppress NK cell-mediated immunotherapy of cancer. *J Immunol* **176**, 1582-7 (2006).
186. Ghiringhelli, F. et al. CD4+CD25+ regulatory T cells inhibit natural killer cell functions in a transforming growth factor-beta-dependent manner. *J Exp Med* **202**, 1075-85 (2005).
187. Cao, X. et al. Granzyme B and perforin are important for regulatory T cell-mediated suppression of tumor clearance. *Immunity* **27**, 635-46 (2007).
188. Barao, I. et al. Suppression of natural killer cell-mediated bone marrow cell rejection by CD4+CD25+ regulatory T cells. *Proc Natl Acad Sci U S A* **103**, 5460-5 (2006).
189. Mahajan, D. et al. CD4+CD25+ regulatory T cells protect against injury in an innate murine model of chronic kidney disease. *J Am Soc Nephrol* **17**, 2731-41 (2006).
190. Taams, L.S. et al. Modulation of monocyte/macrophage function by human CD4+CD25+ regulatory T cells. *Hum Immunol* **66**, 222-30 (2005).
191. Kryczek, I. et al. Cutting edge: induction of B7-H4 on APCs through IL-10: novel suppressive mode for regulatory T cells. *J Immunol* **177**, 40-4 (2006).
192. Kryczek, I. et al. Relationship between B7-H4, regulatory T cells, and patient outcome in human ovarian carcinoma. *Cancer Res* **67**, 8900-5 (2007).
193. Tiemessen, M.M. et al. CD4+CD25+Foxp3+ regulatory T cells induce alternative activation of human monocytes/macrophages. *Proc Natl Acad Sci U S A* **104**, 19446-51 (2007).
194. Lewkowicz, P., Lewkowicz, N., Sasiak, A. & Tchorzewski, H. Lipopolysaccharide-activated CD4+CD25+ T regulatory cells inhibit neutrophil function and promote their apoptosis and death. *J Immunol* **177**, 7155-63 (2006).
195. Kim, J.M., Rasmussen, J.P. & Rudensky, A.Y. Regulatory T cells prevent catastrophic autoimmunity throughout the lifespan of mice. *Nat Immunol* **8**, 191-7 (2007).
196. Tadokoro, C.E. et al. Regulatory T cells inhibit stable contacts between CD4+ T cells and dendritic cells in vivo. *J Exp Med* **203**, 505-11 (2006).

197. Tang, Q. et al. Visualizing regulatory T cell control of autoimmune responses in nonobese diabetic mice. *Nat Immunol* **7**, 83-92 (2006).
198. Itescu, S. et al. Intravenous pulse administration of cyclophosphamide is an effective and safe treatment for sensitized cardiac allograft recipients. *Circulation* **105**, 1214-9 (2002).
199. Lien, Y.H. & Scott, K. Long-term cyclophosphamide treatment for recurrent type I membranoproliferative glomerulonephritis after transplantation. *Am J Kidney Dis* **35**, 539-43 (2000).
200. Polak, L., Geleick, H. & Turk, J.L. Reversal by cyclophosphamide of tolerance in contact sensitization. Tolerance induced by prior feeding with DNCB. *Immunology* **28**, 939-42 (1975).
201. Rollinghoff, M., Starzinski-Powitz, A., Pfizenmaier, K. & Wagner, H. Cyclophosphamide-sensitive T lymphocytes suppress the in vivo generation of antigen-specific cytotoxic T lymphocytes. *J Exp Med* **145**, 455-9 (1977).
202. North, R.J. Cyclophosphamide-facilitated adoptive immunotherapy of an established tumor depends on elimination of tumor-induced suppressor T cells. *J Exp Med* **155**, 1063-74 (1982).
203. Berd, D. & Mastrangelo, M.J. Effect of low dose cyclophosphamide on the immune system of cancer patients: depletion of CD4+, 2H4+ suppressor-inducer T-cells. *Cancer Res* **48**, 1671-5 (1988).
204. Ghiringhelli, F. et al. CD4+CD25+ regulatory T cells suppress tumor immunity but are sensitive to cyclophosphamide which allows immunotherapy of established tumors to be curative. *Eur J Immunol* **34**, 336-44 (2004).
205. Terme, M. et al. Regulatory T Cells Control Dendritic Cell/NK Cell Cross-Talk in Lymph Nodes at the Steady State by Inhibiting CD4+ Self-Reactive T Cells. *J Immunol* **180**, 4679-86 (2008).
206. Lutsiak, M.E. et al. Inhibition of CD4(+)25+ T regulatory cell function implicated in enhanced immune response by low-dose cyclophosphamide. *Blood* **105**, 2862-8 (2005).
207. Attia, P. et al. Autoimmunity correlates with tumor regression in patients with metastatic melanoma treated with anti-cytotoxic T-lymphocyte antigen-4. *J Clin Oncol* **23**, 6043-53 (2005).
208. Maker, A.V., Attia, P. & Rosenberg, S.A. Analysis of the cellular mechanism of antitumor responses and autoimmunity in patients treated with CTLA-4 blockade. *J Immunol* **175**, 7746-54 (2005).
209. Mahnke, K. et al. Depletion of CD4+CD25+ human regulatory T cells in vivo: kinetics of Treg depletion and alterations in immune functions in vivo and in vitro. *Int J Cancer* **120**, 2723-33 (2007).
210. Dannull, J. et al. Enhancement of vaccine-mediated antitumor immunity in cancer patients after depletion of regulatory T cells. *J Clin Invest* **115**, 3623-33 (2005).
211. Attia, P. et al. Selective elimination of human regulatory T lymphocytes in vitro with the recombinant immunotoxin LMB-2. *J Immunother* **29**, 208-14 (2006).
212. Powell, D.J., Jr. et al. Administration of a CD25-directed immunotoxin, LMB-2, to patients with metastatic melanoma induces a selective partial reduction in regulatory T cells in vivo. *J Immunol* **179**, 4919-28 (2007).
213. Pasare, C. & Medzhitov, R. Toll pathway-dependent blockade of CD4+CD25+ T cell-mediated suppression by dendritic cells. *Science* **299**, 1033-6 (2003).
214. Peng, G. et al. Toll-like receptor 8-mediated reversal of CD4+ regulatory T cell function. *Science* **309**, 1380-4 (2005).

215. Wang, H.Y. & Wang, R.F. Regulatory T cells and cancer. *Curr Opin Immunol* **19**, 217-23 (2007).
216. Sutmuller, R.P. et al. Toll-like receptor 2 controls expansion and function of regulatory T cells. *J Clin Invest* **116**, 485-94 (2006).
217. Liu, H., Komai-Koma, M., Xu, D. & Liew, F.Y. Toll-like receptor 2 signaling modulates the functions of CD4+ CD25+ regulatory T cells. *Proc Natl Acad Sci U S A* **103**, 7048-53 (2006).
218. Crellin, N.K. et al. Human CD4+ T cells express TLR5 and its ligand flagellin enhances the suppressive capacity and expression of FOXP3 in CD4+CD25+ T regulatory cells. *J Immunol* **175**, 8051-9 (2005).
219. Pestka, S., Krause, C.D. & Walter, M.R. Interferons, interferon-like cytokines, and their receptors. *Immunol Rev* **202**, 8-32 (2004).
220. Novick, D., Cohen, B. & Rubinstein, M. Soluble interferon-alpha receptor molecules are present in body fluids. *FEBS Lett* **314**, 445-8 (1992).
221. Hiscott, J. Triggering the innate antiviral response through IRF-3 activation. *J Biol Chem* **282**, 15325-9 (2007).
222. Biron, C.A., Nguyen, K.B., Pien, G.C., Cousens, L.P. & Salazar-Mather, T.P. Natural killer cells in antiviral defense: function and regulation by innate cytokines. *Annu Rev Immunol* **17**, 189-220 (1999).
223. Yoneyama, M. et al. Direct triggering of the type I interferon system by virus infection: activation of a transcription factor complex containing IRF-3 and CBP/p300. *Embo J* **17**, 1087-95 (1998).
224. Marie, I., Durbin, J.E. & Levy, D.E. Differential viral induction of distinct interferon-alpha genes by positive feedback through interferon regulatory factor-7. *Embo J* **17**, 6660-9 (1998).
225. Sato, M. et al. Distinct and essential roles of transcription factors IRF-3 and IRF-7 in response to viruses for IFN-alpha/beta gene induction. *Immunity* **13**, 539-48 (2000).
226. Lund, J.M. et al. Recognition of single-stranded RNA viruses by Toll-like receptor 7. *Proc Natl Acad Sci U S A* **101**, 5598-603 (2004).
227. Tabeta, K. et al. Toll-like receptors 9 and 3 as essential components of innate immune defense against mouse cytomegalovirus infection. *Proc Natl Acad Sci U S A* **101**, 3516-21 (2004).
228. Kurt-Jones, E.A. et al. Pattern recognition receptors TLR4 and CD14 mediate response to respiratory syncytial virus. *Nat Immunol* **1**, 398-401 (2000).
229. Liu, Y.J. IPC: professional type 1 interferon-producing cells and plasmacytoid dendritic cell precursors. *Annu Rev Immunol* **23**, 275-306 (2005).
230. Juang, Y.T. et al. Primary activation of interferon A and interferon B gene transcription by interferon regulatory factor 3. *Proc Natl Acad Sci U S A* **95**, 9837-42 (1998).
231. Lindahl, P., Gresser, I., Leary, P. & Tovey, M. Interferon treatment of mice: enhanced expression of histocompatibility antigens on lymphoid cells. *Proc Natl Acad Sci U S A* **73**, 1284-7 (1976).
232. Honda, K. et al. Selective contribution of IFN-alpha/beta signaling to the maturation of dendritic cells induced by double-stranded RNA or viral infection. *Proc Natl Acad Sci U S A* **100**, 10872-7 (2003).
233. Hoebe, K. et al. Upregulation of costimulatory molecules induced by lipopolysaccharide and double-stranded RNA occurs by Trif-dependent and Trif-independent pathways. *Nat Immunol* **4**, 1223-9 (2003).

234. Santini, S.M. et al. Type I interferon as a powerful adjuvant for monocyte-derived dendritic cell development and activity in vitro and in Hu-PBL-SCID mice. *J Exp Med* **191**, 1777-88 (2000).
235. Tough, D.F., Borrow, P. & Sprent, J. Induction of bystander T cell proliferation by viruses and type I interferon in vivo. *Science* **272**, 1947-50 (1996).
236. Cousens, L.P., Orange, J.S., Su, H.C. & Biron, C.A. Interferon-alpha/beta inhibition of interleukin 12 and interferon-gamma production in vitro and endogenously during viral infection. *Proc Natl Acad Sci U S A* **94**, 634-9 (1997).
237. McRae, B.L., Semnani, R.T., Hayes, M.P. & van Seventer, G.A. Type I IFNs inhibit human dendritic cell IL-12 production and Th1 cell development. *J Immunol* **160**, 4298-304 (1998).
238. Cousens, L.P. et al. Two roads diverged: interferon alpha/beta- and interleukin 12-mediated pathways in promoting T cell interferon gamma responses during viral infection. *J Exp Med* **189**, 1315-28 (1999).
239. Santoli, D., Trinchieri, G. & Koprowski, H. Cell-mediated cytotoxicity against virus-infected target cells in humans. II. Interferon induction and activation of natural killer cells. *J Immunol* **121**, 532-8 (1978).
240. Gidlund, M., Orn, A., Wigzell, H., Senik, A. & Gresser, I. Enhanced NK cell activity in mice injected with interferon and interferon inducers. *Nature* **273**, 759-61 (1978).
241. Salazar-Mather, T.P., Ishikawa, R. & Biron, C.A. NK cell trafficking and cytokine expression in splenic compartments after IFN induction and viral infection. *J Immunol* **157**, 3054-64 (1996).
242. Lin, Q., Dong, C. & Cooper, M.D. Impairment of T and B cell development by treatment with a type I interferon. *J Exp Med* **187**, 79-87 (1998).
243. Honda, K., Mizutani, T. & Taniguchi, T. Negative regulation of IFN-alpha/beta signaling by IFN regulatory factor 2 for homeostatic development of dendritic cells. *Proc Natl Acad Sci U S A* **101**, 2416-21 (2004).
244. Takayanagi, H. et al. RANKL maintains bone homeostasis through c-Fos-dependent induction of interferon-beta. *Nature* **416**, 744-9 (2002).
245. Gresser, I. & Bourali, C. Exogenous interferon and inducers of interferon in the treatment Balb-c mice inoculated with RC19 tumour cells. *Nature* **223**, 844-5 (1969).
246. Gresser, I., Bourali, C., Levy, J.P., Fontaine-Brouty-Boye, D. & Thomas, M.T. Increased survival in mice inoculated with tumor cells and treated with interferon preparations. *Proc Natl Acad Sci U S A* **63**, 51-7 (1969).
247. Gresser, I. & Bourali-Maury, C. Inhibition by interferon preparations of a solid malignant tumour and pulmonary metastasis in mice. *Nat New Biol* **236**, 78-9 (1972).
248. Gresser, I., Thomas, M.T. & Brouty-Boye, D. Effect of interferon treatment of L1210 cells in vitro on tumour and colony formation. *Nat New Biol* **231**, 20-1 (1971).
249. Tanabe, T., Kominsky, S.L., Subramaniam, P.S., Johnson, H.M. & Torres, B.A. Inhibition of the glioblastoma cell cycle by type I IFNs occurs at both the G1 and S phases and correlates with the upregulation of p21(WAF1/CIP1). *J Neurooncol* **48**, 225-32 (2000).
250. Dvorak, H.F. & Gresser, I. Microvascular injury in pathogenesis of interferon-induced necrosis of subcutaneous tumors in mice. *J Natl Cancer Inst* **81**, 497-502 (1989).
251. Slaton, J.W. et al. Treatment with low-dose interferon-alpha restores the balance between matrix metalloproteinase-9 and E-cadherin expression in human transitional cell carcinoma of the bladder. *Clin Cancer Res* **7**, 2840-53 (2001).
252. Belardelli, F., Ferrantini, M., Proietti, E. & Kirkwood, J.M. Interferon-alpha in tumor immunity and immunotherapy. *Cytokine Growth Factor Rev* **13**, 119-34 (2002).

253. Salmon, P., Le Cotonnec, J.Y., Galazka, A., Abdul-Ahad, A. & Darragh, A. Pharmacokinetics and pharmacodynamics of recombinant human interferon-beta in healthy male volunteers. *J Interferon Cytokine Res* **16**, 759-64 (1996).
254. Einhorn, S. & Grander, D. Why do so many cancer patients fail to respond to interferon therapy? *J Interferon Cytokine Res* **16**, 275-81 (1996).
255. Gresser, I. et al. Antibody to mouse interferon alpha/beta abrogates resistance to the multiplication of Friend erythroleukemia cells in the livers of allogeneic mice. *J Exp Med* **168**, 1271-91 (1988).
256. Gresser, I. et al. Interferon treatment markedly inhibits the development of tumor metastases in the liver and spleen and increases survival time of mice after intravenous inoculation of Friend erythroleukemia cells. *Int J Cancer* **41**, 135-42 (1988).
257. Deonarain, R. et al. Critical roles for IFN-beta in lymphoid development, myelopoiesis, and tumor development: links to tumor necrosis factor alpha. *Proc Natl Acad Sci U S A* **100**, 13453-8 (2003).
258. Dunn, G.P. et al. A critical function for type I interferons in cancer immunoediting. *Nat Immunol* **6**, 722-9 (2005).
259. Swann, J.B. et al. Type I IFN contributes to NK cell homeostasis, activation, and antitumor function. *J Immunol* **178**, 7540-9 (2007).
260. Bui, J.D., Carayannopoulos, L.N., Lanier, L.L., Yokoyama, W.M. & Schreiber, R.D. IFN-dependent down-regulation of the NKG2D ligand H60 on tumors. *J Immunol* **176**, 905-13 (2006).
261. Seliger, B., Maeurer, M.J. & Ferrone, S. TAP off--tumors on. *Immunol Today* **18**, 292-9 (1997).
262. Talmadge, J.E., Phillips, H., Schindler, J., Tribble, H. & Pennington, R. Systematic preclinical study on the therapeutic properties of recombinant human interleukin 2 for the treatment of metastatic disease. *Cancer Res* **47**, 5725-32 (1987).
263. Trinchieri, G. Interleukin-12: a cytokine at the interface of inflammation and immunity. *Adv Immunol* **70**, 83-243 (1998).
264. Zuniga, E.I., Hahm, B. & Oldstone, M.B. Type I interferon during viral infections: multiple triggers for a multifunctional mediator. *Curr Top Microbiol Immunol* **316**, 337-57 (2007).
265. Ferrantini, M., Capone, I. & Belardelli, F. Interferon-alpha and cancer: mechanisms of action and new perspectives of clinical use. *Biochimie* **89**, 884-93 (2007).
266. Unkeless, J.C. Characterization of a monoclonal antibody directed against mouse macrophage and lymphocyte Fc receptors. *J Exp Med* **150**, 580-96 (1979).
267. van Hall, T. et al. Selective cytotoxic T-lymphocyte targeting of tumor immune escape variants. *Nat Med* **12**, 417-24 (2006).
268. Weiss, A., Wiskocil, R.L. & Stobo, J.D. The role of T3 surface molecules in the activation of human T cells: a two-stimulus requirement for IL 2 production reflects events occurring at a pre-translational level. *J Immunol* **133**, 123-8 (1984).
269. Sanford, K.K., Earle, W.R. & Likely, G.D. The growth in vitro of single isolated tissue cells. *J Natl Cancer Inst* **9**, 229-46 (1948).
270. Ceredig, R., Lowenthal, J.W., Nabholz, M. & MacDonald, H.R. Expression of interleukin-2 receptors as a differentiation marker on intrathymic stem cells. *Nature* **314**, 98-100 (1985).
271. Karre, K., Ljunggren, H.G., Piontek, G. & Kiessling, R. Selective rejection of H-2-deficient lymphoma variants suggests alternative immune defence strategy. *Nature* **319**, 675-8 (1986).

272. Sutmuller, R.P. et al. Synergism of cytotoxic T lymphocyte-associated antigen 4 blockade and depletion of CD25(+) regulatory T cells in antitumor therapy reveals alternative pathways for suppression of autoreactive cytotoxic T lymphocyte responses. *J Exp Med* **194**, 823-32 (2001).
273. Yu, P. et al. Intratumor depletion of CD4+ cells unmasks tumor immunogenicity leading to the rejection of late-stage tumors. *J Exp Med* **201**, 779-91 (2005).
274. Blankenstein, T. & Qin, Z. The role of IFN-gamma in tumor transplantation immunity and inhibition of chemical carcinogenesis. *Curr Opin Immunol* **15**, 148-54 (2003).
275. Finkelman, F.D. & Morris, S.C. Development of an assay to measure in vivo cytokine production in the mouse. *Int Immunol* **11**, 1811-8 (1999).
276. Shresta, S., Pham, C.T., Thomas, D.A., Graubert, T.A. & Ley, T.J. How do cytotoxic lymphocytes kill their targets? *Curr Opin Immunol* **10**, 581-7 (1998).
277. Kayagaki, N. et al. Polymorphism of murine Fas ligand that affects the biological activity. *Proc Natl Acad Sci U S A* **94**, 3914-9 (1997).
278. Qin, Z. & Blankenstein, T. CD4+ T cell--mediated tumor rejection involves inhibition of angiogenesis that is dependent on IFN gamma receptor expression by nonhematopoietic cells. *Immunity* **12**, 677-86 (2000).
279. Galon, J. et al. Type, density, and location of immune cells within human colorectal tumors predict clinical outcome. *Science* **313**, 1960-4 (2006).
280. Chen, M.L. et al. Regulatory T cells suppress tumor-specific CD8 T cell cytotoxicity through TGF-beta signals in vivo. *Proc Natl Acad Sci U S A* **102**, 419-24 (2005).
281. Suri-Payer, E. & Fritzsching, B. Regulatory T cells in experimental autoimmune disease. *Springer Semin Immunopathol* **28**, 3-16 (2006).
282. Lechner, M., Lirk, P. & Rieder, J. Inducible nitric oxide synthase (iNOS) in tumor biology: the two sides of the same coin. *Semin Cancer Biol* **15**, 277-89 (2005).
283. Zamanakou, M., Germenis, A.E. & Karanikas, V. Tumor immune escape mediated by indoleamine 2,3-dioxygenase. *Immunol Lett* **111**, 69-75 (2007).
284. Rock, K.L. & Shen, L. Cross-presentation: underlying mechanisms and role in immune surveillance. *Immunol Rev* **207**, 166-83 (2005).
285. Chambers, B. et al. Induction of protective CTL immunity against peptide transporter TAP-deficient tumors through dendritic cell vaccination. *Cancer Res* **67**, 8450-5 (2007).
286. Richards, J.O. et al. Tumor growth impedes natural-killer-cell maturation in the bone marrow. *Blood* **108**, 246-52 (2006).
287. Hwang, S.Y. et al. A null mutation in the gene encoding a type I interferon receptor component eliminates antiproliferative and antiviral responses to interferons alpha and beta and alters macrophage responses. *Proc Natl Acad Sci U S A* **92**, 11284-8 (1995).
288. Sakaguchi, S. Regulatory T cells in the past and for the future. *Eur J Immunol* **38**, 901-937 (2008).
289. Hontsu, S. et al. Visualization of naturally occurring Foxp3+ regulatory T cells in normal and tumor-bearing mice. *Int Immunopharmacol* **4**, 1785-93 (2004).
290. Ghiringhelli, F. et al. Tumor cells convert immature myeloid dendritic cells into TGF-beta-secreting cells inducing CD4+CD25+ regulatory T cell proliferation. *J Exp Med* **202**, 919-29 (2005).
291. Valzasina, B., Piconese, S., Guiducci, C. & Colombo, M.P. Tumor-induced expansion of regulatory T cells by conversion of CD4+CD25- lymphocytes is thymus and proliferation independent. *Cancer Res* **66**, 4488-95 (2006).
292. Fazilleau, N., Bachelez, H., Gougeon, M.L. & Viguier, M. Cutting edge: size and diversity of CD4+CD25high Foxp3+ regulatory T cell repertoire in humans: evidence for

similarities and partial overlapping with CD4+CD25- T cells. *J Immunol* **179**, 3412-6 (2007).
293. Wolf, A.M. et al. Increase of regulatory T cells in the peripheral blood of cancer patients. *Clin Cancer Res* **9**, 606-12 (2003).
294. Trzonkowski, P., Szmit, E., Mysliwska, J., Dobyszuk, A. & Mysliwski, A. CD4+CD25+ T regulatory cells inhibit cytotoxic activity of T CD8+ and NK lymphocytes in the direct cell-to-cell interaction. *Clin Immunol* **112**, 258-67 (2004).
295. Simon, A.K. et al. Regulatory T cells inhibit Fas ligand-induced innate and adaptive tumour immunity. *Eur J Immunol* **37**, 758-67 (2007).
296. Casares, N. et al. CD4+/CD25+ regulatory cells inhibit activation of tumor-primed CD4+ T cells with IFN-gamma-dependent antiangiogenic activity, as well as long-lasting tumor immunity elicited by peptide vaccination. *J Immunol* **171**, 5931-9 (2003).
297. Wald, O. et al. IFN-gamma acts on T cells to induce NK cell mobilization and accumulation in target organs. *J Immunol* **176**, 4716-29 (2006).
298. Sarween, N. et al. CD4+CD25+ cells controlling a pathogenic CD4 response inhibit cytokine differentiation, CXCR-3 expression, and tissue invasion. *J Immunol* **173**, 2942-51 (2004).
299. Mosser, D.M. The many faces of macrophage activation. *J Leukoc Biol* **73**, 209-12 (2003).
300. Balkwill, F., Charles, K.A. & Mantovani, A. Smoldering and polarized inflammation in the initiation and promotion of malignant disease. *Cancer Cell* **7**, 211-7 (2005).
301. Sica, A. & Bronte, V. Altered macrophage differentiation and immune dysfunction in tumor development. *J Clin Invest* **117**, 1155-66 (2007).
302. Bettelli, E. et al. Reciprocal developmental pathways for the generation of pathogenic effector TH17 and regulatory T cells. *Nature* **441**, 235-8 (2006).
303. Nakae, S., Iwakura, Y., Suto, H. & Galli, S.J. Phenotypic differences between Th1 and Th17 cells and negative regulation of Th1 cell differentiation by IL-17. *J Leukoc Biol* **81**, 1258-68 (2007).
304. Ouyang, W., Kolls, J.K. & Zheng, Y. The biological functions of T helper 17 cell effector cytokines in inflammation. *Immunity* **28**, 454-67 (2008).
305. Sica, G.L. et al. B7-H4, a molecule of the B7 family, negatively regulates T cell immunity. *Immunity* **18**, 849-61 (2003).
306. Collison, L.W. et al. The inhibitory cytokine IL-35 contributes to regulatory T-cell function. *Nature* **450**, 566-9 (2007).
307. Kelly, J.M., Takeda, K., Darcy, P.K., Yagita, H. & Smyth, M.J. A role for IFN-gamma in primary and secondary immunity generated by NK cell-sensitive tumor-expressing CD80 in vivo. *J Immunol* **168**, 4472-9 (2002).
308. Kerbel, R. & Folkman, J. Clinical translation of angiogenesis inhibitors. *Nat Rev Cancer* **2**, 727-39 (2002).
309. Folkman, J. Successful treatment of an angiogenic disease. *N Engl J Med* **320**, 1211-2 (1989).
310. Ezekowitz, R.A., Mulliken, J.B. & Folkman, J. Interferon alfa-2a therapy for life-threatening hemangiomas of infancy. *N Engl J Med* **326**, 1456-63 (1992).
311. Griffioen, A.W., Damen, C.A., Martinotti, S., Blijham, G.H. & Groenewegen, G. Endothelial intercellular adhesion molecule-1 expression is suppressed in human malignancies: the role of angiogenic factors. *Cancer Res* **56**, 1111-17 (1996).

# 9 ABBREVIATIONS

(listed in alphabetical order)

| | |
|---|---|
| 1MT | 1-Methyl- L -Tryptophan |
| α- | anti- |
| ACK | Ammonium Chloride potassium phosphate buffer |
| ADCC | Antibody-Dependent Cell-mediated Cytotoxicity |
| APC | AlloPhycoCyanin |
| APC | Antigen Presenting Cells |
| BCR | B Cell Receptor |
| bFGF | basic Fibroblast Growth Factor |
| BM | Bone Marrow |
| CD | Cluster of Differentiation |
| CSF | Colony Stimulating Factor |
| CFSE | CarboxyFluorescein Succinimidyl Ester |
| cpm | counts per minute |
| CTLA-4 | Cytotoxic T-lymphocyte-associated Antigen-4 |
| Cy5 | Cyanine 5 |
| DC | Dendritic Cells |
| $ddH_2O$ | double distilled water |
| DLN | Draining LN |
| DMSO | DiMethylSulfOxide |
| ELISA | Enzyme-Linked ImmunoSorbent Assay |
| EMCV | EncephaloMyoCarditis Virus |
| E:T | Effector to Target |
| FACS | Fluorescence-Activated Cell Sorting |
| FITC | Fluorescein-IsoThioCyanate |
| FSC | Forward SCatter |
| g | gram |
| GM-CSF | Granulocyte/Macrophage CSF |
| GITR | Glucocorticoid-Iinduced TNF-receptor family-Related |
| h | hour |

| | |
|---|---|
| HLA | Human Leukocyte Antigen |
| HSV | Herpes Simplex Virus |
| IBD | Inflammatory Bowel Disease |
| ICAM | InterCellular Adhesion Molecule |
| IDO | Indoleamine-pyrrole 2,3-dioxygenase |
| IFN | Interferon |
| IFNAR1 | Interferon-α Receptor 1 |
| Ig | Immunoglobulin |
| IL | InterLeukin |
| iMC | immature Myeloid Cells |
| iNOS | inducible Nitric Oxide Synthase |
| i.p. | intraperitoneal |
| i.v. | intravenous |
| IPEX | Immune dysregulation, Polyendocrinopathy, Enteropathy, X-linked |
| L/D-NMMA | L/D-$N^G$-MonoMethyl Arginine |
| LN | Lymph Node |
| LPS | LipoPolySaccharide |
| mAb | monoclonal Antibody |
| MACS | Magnetic Cell Sorting |
| μC | microCurie |
| MCA | MethylCholAnthrene |
| MCMV | Murine CytoMegaloVirus |
| MDA5 | Melanoma Differentiation-Associated protein 5 |
| MDSC | Myeloid-Derived Suppressor Cells |
| MHC | Major Histocompatibility Complex |
| Mϕ | Macrophage |
| MFI | Mean Fluorescence Intensity |
| μg | microgram |
| min | minute |
| MIP | Macrophage Inflammatory Protein |
| μl | microlitre |
| ml | mililitre |

| | |
|---|---|
| μM | microMolar |
| mM | miliMolar |
| MME | Macrophage MetalloElastase |
| MMP | Matrix MetalloProteinase |
| MSC | Myeloid Suppressor Cells |
| NK | Natural Killer |
| NKG2D | NK Group 2 member D |
| nm | nanometer |
| NO | Nitric Oxide |
| NOD | Nucleotide-Oligomerization Domains |
| OD | Optical Density |
| O/N | Over Night |
| PAMP | Pathogen-Associated Molecular Patterns |
| PBL | Peripheral Blood Lymphocytes |
| PBS | Phosphate Buffered Saline |
| pDC | plasmacytoid DC |
| PD-ECGF | Platelet-Derived Endothelial Cell Growth Factor |
| PE | PhycoErythrin |
| PFA | ParaFormAldenhyde |
| pg | picogram |
| pH | potential Hydrogeni |
| PI | Propidium Iodide |
| PGE2 | Prostaglandin E synthase 2 |
| Poly(I:C) | PolyInosinic-PolyCytidylic acid |
| Prf | Perforin |
| PRR | Pattern-Recognition Receptors |
| RAE-1 | Retinoic Acid Early inducible-1 |
| RAG | Recombination-Activation Gene |
| rpm | rounds per minute |
| RT | Room Temperature |
| s.c. | subcutaneous |
| SD | Standard Deviation |
| S/N | SuperNatant |
| SSC | Side SCatter |

| | |
|---|---|
| TAA | Tumor-Associated Antigens |
| TAM | Tumor Associated Macrophages |
| Tcon | conventional T cells |
| TCR | T Cell Receptor |
| TGF-β | Transforming Growth Factor-β |
| TID | Type I Diabetes |
| TLR | Toll-Like Receptors |
| TNF | Tumor Necrosis Factor |
| TRAIL | TNF–Related Apoptosis-Inducing Öigand |
| Treg | Regulatory T cells |
| TSA | Tumor-Specific Antigens |
| VEGF | Vascular Endothelial Growth Factor |
| wt | wild type |

# 10 ACKNOWLEDGEMENTS

I would like to thank, first of all, my supervisor PD Dr. Adelheid Cerwenka for giving me the opportunity to work in her lab, and for the challenging project I took over. I am thankful for all her support during my PhD, for the scientific knowledge I gained from her and for the opportunities to present my work in scientific conferences and interact with important scientists.

I would like to thank our valuable collaborators for this project: PD Dr. Elisabeth Suri-Payer for her expertise in the field of regulatory T cells, the numerous interesting discussions and her guidance; Prof. Dr. Rainer Zawatzky for his valuable knowledge on type I IFN; and Dr. Thorbald van Hall for providing us reagents and expertise on TEIPP peptides.

Moreover, I would like to thank Prof. Dr. Günter Hämmerling for accepting to be my first referee; Prof. Dr. Peter H. Krammer, Prof. Dr. Henning Walczak and their group members for all the fruitful discussions and suggestions during my presentations in their Work In Progress; Prof. Dr. Hideo Yagita, Dr. Christine Falk, Dr. Rüdiger Arnold, Dr. Natalio Garbi for providing reagents, mice, technical support and scientific knowledge. Klaus Hexel and Dr. Steffen Schmitt for the long FACS sorting appointments; Dr. Christian Ackermann and Dr. Ulrike Engel for their assistance at the Nikon Imaging Center; and all the personnel of the DKFZ animal facility for their support in animal care and breeding.

Many special thanks to all the lab members of the Innate Immunity lab, as well as the A160 and A150 members, for the friendly working atmosphere and the exciting activities. In particular, I would like to thank Marco Wendel and Dr. Carola Schellack for the fruitful collaboration in this project; Ana Stojanovic for the scientific and personal interaction and for reading my thesis; Dr. Norman Nausch and Dr. Kai Zanzinger for collaborating and exchanging ideas; Joachim Neuert, Sandra Weiler, Melanie Rutz and Diana Vobis for technical assistance; Dr. Anja Tessarz for being patient with all my questions and for introducing me to German culture; and Martina Kegel for reading my thesis.

Finally, I would like to thank most of all my family – my mother, my grand-mother and my sister – and my life partner, Βασιλη, who although from a distance they were the stronger supporters of my efforts.